Characterization of the secretins, large outer membrane channels of Gram-negative bacteria

A thesis presented in partial fulfillment of the requirements for the degree of

Doctor of Philosophy

In

Biochemistry

at Massey University, Palmerston North

New Zealand

Sofia Khanum

2015

Dedicated to my mother

Acknowledgements

"In the name of Allah, the Most Gracious, the Most Merciful"

First of all I would like to acknowledge my supervisor Dr. Jasna Rakonjac for her continuous support and critical evaluation of my work throughout my PhD. Indeed it was due to her encouragement and innovative thinking that polished my skills and enabled me to do well. I would also like to thank my co-supervisor Dr. Gill Norris for her valuable feedback. A special thanks to my lab fellows Wesley Wen, and Julian Spagnuolo at Helipad. I would also like thank the staff at Institute of Fundamental Sciences; their cooperation and kindness will be treasured always.

I would like to extend my gratitude to my sweet friends Sadia Sattar, Shazrah Salam, Sadia Tahir and Amber Faisal for their continuous support, understanding, cooperation and care; they indeed made things easier for me at the time of stress by just being around apart from giving me valuable suggestions during my research and writing this thesis.

A special thanks to my family.

My parents remained a source of contentment for me always, particularly during this course of study. My parents' continuous encouragement, support and suggestions for my study throughout these five years is remarkable. A special thanks to my parents for letting me pursue my dream of higher education.

This thesis would have never been possible without my loving husband Khurram Iqbal. You were always around at times I thought that it is impossible to continue, you helped me to keep things in perspective. I am grateful to you for your remarkable patience and unwavering love and support over the course of my research, and also for the countless days of daddy daycare to our daughters. My daughters Mahin and Mahrosh, I owe you lots and lots of fun hours. I couldn't imagine doing my PhD without you; you really gave me the reason to continue.

Not to forget the support of my sisters Jamila, Anila along with the continuous encouragement of my brother Waseem. Lastly I would like to say thanks to my nephews Hannan, Ahmed, Ali and my niece Shiza for their lovely smiles in stressful days.

Abstract

Secretins, a family of large outer membrane channels, mediate secretion and/or assembly of virulence factors and/or complex proteinaceous structures, such as rods, type IV pili and filamentous bacteriophage. Secretins form large radially-symmetric channels composed of 12 to 14 identical subunits, with internal diameters of up to 10 nm, whose lumen is interrupted by a septum/plug structure that very likely represents a gate or a valve. The identity of septum in the primary sequence of secretins has not been determined as yet, however the cryo-EM and SPA analyses point to the C-terminal domain forming these structures, whereas mutagenesis specifically identified two regions in this domain, named GATE1 and GATE2, as having an important role in gating of the filamentous phage secretion system secretin pIV. However, it is not known whether these regions are also involved in gating of the secretins from type II and type III secretion systems.

In this work, twelve "leaky-gate" mutants in the secretin PulD from the type II secretion system (T2SS), selected from a random mutant library based on ability to utilise 829 Da oligosaccharide maltopentaose in the absence of maltoporin, were analysed in detail. Most of PulD leaky-gate mutants clustered in the GATE1 and GATE2 regions. All point mutants were positive for secretion of the cognate PulD substrate, enzyme Pullulanase (PulA), whereas a 5-residue in-frame deletion (Δ477-481) was negative. Two severely leaky GATE1 region mutants, G458S and Δ477-481, sensitised *E. coli* to all tested antibiotics whose molecular weight is too high to pass through porins: rifamycin SV (720 Da), bacitracin (1423 Da) vancomycin (1449 Da) and daptomycin (1621 Da). The GATE1 of this secretin is therefore a potential drug target, for design of molecules that can sensitise secretin-containing pathogenic Gram-negative bacteria to > 600 Da antibiotics and/or block the secretion of substrates, including virulence factors.

Engineered chimeras between PulD and pIV were used to probe functional compartmentalisation among the secretin domains and the segments involved in gating. This analysis showed that the N-terminal domains, GATE1 region and channel-forming secretin homology domain are interdependent with respect to function in secretion/assembly of the substrates, and to different extends for folding and multimerisation.

This work further analysed the gating properties of the type III secretion system (T3SS) secretins EscC and InvG. When expressed in *E. coli* K12, these secretins were naturally "leaky" and mistargeted to the inner membrane, resulting in growth retardation. The survival of *E. coli* expressing these secretins depended on the PspF, positive regulator of the key inner membrane stress response Psp. Therefore, in the T3SS secretin-expressing or toxin-secreting cells, PspF is a potential target for design of molecules that could kill T3SS-containing toxin-secreting Gram-negative bacteria.

Table of Contents

List of Tables

List of Figures

List of Abbreviations

ADP	Adenosine diphosphate
AMP	Adenosine monophosphate
ARFs	ADP ribosylation factors
ATPase	Adenosine triphosphatase
Bac	Bacitracin
Bae	Bacterial adaptive response
Bp	Base pairs
cAMP	Cyclic AMP
CDS	Coding sequence
CFU	Colony forming unit
Cm	Chloramphenicol
Cpx	Conjugative pilus expression response
Cryo-EM	Cryo Electron Microscopy
CtxAB	Cholera toxin AB
Da	Dalton
DNA	Deoxyribonuclic acid
DNS	3,5-dinitrosalicyclic acid
DOC	Deoxycholate
EHEC	Enterohaemorrhagic *Escherichia coli*
EDTA	Ethylenediaminetetraacetic acid
EOP	Efficiency of plating
EPEC	Enteropathogenic *Escherichia coli*
ESRs	Envelope stress responses
ETEC	Enterotoxigenic *Escherichia coli*
FPSS	Filamentous phage secretion system
GST	Glutathione S-transferase
IPTG	Isopropyl β-D-1-thiogalactopyranoside
Kn	Kanamycin
LEE	Locus of enterocyte effacement
MIC	Minimal inhibitory concentration
MW	Molecular weight

OD	Optical density
PCR	Polymerase chain reaction
Pfu	Plaque forming unit
Pi	Inorganic phosphate
PKA	Protein kinase A
Psp	Phage shock protein response
R	Resistant
Rcs	Regulation of capsular synthesis
RF	Replicative form
RpoE	RNA polymerase, extracytoplasmic stress sigma factor
S	Sensitive
SDS-PAGE	Sodium dodecyl sulfate-polyacrylamide
SecYEG	General secretory translocon
SPA	Single particle analysis
SPI	Salmonella pathogenicity island
spp.	species
sv.	serovar
T2SS	Type II secretion system
T3SS	Type III secretion system
T4PBS	Type IV pilus biogenesis system
Tat	Twin-arginine translocon
TCA	Trichloroacetic acid
TEM	Transmission electron microscope
Tet	Tetracycline
Van	Vancomycin
WT	Wild type
Ysa-PI	Yersinia pathogenicity islands

Chapter 1: Literature Review

1.1. Introduction

Bacterial interaction with their environment is in great part mediated by structures located on the bacterial surface or the factors secreted into the extracellular space. In bacteria, protein secretion is vital for nutrient acquisition, virulence with secretion of effector molecules and toxins, and for inter- and intra-species communication. In Gram-negative bacteria due to their double membrane system, secretion is complex, because the proteins that are destined for secretion, or those building extracellular structures such as pili, must cross two membranes to reach the exterior of the cell (Dautin and Bernstein, 2007). To avoid this difficulty, Gram-negative bacteria evolved specialized systems for protein secretion and to date multiple different systems have been identified in Gram-negative bacteria (Economou et al., 2006). These systems are complex and diverse in their structures, all of them containing an obligatory outer membrane channel that is an exit port for the secreted substrate. There are several families of the large outer membrane channels in the secretion systems of Gram-negative bacteria, of which most common are channels of the secretin family, found in four known secretion systems: type II secretion system (T2SS), type III secretion system (T3SS), type IV pilus biogenesis system (T4PBS) and filamentous phage assembly-secretion system (FPSS). Secretins, which are the subject of this study, are crucial for these secretion systems, as without the secretin channels these systems are not able to assemble or secrete their substrates, many of which are the key virulence factors in colonisation and invasion of the host by pathogenic bacteria.

1.2. Secretion Systems

Secretion systems containing the secretins are categorised into two groups based on whether the proteins are exported directly from cytoplasm to the extracellular space, or cross the inner membrane via the SecYEG or Tat translocons before being shuttled to the exterior. Among the secretion systems that use secretins, T3SS involves in first type of secretion and has components which make a continuous tunnel from cytoplasm across the whole envelope (inner membrane, periplasm, cell wall and outer membrane). In contrast, the T2SS proteins destined for export are first transported

across the inner membrane into the periplasm using general secretory pathway or translocon (SecYEG) and are then exported across the outer membrane through the secretin channel through the action of a large number of inner membrane and periplasmic components of the T2SS. Both Sec/Tat pathways transport proteins across the inner membrane, without disturbing the inner membrane integrity and function. The proteins transported through SecYEG have specific signal sequences (type I signal sequence, lipoprotein signal sequence, prepilin signal sequence), whereas the Tat-targeted proteins have a Tat signal sequence at their N-termini. Generally, Sec pathway transport unfolded proteins across the inner membrane as well as mediate protein insertion in the inner membrane, while Tat pathways transport folded/semi-folded proteins or the proteins contained cofactors (Natale et al., 2008; Xie and Dalbey, 2008). In contrast, the signals for targeting of proteins to the T2SS, once they are in the periplasm, are less clear (Pineau et al., 2014). Targeting of proteins for secretion by their cognate T3SS involves N-terminal peptides that interact with specific chaperones or 5' end of mRNA (Anderson and Schneewind, 1997).

1.2.1 Type II secretion system (T2SS)

T2SS is used by many Gram-negative bacteria for the transportation of folded proteins from periplasm to extracellular milieu through the outer membrane. Due to dynamic nature of T2SS, its fully assembled machinery has not yet been purified and visualized; however, it has been proposed that the components of T2SS apparatus span both inner and outer membrane. The nomenclature of proteins and genes differ between the systems and organisms, however it is generally denoted as general secretory pathway (Gsp), and often annotated as such with the individual gene and protein annotation being represented by the same letter for the same component in different organisms. Apparatus of T2SS is encoded by 12-15 genes designated as *gsp* (the general secretory pathway), which are organized into a large operon *gspCDEFGHIJKLMNO* (Sandkvist, 2001). Proteins encoded by these genes are inserted into or translocated across the inner membrane through SecYEG pathway and assembled into four sub-assemblies which include cytoplasmic ATPase, inner membrane platform, pseudopilus and outer membrane platform (Korotkov et al., 2012). Inner membrane platform of T2SS is made up of multiple copies of four proteins: GspC, GspF, GspL and GspM (Figure 1.1), while the outer membrane platform is made up of single protein called secretin, denoted as GspD. The secretin channel GspD is a multimer made of 12 identical

subunits in the outer membrane and it interacts with the inner membrane platform through GspC. Cytoplasmic ATPase, GspE, provides energy to this system for the secretion process and is a peripheral membrane protein associated with the inner membrane platform (Lybarger et al., 2009; Sandkvist et al., 1999). Recent studies based on crosslinking, immune-precipitation and co-purification demonstrate that GspC is the only protein of the inner membrane platform that interacts with the outer membrane secretin GspD (Korotkov et al., 2011). It was also suggested that GspC may regulate the secretion process, and play a key role in cross-envelope assembly of T2SS, which is demonstrated by its interaction with pseudopilus proteins (Lee et al., 2000).

Pseudopilus of T2SS is formed by four minor (GspH, GspI, GspJ and GspK) and one major (GspG) pseudopilin. These pseudopilins derived their names from the type 4 pilins, due to homology of the amino terminal sequence to the type 4 pilins, including the pre-pilin signal sequence. Like type IV pilins, pseudopilins use Sec pathway for the insertion into the inner membrane, through their positively charged short N-terminal sequence which is cleaved by a specific aspartic protease, called prepilin peptidase as the pseudopilus assembles (Arts et al., 2007; Francetic et al., 2007). Mature pseudopilins transiently reside in the inner membrane and then at the time of secretion minor pilin GspK forms heterotrimer with two other pseudopilins, GspI and GspJ, in order to form the tip of the pseudopilus (Durand et al., 2011). However, it still remains to be found when and how additional two pilins, GspH and multiple copies of GspG, become part of this pilus and how the pseudopilus interacts with ATPase GspE to harvest energy for GspG elongation that is presumed to be required for the substrate secretion (Korotkov et al., 2012).

Range of substrates transported by T2SS varies from a single substrate in some species to more than 20 in others (Sandkvist, 2001). These substrates have wide range of functions, but are mostly enzymes including proteases, lipases, phosphatases and some toxins that post-translationally modify intracellular host signalling molecules, such as CtxAB of *Vibrio cholerae* (Matson et al., 2007). Substrates of T2SS with their N-terminal signal peptides are initially transported to the periplasm through Sec/Tat pathways. In the periplasm, after cleavage of signal peptides these substrates interact with the periplasmic domain of GspC/secretin and pseudopilus tip (Douzi et al., 2011). These multiple interactions stimulate the ATPase activity of GspE, and facilitate the

addition of pseudopilins to the growing pseudopilus, which is hypothesised to act as a piston and push the substrate through the secretin channel into the extracellular medium (Douzi et al., 2011).

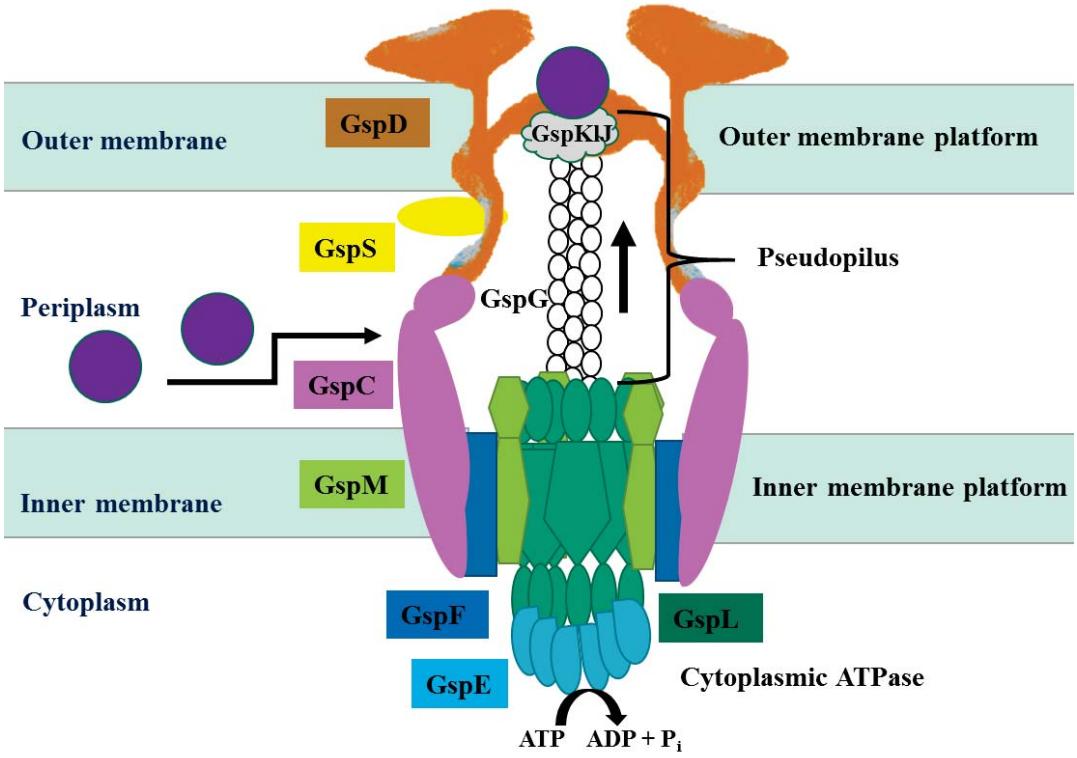

Figure 1.1 Hypothetical model of T2SS of Gram-negative bacteria and its mechanism of action.

Secretion starts when GspC interact with secretin GspD and exoprotein (substrate for secretion) in the periplasm, and transmits signal to ATPase, GspE, through GspLMF. Elongation of pseudopilus starts at the expense of energy released by ATP hydrolysis. The inner membrane protein GspL probably interacts with GspE (ATPase) and GspG (the major pseudopilin) and adds subunits to the growing pseudopilus. The exoprotein moves upwards with growing pseudopilus and finally interacts with GspD. At this stage GspD undergoes a major conformational change which results in the opening of the septum and the exoprotein is eventually released to the extracellular space. Purple circles present the exoprotein, and arrows show the direction of secretion. Figure is adopted from (Korotkov et al., 2012) with permission.

1.2.2 Type III secretion system (T3SS)

Type III secretion system (T3SS) is a widespread secretion system among Gram-negative bacterial pathogens. This macromolecular nano-machine, which is also known as injectisome, is used by bacterial pathogens to inject toxins and other "effectors" of pathogenicity directly from bacterial into the host cell cytoplasm (Buettner, 2012; Galan and Collmer, 1999). Effectors released by T3SS modulate various cellular functions of the host cells and make them accessible for bacterial invasion and infection (Galan, 2009).

T3SS is composed of twenty or more proteins. A number of these proteins (but not the outer membrane channel) are conserved with the flagellar system. Because of this it has been widely accepted that T3SS is evolutionarily derived from flagellar system (McCann and Guttman, 2008). Approximately 10 genes encoding the flagellar basal body are homologous with T3SS proteins, most of those localising to the inner membrane (Blocker et al., 2003). Homology between the T3SS and flagellar system is also seen in the flagellar hook, which is homologous to the proteins forming the needle base of T3SS.

Depending on the organism, most or all of the genes encoding components of T3SS are clustered on the chromosome in so-called "pathogenicity islands". Typical examples of these pathogenicity islands are locus of enterocyte effacement (LEE)- in enteropathogenic and enterohemorrhagic *E. coli*, and *Salmonella* pathogenicity islands (SPI) in *Salmonella* spp. These clusters not only contain genes encoding the structural components of the T3SS apparatus, but also the genes that encode up to twenty or so effectors and regulatory molecules (Deng et al., 2004; Elliott et al., 2000). *Salmonella* are the only group described so far to contain two T3SSs, encoded by two distinct gene clusters, termed as *Salmonella* Pathogenicity Island 1 and 2 (SPI-1 and SPI-2). Presumably both systems have been acquired by independent events of horizontal gene transfer, with SPI-2 being the more recent acquisition. In a model for the evolution of pathogenesis of *Salmonella* infections, *Salmonella* may have initially evolved to a pathogen capable of localized gastrointestinal infections (SPI-1 function) and later extended its pathogenic potential towards systemic infections (SPI-2 function) (Fabrega and Vila, 2013; Schmidt and Hensel, 2004). These two T3SSs are required at different stages of infection; SPI-1 for initial invasion of the host intestinal mucosa

and SPI-2 is for subsequent systemic spread of infection that includes invasion of the macrophage (Galan, 1999; Lostroh and Lee, 2001).

T3SS exists in more than twenty five species of Gram-negative bacteria and its apparatus is very similar among all these bacterial species (Cornelis, 2006). Structurally, T3SS is a complex macromolecular assembly, including structural proteins, cytoplasmic chaperones and accessory proteins. The system is composed of a basal body traversing the whole bacterial envelope (inner membrane, periplasm, peptidoglycan and outer membrane) that morphologically looks as a stack of variable size rings. A needle lodged inside the basal body completes the injectisome (Figure 1.2) (Kimbrough and Miller, 2000). Recent cryo electron microscopy and single particle analysis resolved the structure of *Salmonella* and *Shigella* needle complexes at sub-nanometer resolution, revealing detailed organization of individual substructures (Hodgkinson et al., 2009; Marlovits et al., 2004; Sani et al., 2007; Schraidt et al., 2010; Schraidt and Marlovits, 2011).

Assembly of T3SS apparatus occurs in a step-wise fashion. It starts with the basal body formation in the inner and outer membrane and after that assembly of needle sub-structures takes place. As mentioned earlier, basal body is composed of rings of different diameters, which can be referred to as inner membrane ring and outer membrane ring, connected with a smaller-diameter barrel. The inner membrane ring is proposed to be the first ring to assemble within the basal body. Recent surface labelling and single particle analysis studies revealed that this inner membrane ring is formed by two proteins that are homologous in various T3SSs, but named differently: YscJ and YscD in *Yersinia,* MxiJ and MxiG in *Shigella,* PrgK and PrgH in *Salmonella* (Kimbrough and Miller, 2000; Schraidt et al., 2010). Moreover, cryo-electron microscopic studies of the *Salmonella* T3SSs revealed that the inner membrane ring formed by PrgK and PrgH has 24-fold radial symmetry and is most likely composed of 24 subunits of each protein. Data also indicated that PrgK formed a smaller inner membrane ring that is covered by a larger outer ring made of PrgH subunits. Similar 24-fold radial symmetry was also observed for EscJ, a homologue which forms the inner membrane ring of enteropathogenic *E. coli* T3SS (Schraidt and Marlovits, 2011; Yip et al., 2005). The outer membrane ring of type III secretion apparatus corresponds to a secretin family channel. Secretins EscC, InvG and YscC form the outer membrane

ring in the EHEC, *Salmonella* Typhimurium and *Yersinia* spp, respectively (Figure 1.2) (Kosarewicz et al., 2012; Koster et al., 1997; Kubori et al., 2000).

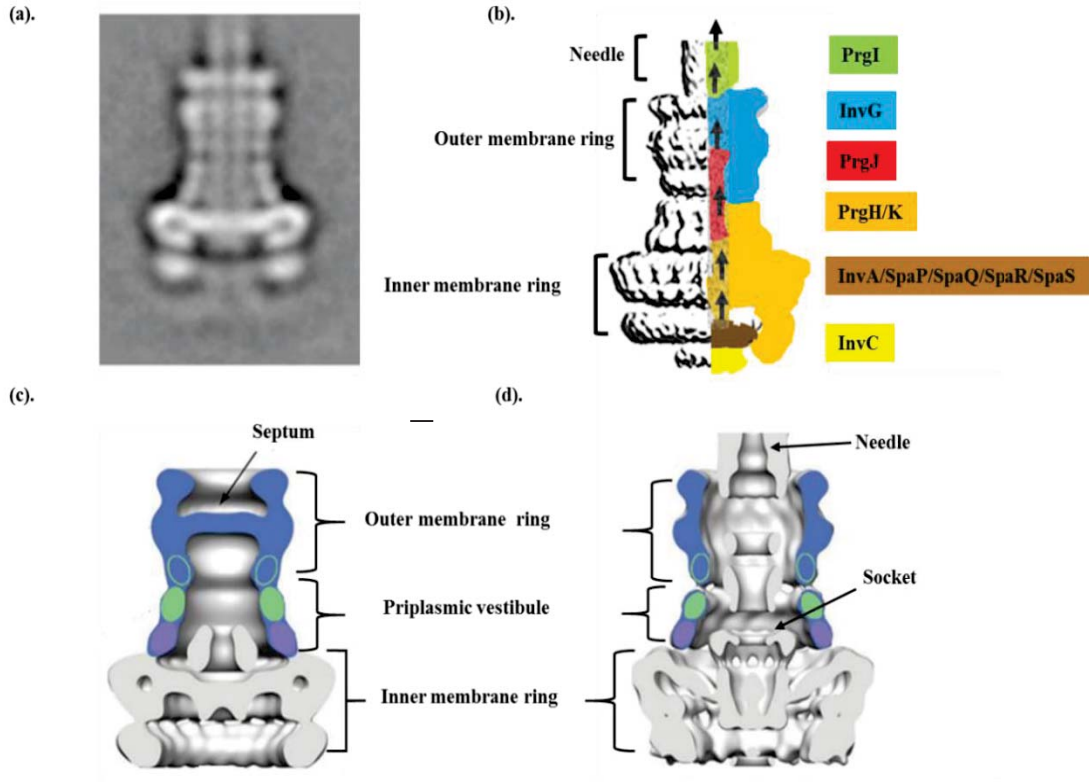

Figure 1.2 Organization of basal body and needle sub-structure of T3SS.

(a). Averaged image obtained from negatively stained needle complex micrographs of *Salmonella enterica sv.* Typhimurium (Schraidt et al., 2010). **(b).** Structure obtained from the single particle analysis of the unstained cryo-EM at 10 Å resolution. The structure is overlapped with cartoon model, indicating proposed organization of the major structural components (PrgH, PrgK, PrgJ, InvG and PrgI) and export apparatus (InvA, SpaP, SpaQ, SpaR, SpaS) with ATPase (InvC). Arrows indicate the direction of secretion (Marlovits et al., 2004; Schraidt and Marlovits, 2011). **(c).** A slice view through the base complex of *Salmonella enterica sv.* Typhimurium T3SS in closed state (Marlovits et al., 2004); there is no substrate (needle components). **(d).** A slice view of the needle complex, from *Shigella flexneri* T3SS featuring an open secretin channel containing the lodged needle components (Hodgkinson et al., 2009). (c-d) Above the inner membrane ring, the secretin (blue) occupies the top part of the T3SS, circles in blue secretin represent locations of the N-terminal subdomains N0 (purple ovals), N1 (light-green ovals) and N3 (light-green ovals) (Sanowar et al., 2010; Schraidt et al., 2010). Adopted from (Hodgkinson et al., 2009; Marlovits et al., 2004; Sanowar et al., 2010; Schraidt et al., 2010; Schraidt and Marlovits, 2011) with permission.

In the needle complex, secretin is occupied by the needle, a rod-like appendage made up of multiple copies of a single subunit. Prior to assembly of the needle, the empty T3SS (the basal body) is a hollow structure, sealed across the apical side (at the level of outer membrane) by septum which is part of the secretin channel (Figure 1.2c). The basal body is also closed across the base (at the level of the inner membrane) with the basal plate. Evidence for the sealing structures across the basal body comes from densities observed in the structures obtained by cryo-electron microscopy and single particle analysis (Figure 1.2). However, the roles of the densities that span the basal body in maintaining physiological outer and inner membrane barrier functions have not been investigated in functional studies (Loquet et al., 2012; Schraidt and Marlovits, 2011).

Basal plate of T3SS is formed by five highly conserved inner membrane proteins (InvA, SpaP, SpaQ, SpaR and SpaS in *Salmonella* spp.) known as export apparatus of T3SS. The cytoplasmic components which are essential for secretion are conserved across all T3SSs include: an ATPase (InvC) and the linker protein (OrgB) which recruits InvC to the platform formed by SpaO/OrgA in *Salmonella*. It seems that a component of the basal plate interacts with substrates (or substrate-chaperone complexes) and confers specificity to the T3SS (Cornelis, 2006; Minamino et al., 2011). When needle assembly starts, a protrusion appears from the base, which acts like socket/anchor for the needle. During needle assembly, both inner and outer membrane rings undergo conformational change. These changes transform the secretin InvG from a barrier to a scaffold in the outer membrane and across the periplasm that holds the needle (Figure 1.2d) (Marlovits et al., 2004).

Needle assembly starts soon after the basal body formation. Needle subunits are assembled in the basal body after passing through the basal plate, which recognizes them as the primary substrates of T3SS. Needle itself is composed of a single protein EscF, PrgI and MxiH in EHEC, *Salmonella* and *Shigella*, respectively. Inside the base, the needle is connected to a substructure, called inner rod, which passes through the entire length of the base, serving as a structural base for the needle and a channel for the passage of the needle subunits across the periplasmic segment of the basal body (Figure 1.2). This inner rod is made of protein called EscA and PrgJ in EHEC and *Salmonella*, respectively (Marlovits et al., 2004; Roe et al., 2003; Zhong et al., 2012). Inside the basal body, inner rod is anchored to a socket-like structure at the bottom,

which may serve as an adaptor between the helical inner rod and the inner membrane ring of the basal body (Figure 1.2). Once the needle reaches certain length, the needle complex assembly is completed. The completion of the needle complex is thought to change its substrate recognition complex structure, becoming competent for the secretion of effector proteins that are to be delivered into the host cell (Kubori et al., 2000; Lefebre and Galan, 2014). On contact with the host cell, the needle complex secretes a pair of translocator proteins called EspB/EspD and SipB/SipC in EHEC and *Salmonella*, respectively that is delivered to the host cell surface (Wachter et al., 1999). These proteins insert into the host membrane, making a translocator pore and attaching the needle complex to the host cell. The effector proteins are injected into the host cell using the conduit made of the needle complex and the pore (Miki et al., 2004).

1.2.3 Type IV pilus biogenesis system (T4PBS)

Type IV pili (T4P) are 1-5 µm long helical fibers composed of small structural subunits called pilins, and displayed by a wide variety of Gram-positive, Gram-negative and archaeal species (Albers and Pohlschroeder, 2009; Giltner et al., 2012). Bacteria use these fibres/pili for adhesion to host cells, biofilm formation, cellular invasion, DNA uptake and twitching/gliding motility (Craig and Li, 2008). T4P are related to the pseudopilus of the type II secretion system (T2SS) in terms of polymerization of pilin subunits described in the previous section (Ayers et al., 2010). Generally, T4P are categorized into two types: IVa and IVb, based on the composition of pilus genes and the structure of the major pilin (Burrows, 2005; Craig and Li, 2008; Hansen and Forest, 2006). Genes encoded T4PBS are either scattered on the chromosomes in some bacterial species or found in the form of clusters in others like *pil* genes of *Pseudomonas aeruginosa* and *Neisseria* spp, while in some, T4P genes reside on a plasmid like *tcp* and *bfp* genes of *Vibrio cholerae* and EPEC, respectively (Mattick et al., 1996; Mohammadi-Barzelighi et al., 2011; Sohel et al., 1996).

Details of T4P biogenesis are not yet fully understood. It is known that the minor and major prepilins are inserted into the cytoplasmic membrane via their hydrophobic N-terminal pre-pilin signal sequence by the SecYEG translocon. Later on, the N-terminus of the signal sequence is cleaved at a specific site by enzyme prepilin peptidase and the mature pilin subunits assemble into pilus by the T4P assembly machinery at the inner membrane, in a similar fashion to what was demonstrated for the pseudopilus of

the T2SS. The inner membrane components of the *Neisseria meningitidis* T4PBS include membrane-associated cytoplasmic ATPase PilF, integral inner membrane protein PilG (whose function is unknown). The outer membrane component is the secretin family channel PilQ. The assembling T4P pilus requires the secretin channel to cross the outer membrane and become exposed on the cell surface. Interestingly, Type IV pilus is used for the twitching motility which is mediated by assembly/extrusion, followed by retraction of the type IV pili. During retraction, pilins are disassembled from the base using the energy provided by another cytoplasmic ATPase, PilT, in *Neisseria* spp. Adhesion of bacteria to the host cells via T4P is most commonly mediated by the major pilin, however in some bacterial species separate proteins are present at the tip of the fibre, for example PilC in *Neisseria* spp. (Figure 1.3) (Francetic et al., 2007; Satyshur et al., 2007; Thanassi et al., 2012).

T4PBS is closely related to T2SS. It was reported that proteins involved in the function or structure of T2SS and T4PBS overlap in some species. For example, it has been shown that the type 4 pilin subunit PilA that comprises the adhesive type 4 pilus of *P. aeruginosa* is also required for efficient secretion of exoenzymes (Lu et al., 1997) via the T2SS . Moreover, some T4PBS have reported to have secretory functions (Han et al., 2007; Kirn et al., 2003). For example, in *Vibrio cholerae,* T4 toxin co-regulated pilus (TCP) biogenesis machinery is required for the translocation of colonization factor (TcpF) which is important for the colonization of infant murine intestine by the *Vibrio* (Kirn et al., 2003). These observations led to the hypothesis that T2SS use a short "pseudopilus" as a piston whose the assembly and retraction "pumps" a secreted protein (substrate) across the outer membrane secretin channel (Yamagata et al., 2012). Despite many similarities, the two systems each have a unique set of components that are not present in the other (Sauvonnet et al., 2000). These observations probably reflect the divergent evolution of the T2SS and T4PBS systems (Peabody et al., 2003).

1.2.4 Filamentous phage secretion system (FPSS)

Filamentous phages are rod-shaped bacterial viruses 1-2 μm in length, that infect a wide variety of Gram-negative bacteria, including *Escherichia* (Marvin and Hohn, 1969), *Salmonella*, *Yersinia*, *Pseudomonas*, *Xanthomonas*, *Thermus*, *Neisseria* and *Vibrio* (Rakonjac et al., 2011; Russel and Model, 2006). The virion of filamentous phage is composed of five proteins, one major coat protein (pVIII) that forms the shaft

of the filament, presents in thousands of copies, and two pairs of minor virion proteins, pVII/pIX, and pIII/pVI. Unlike majority of bacteriophages, which are assembled in the cytoplasm and released by lysis of the host cell, filamentous phages are assembled and released from the cell surface using special secretion system known as filamentous phage secretion system (FPSS) without killing the host cells. This FPSS is an assembly/secretion complex, composed of three morphogenic phage proteins: pI, a presumed ATPase, and pXI that form a complex in the inner membrane, and a large channel of the secretin family, pIV that traverses the outer membrane and periplasm (Opalka et al., 2003). In the host periplasm, pIV through its N-terminal domain interacts with C-terminal domains of pI and pXI to form a large export/assembly channel at assembly sites of filamentous phage (Feng et al., 1999).

Filamentous phage genome is replicated by rolling-circle replication, one strand at the time, generating single-genome-length circular ssDNA. The substrate for packaging is a rod-shaped complex of the genome with phage-encoded ssDNA-binding protein pV. The whole genome, apart from a hairpin loop that serves as a packaging signal, is covered by pV. Meanwhile, the minor and major virion proteins are inserted into the inner membrane; as well as the pI/pIX inner membrane component of assembly machinery; whereas the secretin pIV is secreted to the periplasm and then targeted to the outer membrane. Assembly process starts when packaging signal (PS) protruding from pV-ssDNA complex interacts with the cytoplasmic domain of pI and C-terminal ends of minor coat proteins pVII and pIX (Rapoza and Webster, 1995; Russel, 1991). As the ssDNA traverses bacterial inner membrane, pV dimers are successively removed and replaced by the major coat protein (pVIII) embedded in the membrane (Figure 1.4) and assembled phage particle comes out of the cell through the secretin channel pIV that traverses the periplasm and outer membrane (Marvin et al., 2014; Rakonjac and Conway, 2006; Rakonjac et al., 1999).

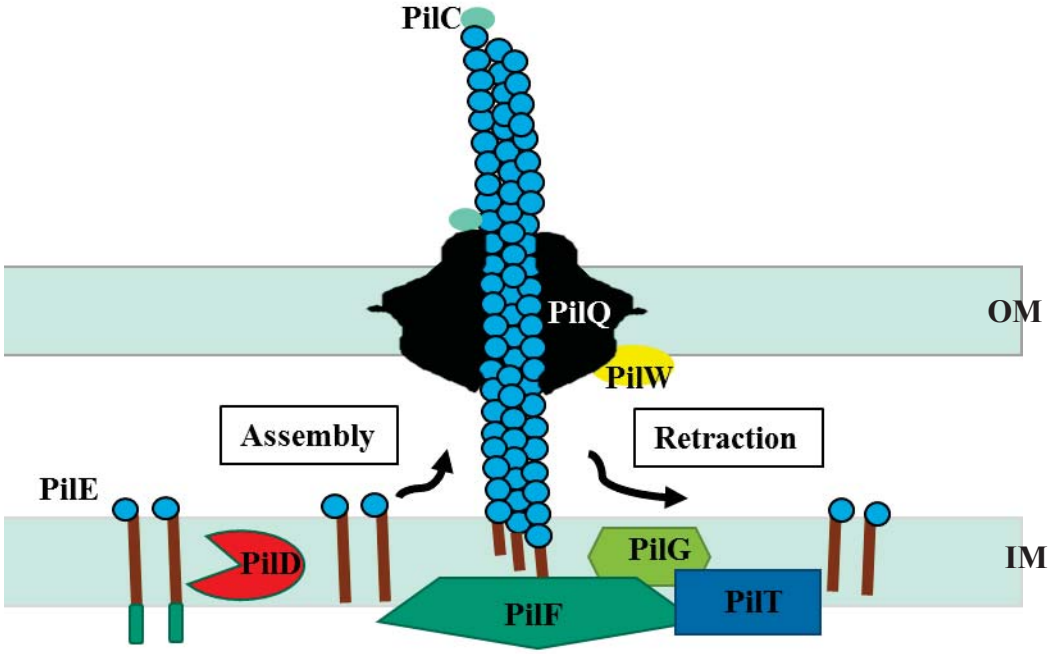

Figure 1.3 Schematic presentation of the type IV pilus biogenesis system (T4PBS).

Model for biogenesis of type IV pili of *Neisseria meningitidis*. PilD, the prepilin peptidase cleaves the N-terminal pre-pilin signal sequence in the inner membrane, followed by the assembly of mature pilin subunits including the major PilE subunit. PilF, the cytoplasmic ATPase, provides energy for this process. PilQ secretin of the *Neisseria meningitidis* T4PBS provide an exit channel for the pilus to traverse the outer membrane. PilT cytoplasmic ATPase powers the retraction process, while the minor pilin PilC was proposed to function as adhesin when displayed at the tip of the pilus or promote retraction when attached to the outer membrane.OM, outer membrane; IM, inner membrane (Thanassi et al., 2012).

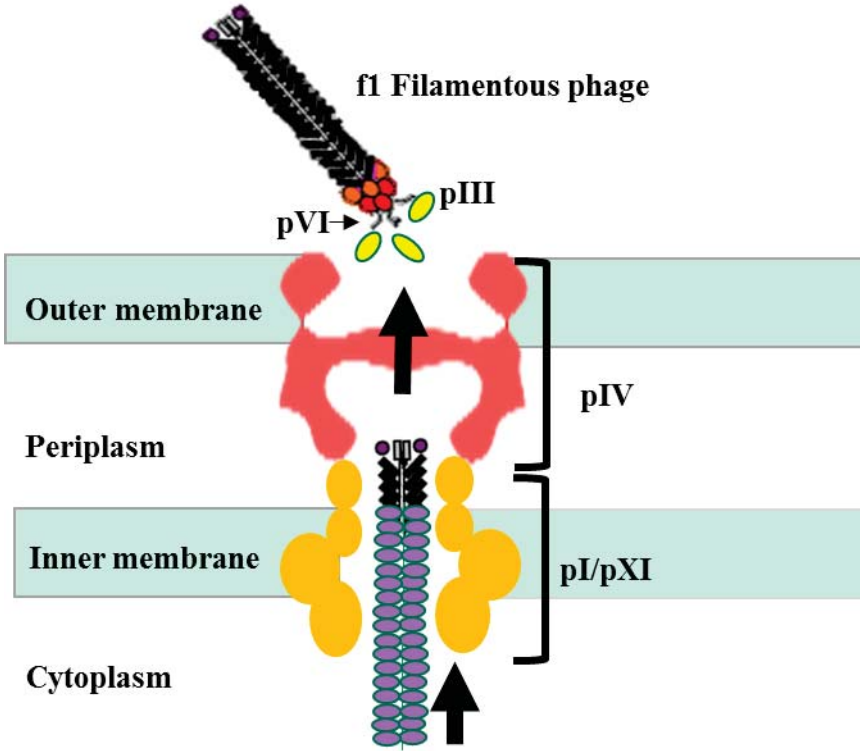

Figure 1.4 Schematic presentation of filamentous phage secretion system (FPSS).

Model of filamentous phage secretion system. Process of filamentous phage assembly starts when ssDNA-pV complex of filamentous phage genome interacts with the inner membrane assembly machinery (pI/pXI) of FPSS, followed by replacement of pV molecules with major phage coat protein as phage genome traverses the inner membrane. Minor proteins pIII and pVI are added once the complete genome is coated, and the virion is released from the host cell. Figure adapted from (Rakonjac et al., 2011) with permission.

1.3 The role of bacterial secretion systems in pathogenesis

Pathogenic Gram-negative bacteria use their secretion systems to colonise their respective hosts, invade the host cells and manipulate the immune response by secreting a variety of toxins, enzymes and virulence factors. Some secretion systems help in the attachment to the host cell surface, which is vital part of bacterial colonisation during infection. These secretion systems are widespread among Gram-negative bacterial pathogens. A well-studied example is the T3SS of enterohemorrhagic *Escherichia coli* (EHEC). The EHEC causes numerous food and waterborne outbreaks of diarrhoea and haemolytic uremic syndrome (HUS) throughout the world (Leotta et al., 2008). A prominent feature of the disease caused by EHEC is the formation of attaching and effacing lesions (A/E lesions). Formation of these lesions are accompanied by destruction of microvilli and rearrangement of host cell cytoskeleton (Nataro and Kaper, 1998). Bacteria form these lesions using effectors secreted by their T3SS, which mediate attachment to the host cells and modification of cytoskeleton to form characteristic pedestals that are part of the effacement phenotype (Hueck, 1998). Similarly, *Salmonella enterica* sv. Typhimurium (*S.* Typhimurium) causes broad range of diseases including gastroenteritis, bacteraemia and enteric fever in variety of vertebrate hosts. *S.* Typhimurium, which is one of the major human pathogens, invades the intestinal epithelial cells with the help of T3SS (Galan and Zhou, 2000). In addition, T3SS effectors also inhibit activation of phagocytes, and delay the immune response (Galan and Collmer, 1999). Past studies revealed that any disturbance in the secretion of effectors proteins abolishes the ability of *S.* Typhimurium to invade the host cells. Moreover, without the secretory effector proteins, a reduction in *S.* Typhimurium persistence and cytotoxicity was observed in cell culture and murine models (Miki et al., 2004).

S. Typhimurium uses two T3SS encoded by SP1-1 and SPI-2 respectively, which allow delivery of effector proteins into the cytoplasm of two different types of host cells to manipulate cell signaling and vesicular trafficking (Hapfelmeier et al., 2005). It was shown *in vitro* that effector proteins translocated via the SPI-1 T3SS reorganize host cell structure, trigger invasion into fibroblasts and epithelial cells, establish a permissive intracellular niche, and induce expression of pro-inflammatory cytokines and chemokines and induce cell death (Chen et al., 1999; Hardt et al., 1998; Hernandez

et al., 2004; Hernandez et al., 2003). The SPI-2 T3SS is expressed after *S.* Typhimurium has entered a macrophage. SPI-2 effector proteins manipulate vesicular trafficking, inhibit macrophage activation and pyroptosis and thereby enhance intracellular survival and proliferation of *Salmonella* (McGhie et al., 2009)

Type II secretion systems (T2SS) are also employed by Gram-negative bacteria to establish diseases in their respective hosts, by secretion of various types of toxins, enzymes and virulence factors. These include human pathogens *Pseudomonas aeruginosa*, *Yersinia enterocolitica, Vibrio cholerae*, *Legionella pneumophila,* enterohaemorrhagic *E. coli* (EHEC), enterotoxigenic *E. coli* (ETEC) and *Klebsiella* spp., fish and amphibian pathogen *Aeromonas hydrophila* and plant pathogens *Dickeya dadantii* and *Erwinia carotovora* (Jyot et al., 2011; Lathem et al., 2002; Rossier et al., 2004; Toth and Birch, 2005). For instance, *Vibrio cholerae* and ETEC use their T2SSs to secrete cholera toxin and heat-labile enterotoxin, respectively, which are hallmark virulence factors of cholera and diarrhoea in the children (Sithivong et al., 2010; Vicente et al., 2005). Once secreted, heat-labile enterotoxin of ETEC and cholera toxin bind preferentially to gangliosides on eukaryotic cell surface (Angstrom et al., 1994). Following internalization of the toxin, the enzymatically active subunit of toxin is activated by ADP ribosylation factors (ARFs). Activated toxin catalyses the ADP ribosylation of the heterotrimeric GTPase Gsα, consequently activating adenylate cyclase. Increased cAMP concentration activates cAMP-dependent protein kinase A (PKA), that ultametily leads to phosphorylation of the multiple serines of the chloride channel (Sheppard and Welsh, 1999). This leads to the secretion of fluids and electrolytes and diarrhea (Dorsey et al., 2006). In *Vibrio cholerae*, it was also demonstrated that T2SS has a role in biofilm formation by secreting the biofilm matrix proteins into the culture supernatant (Johnson et al., 2014).

Surface structures such as polymeric fibres formed by the T4PBS of several pathogenic bacteria including *Vibrio cholerae*, *Pseudomonas aeruginosa* and *Neisseria gonorrhoeae* aid the virulence with variety of diverse functions such as DNA uptake, twitching motility, host cell attachment and biofilm formation. Some T4PBS secrete specific exoproteins as well (Hager et al., 2006; Han et al., 2007; Kirn et al., 2003).

Filamentous phage have been demonstrated to have effect on virulence either by horizontal transfer of virulence factors such as cholera toxin (Waldor and Mekalanos,

1996), or by supporting biofilm formation in *Pseudomonas aeruginosa* (Rice et al., 2009) or via unknown mechanisms in plant pathogens *Xantomonas* and *Ralstonia* (Askora et al., 2009; Tseng et al., 1990).

In conclusion, these four secretion systems, despite their diverse structure and function, have a conserved outer membrane component, a large channel of the secretin family. Members of this family share sequence and structural homology, in particular the channel-forming secretin homology or C-domain (pfam:PF00263). Several recent studies based on the fusion of fluorescent proteins with the different components of these secretion systems, provide evidence that secretins promote the assembly of these secretion systems. It was reported that the assembly of T3SS in *Yersinia* and T2SS of *Klebsiella* and *Vibrio* start with secretin ring formation in the outer membrane (Buddelmeijer et al., 2009; Diepold et al., 2010; Lybarger et al., 2009).

1.4 Secretins

Secretins are multi-domain proteins that form large channels in the outer membrane of Gram-negative bacteria. Genetic and biochemical analyses revealed that the secretins had two distinct functional domains: a C-terminal trans-membrane domain and an N-terminal periplasmic domain (Chami et al., 2005) (Figure 1.5a). The C-terminal domain, known as the "Secretin homology domain", is the most conserved domain of this family. This domain mediates insertion into the membrane and formation of the channel. This domain is followed, in some secretins, by an S domain that is required for assembly and outer membrane insertion.

The periplasmic N-terminal domain is less conserved than the secretin homology domain. The N-terminal domain interacts with the integral (inner) membrane and periplasmic proteins of the cognate secretion system and in some secretins confers specificity to the secretion process (Korotkov et al., 2011). The N-terminal domain is further subdivided into two to four independently folding sub-domains (N0 to N3) (Bitter et al., 1998). Strikingly, bioinformatics studies suggested that secretins of T4PBS contained one or two extra domains at their N-terminal end which are known as B1 and B2, predicted to be rich in β sheets (Berry et al., 2012). To date, structures of N-terminal and S-domains of type II and type III secretins have been resolved by crystallography, but no high-resolution structure of the secretin homology (C-terminal) domain (pfam:PF00263) is available as yet.

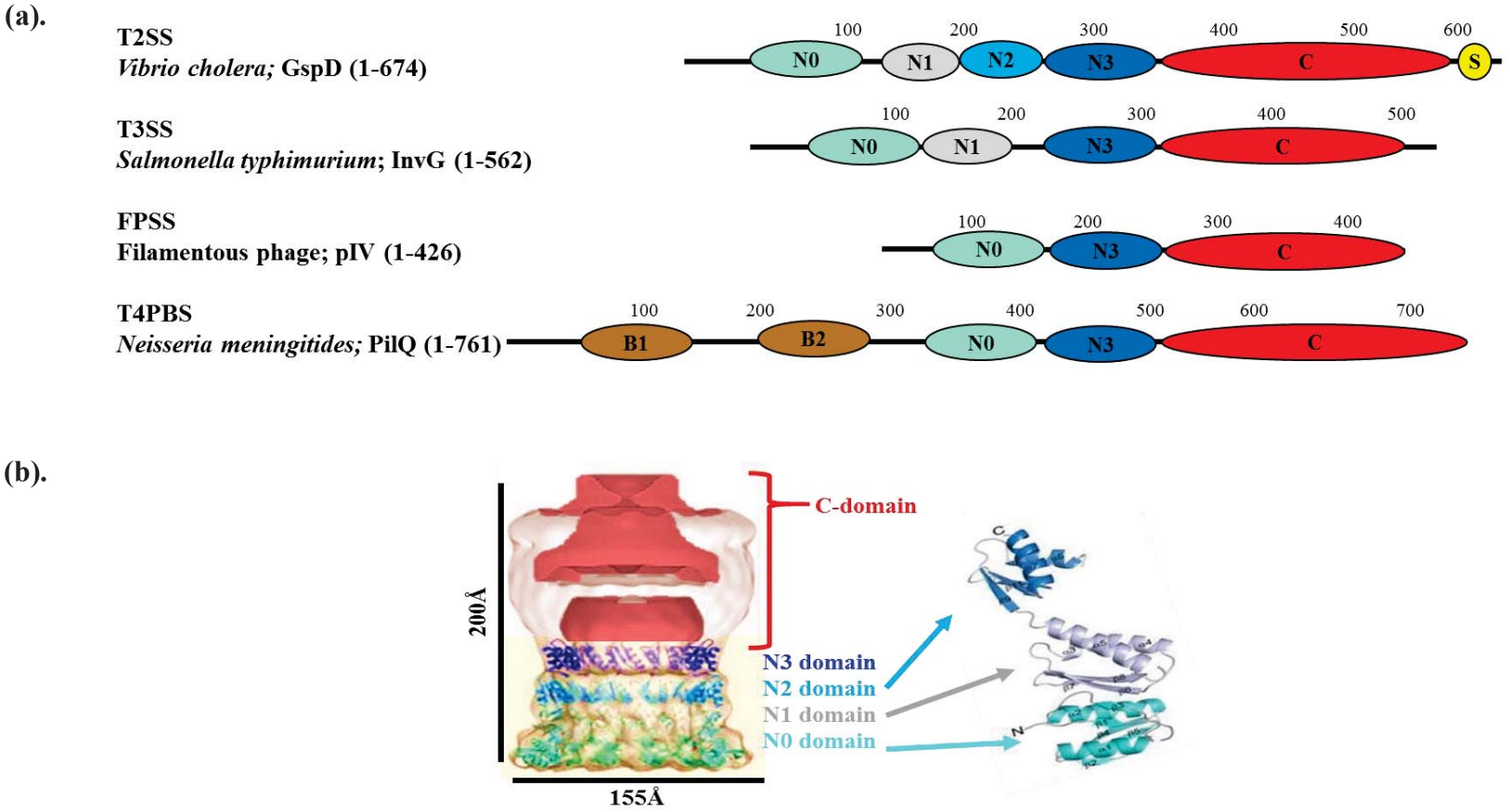

Figure 1.5 Modular organization of the secretin domains and their structures.

(a). Comparison of domain architecture among secretins of different secretion systems. Secretins of type II secretion system contain four N-terminal sub-domains N0 (cyan), N1 (grey) N2 (light blue) and N3 (dark blue) followed by the C-domain or secretin homology domain (red) and S domain (yellow). Secretins of T3SS and FPSS lack one and two N-terminal sub-domains, respectively, while T4PBS secretin PilQ contains two additional domains at the N-terminus, denoted B1 and B2 (brown) (Berry et al., 2012; Genin and Boucher, 1994; Martin

et al., 1993; Reichow et al., 2010). **(b).** Left side, crystal structures of N-terminal sub-domains (N0, N1 and N2) fitted into the structure obtained by cryo-EM and single particle analysis of GspD secretin from ETEC (Korotkov et al., 2009); right, a close-up of the N-terminal sub-domains N0 (cyan), N1 (grey) N2 (light blue), and N3 (dark blue) presented as ribbon diagrams

1.4.1 Secretins: the N-terminal domain(s)

The periplasmic N-terminal domain of secretins is thought to protrude deep into the periplasm where it interacts with the secreted proteins and periplasmic components of secretion machinery (Douet et al., 2004). In the past several years, crystal structures of N-terminal domains from four secretins have been determined; N0, N1 and N2 of two T2SS secretins, GspD from ETEC and XcpQ from *Pseudomonas aeruginosa*, as well as two T3SS secretins, EscC and InvG from EHEC and *S. typhimurium*, respectively. Crystal structures of the EscC, GspD and XcpQ N-terminal domains, despite the low sequence identity, display structural similarities in their subdomains. Subdomains N1 and N2 share KH fold that is also found in the inner-membrane-ring-forming proteins of the T3SS, while their N0 domains are related to the signalling domain of the outer membrane TonB-dependent receptor (TonB is an inner membrane protein which senses signal from outside of the bacterial cells and energises opening of the plugs in outer membrane channels such as BtuB and FhuA, in order to import the cognate substrates, cobalamin and ferrichrome, respectively). Strikingly, periplasmic N-terminal domain of EscC, secretin of the EHEC T3SS, shows two N-terminal subdomains N0 and N1 share similar fold to those observed in the N0 and N1 of GspD of ETEC. However, the angle between N0 and N1 of EscC is found to be more flexible than that in GspD (Korotkov et al., 2009; Spreter et al., 2009; Van der Meeren et al., 2013). According to the sequence similarities between N3 and N1/N2 domains, it is predicted that N3 domain adopts similar fold to that of N1 and N2 (Figure 1.5b) (Korotkov et al., 2009).

Secretin N-terminal domain has been shown to interact with the cognate periplasmic and inner membrane components of secretion systems, providing specificity. A systematic two-hybrid protein-protein interaction analysis reported that pseudopilin GspJ of *Dickeya dadantii* T2SS interacts with the N-terminal domain of GspD (Bouley et al., 2001; Douet et al., 2004). Furthermore, it was demonstrated directly that the inner membrane component of *Vibrio cholera*e T2SS, of GspC, interacts with the periplasmic domain of GspD (Korotkov et al., 2006). The ultimate proof of interaction was the crystal structure of complex formed between GspC and N0 domain of GspD N0-N1 co-crystalised fragment from ETEC (Korotkov et al., 2011). A recent surface plasmon resonance dissection of interaction between *Pseudomonas aeruginosa* GspD and GspC, however, indicates that in this system the interaction is mediated by N3

rather than N0 domain (Douzi et al., 2011). The N0 vs. N3 domain interaction with GspC could be due to differences in their GspC structures between EPEC and *P. aeruginosa* T2SS. Alternatively, it may be possible that GspC of the inner membrane complex binds both domains, and the binding has functional meaning. For example, double N0 and N3 domain interaction could stabilize the complex; or alternatively sequential binding to these two domains may be involved in function or assembly of T2SS (Korotkov et al., 2012). These observations suggest that secretins associated with different secretion systems have diversified in their periplasmic domains, which determine the specificity for the periplasmic and inner membrane portion of the T2SS complex.

1.4.2 Secretin homology (or C-terminal) domain

The secretin homology domain or C-terminal domain is highly conserved among secretins. It spans the outer membrane and represents the core domain that is necessary and in some cases sufficient to form the channel as seen by cryo-EM and single particle analysis. In the absence of high-resolution structure, it remains unclear as to the folding of the primary amino acid sequence of the secretin homology domain into the tertiary and quaternary structures. The TMBETA algorithm (Gromiha et al., 2005) based on porins and some older predictions estimated between 10 and 14 amphipathic transmembrane β strands in the C-terminal secretin homology domain (Genin and Boucher, 1994). It is likely that the, using this is overestimate, as was the case for the iron transporter FhuA which was predicted to have 32 transmembrane β-strands, while the crystal structure revealed 22 strands (Ferguson et al., 1998) or TolC, predicted to have 21 transmembrane β-strands per subunit, but the high-resolution structure of this protein, which has a large periplasmic domain, revealed only 4 (Koronakis et al., 2000).

Architecture of the secretins is very different from porins, as the membrane-spanning portion of the C-domain is only a minor segment of the overall structure. This means that the predicted transmembrane β strands in the C-terminal domain are unlikely to be arranged in the obvious strand-turn-strand β-hairpin structures that are present in porin β-barrels. Instead, the transmembrane β strands of secretins are likely separated by long “loops” or more likely elaborate extracellular and periplasmic structures that form the “cup” and “saucer” observed by cryo-EM and single particle analysis (Yen

et al., 2002). A recent cryo-EM and single particle analysis of the channel assembled from the PulD fragment comprising N3 and C-domain suggests that there are only four transmembrane segments per subunit (Tosi et al., 2014), consistent with only a small portion of the protein spanning the membrane.

Given all these considerations, modelling of secretins as β-barrels using algorithms trained on porin-family β-barrel structures is not informative (Martelli et al., 2002; Wimley, 2002). Besides the most common single-wall barrel arrangement, there are alternative solutions for membrane spanning structures found in a minor fraction of outer membrane proteins, such as in the Wza (extracellular polysaccharide export) and VirB10 (type IV secretion system), which have transmembrane α helices. There is a possibility that secretins too have transmembrane α helices (Chandran et al., 2009).

Structural studies using cryo-EM and single particle analysis of the secretin homology domain from the *P. aeruginosa* T3SS secretin PscC showed that the secretin homology domain is the core domain, necessary and sufficient for assembly of the channel and insertion into the outer membrane, and that it does not require the N3 domain, whereas the fragment forming the channel in the case of *Klebsiella oxytoca* T2SS secretin PulD was composed of N3 and C-terminal domains (Guilvout et al., 2008; Guilvout et al., 2014; Guilvout et al., 2011).

These findings strongly suggest that there is structural demarcation between secretin N and C-terminal domains, and that these moieties of the protein may fold independently. However, their functional demarcation in substrate secretion within the context of the secretin and the complete secretion system is not established yet.

1.4.3 Secretin targeting to the outer membrane

Secretins are assembled in the form of homo-multimeric channels in the outer membrane of Gram-negative bacteria. Regardless of the similarity in the overall architecture of the channels formed by secretins, their mechanism of targeting monomers to the outer membrane and assembly varies both between and within the systems. Some secretins, like pIV of FPSS, are presumably self-targeted to the outer membrane, as they do not have any accessory chaperones or outer membrane-targeting sequences. These secretins typically insert into inner, as well as outer membrane. Other secretins contain an S-domain at the C-terminus and require interaction with a cognate

periplasmic chaperone (called pilotin) for targeting and assembly in the outer-membrane (Hardie et al., 1996). MxiM/PulS/InvH are the pilotins of the MxiD/PulD/InvG secretins in *Shigella*, *Klebsiella oxytoca* and *S.* yphimurium, respectively (Chami et al., 2005; Daefler and Russel, 1998; Lario et al., 2005). Without the cognate pilotins, secretins that contain an S domain fail to insert into the outer membrane or do so very inefficiently. In the absence of PulS, PulD secretin is degraded. If expressed in a host with deletion of periplasmic protease DegP, it assembles into a multimer in the inner membrane and induces an envelope stress response, the phage shock protein response (Collins et al., 2007; Jovanovic et al., 2006). Recent crystallographic studies of the pilotin MxiM of *Shigella* revealed the high resolution structure of pilotin complex with the pilotin-binding domain of secretin MxiD. This structure shows that S domain of the secretin forms a C-terminal helix which mediates the secretin homology domain insertion into the outer membrane by displacing lipid from a pocket of the pilotin, allowing insertion into the outer membrane by interacting with membrane lipids (Lario et al., 2005). However, pilotin-binding domains are very poorly conserved among secretins, suggesting that the mechanisms of their action may be diverse. Interestingly, it was found by constructing a chimera of secretin pIV (which does not have a pilotin-binding domain) to the pilotin-binding domain of a T2SS secretin, PulD (pIV-$PulD_{65}$) or of a T3SS secretin InvG (pIV-$InvG_{43}$) that function of the pilotin binding domain and their dependence on their cognate pilotin are transferable (Daefler et al., 1997a; Daefler and Russel, 1998).

Pilotins with their type II (lipoprotein) N-terminal signal sequence are transported across the inner membrane by the SecYEG translocon followed by transfer to the inner leaflet of the outer membrane through the Lol system for outer membrane targeting of lipoproteins. It is proposed that pilotins bind to the secretin monomers in the periplasm and the complex is then co-transported to the outer membrane through the Lol system. This was supported by analysis of the PulS/PulD targeting in LolA mutants which prevented transfer to LolB. In these mutants PulS-PulD failed to be targeted to the outer membrane and instead were inserted into the inner membrane (Collin et al., 2011). Pilotins of the S-domain-containing secretins have mostly been identified as they are most commonly encoded in the same operon or gene clusters, however there are some S-domain-containing secretins that are not accompanied by any obvious

pilotin-encoding CDSs within the gene cluster. Some T2SS secretins, like EpsD of *Vibrio cholerae* and ExeD of *Aeromonas hydrophila* were originally thought to lack a pilotin, despite containing each an S-domain. However, recently EpsD cognate pilotin, AspS (encoded by an unlinked gene), has been identified in *V. cholerae* and Gram-negative bacteria that have acquired a *Vibrio*-like T2SS (Dunstan et al., 2013). Besides the S-domain and pilotin, another lipoprotein-dependent outer membrane targeting pathway was identified in secretin HxcQ of T2SS from *P. aeruginosa*. HxcQ is itself a lipoprotein and is targeted to the outer membrane through the Lol pathway.

Some secretins require accessory proteins other than pilotins for their stability and assembly. For example, in the *Vibrio* species, proteins GspA/B were thought to be important for the expression of the T2SS secretin, however they may be important for stability (Strozen et al., 2011). GspA, like pI of filamentous phage, spans the inner membrane and has domains in both cytoplasm and periplasm. Both GspA and pI have cytoplasmic ATPase domains and interact with their respective secretins, raising possibility that they might be evolutionary related. Another inner membrane protein, MxiJ of *S. flexneri* T3SS, is involved in secretin assembly (Schuch and Maurelli, 2001). Roles of T2SS and T3SS accessory proteins other than pilotins in assembly and targeting of secretins remain yet to be fully determined. For example, it was found recently that mutation in peptidoglycan-binding protein FimV of *Pseudomonas aeruginosa* is required for folding and assembly of the type IV pilus secretin PilQ (Wehbi et al., 2011).

Initial evidence of pilotin interaction with the complete secretin channel comes from the cryo-EM and single particle analysis of PulD alone and PulD-PulS complex exposed to limited proteolysis. It was found that 12 spokes emanate radially from the channel formed by PulD-PulS complex, but not PulD alone. This also proves the location of PulS in the PulD complex, as a peripherally located density at the level of the inner leaflet of the outer membrane corresponding to each PulD subunit, signifying a 1:1 stoichiometry between the secretin and the pilotin (Nouwen et al., 1999). This can be variable as the PilQ of *N. meningitidis* showed fourfold symmetry in its cryo-EM images, which lacked any spokes (Collins et al., 2004). Variability in the mode of pilotin binding to secretin and functional implications of this interaction is further illustrated by the fact that deletion of 96 amino acids at the C-terminal end of the secretin YscC, corresponding to the pilotin-binding domain, did not prevent the

cognate pilotin YscW to target the secretin to the outer membrane, resulting in channel assembly (Burghout et al., 2004a). Therefore pilotin YscW interacts with the YscC sequence different from the S-domain.

1.4.4 Structural similarities and differences within the secretin family

Low resolution structures obtained by cryo-electron microscopic studies of purified secretins and single particle analysis revealed that, depending on the family member and secretion system, secretins formed radially symmetrical homo-multimeric channels containing, depending on the secretin, 12 to 15 monomers. The T2SS secretins such as prototypical PulD and GspD of *Klebsiella oxytoca* and *Vibrio cholerae*, respectively, are 12-mers and have dodecameric radial symmetry. The T4PBS secretins are also 12-mers, however they were found to have 12-fold or 4-fold symmetry in *P. aeruginosa* and *N. meningitidis*, respectively. Secretins of T3SS come in different symmetries. For example, MxiD from *Shigella flexneri* displays 12-fold symmetry, whereas InvG from *Salmonella enterica* sv. Typhimurium displays 15 fold symmetry (Berry et al., 2012; Chami et al., 2005; Hodgkinson et al., 2009; Reichow et al., 2010; Schraidt and Marlovits, 2011). Only the secretin of the Ff filamentous phage assembly/secretion system was found to have 14-fold symmetry (Opalka et al., 2003).

Given that the conserved secretin-homology (or C-terminal) domain forms the core of the channel and dictates the assembly process, secretins of different secretion systems are expected to have common structural features despite their different functions (Guilvout et al., 2006). Secretins with different symmetries are expected to have different diameters, however the secretin channels whose structure was determined by EM and single particle analyses: pIV, YscC, GspD, PulD, MxiD, and InvG closely correspond to each other in diameter (Kowal et al., 2013; Reichow et al., 2010)(Chami et al., 2005; Hodgkinson et al., 2009; Schraidt and Marlovits, 2011). The structures of prototypical T2SS (GspD) secretins EpsD and PulD of *Vibrio cholerae* and *Klebsiela oxtoca* obtained by cryo-EM and single particle analysis (SPA) display two general regions, a saucer-like chamber at the level of outer membrane, and a cup-like chamber opening into the periplasm. The saucer and the cup correspond to a small extracellular chamber and a large periplasmic vestibule (155Å in diameter and 200Å in depth), respectively, in the cross-section of these structures. In a closed state, periplasmic

vestibule is sealed at the middle by a periplasmic structure that appears as a solid dense mass named "septum" or "plug" in cryo-EM (Reichow et al., 2010; Tosi et al., 2014) that possibly corresponds to gate of the channel that has to completely open to allow passage of substrates, which are often nearly as large as the diameter of the "cup". Analyses of other secretins using the same method revealed that they have similar structures, including the cup and saucer, but also display some architectural differences. T2SS secretins like GspD (EpsD) contain an extracellular cap with a 10Å opening which is missing from the T3SS secretin YscC. Furthermore, the GspD saucer is smaller than that of YscC. The size of the periplasmic segments and the arrangement of the septum/gates are different between different secretins, corresponding to difference in the size of their N-terminal domains and the number of N-terminal subdomains (Figure 1.6).

Different levels of the secretin barrel are often labelled as "rings" of density: N, M and C-ring, indicating the N-to-C direction of each subunit in the multimer (Opalka et al., 2003). However, it appears that in many structures the N subdomains up to N3 or even up to the secretin homology domain may be disordered and are excluded from the averaged images obtained in single particle analysis.

The T4PBS secretin PilQ shows some key structural differences from the T2SS and T3SS secretins PilQ is more compact and closed at the top and the bottom, whereas other secretins, including pIV, have open periplasmic chamber. This difference might be due to the presence of the B1 and B2 domains in PilQ, which are absent from other secretins (Horstman and Darwin, 2012). Moreover, the periplasmic septum found in other secretins which bisects the secretin chamber and effectively divides it into two, is absent from the *Neisseria* PilQ which displays a large central cavity running through the centre of the complex, and sealed at both the top and bottom (Collins et al., 2004).

Recent structural analysis of the channels formed by N3C-domain of PulD from *Klebsiella oxytoca* and C-domain of T3SS secretin PscC from *Pseudomonas aeruginosa* revealed some subtle features that were missing from previous studies. PscC has 64% sequence identity with T3SS YscC, but displays notable differences. YscC has segmented surface, rather than smooth observed in PscC; furthermore the protrusion present at the base of YscC is absent from the PscC.

This analysis also revealed details of the septum in the PulD^{N3C} cross section at ≤ 10 Å resolution. The septum presented as a grid-like structure located ~100 Å from the edge of the saucer, protruding ~30 Å from the main wall of the channel and forming a connecting ring around a spherical plug. Other new features observed in this study were layers of density within the periplasmic constriction region of PulD (Tosi et al., 2014).

Overall, although a high-resolution structure of the secretin core channel domain that would allow tracing of the protein backbone is not available as yet, it is clear that significant structural differences exist between different secretin types, and also that such structures must be dynamic to allow passage of secreted pilus fibres, filamentous bacteriophage and exoprotein substrates.

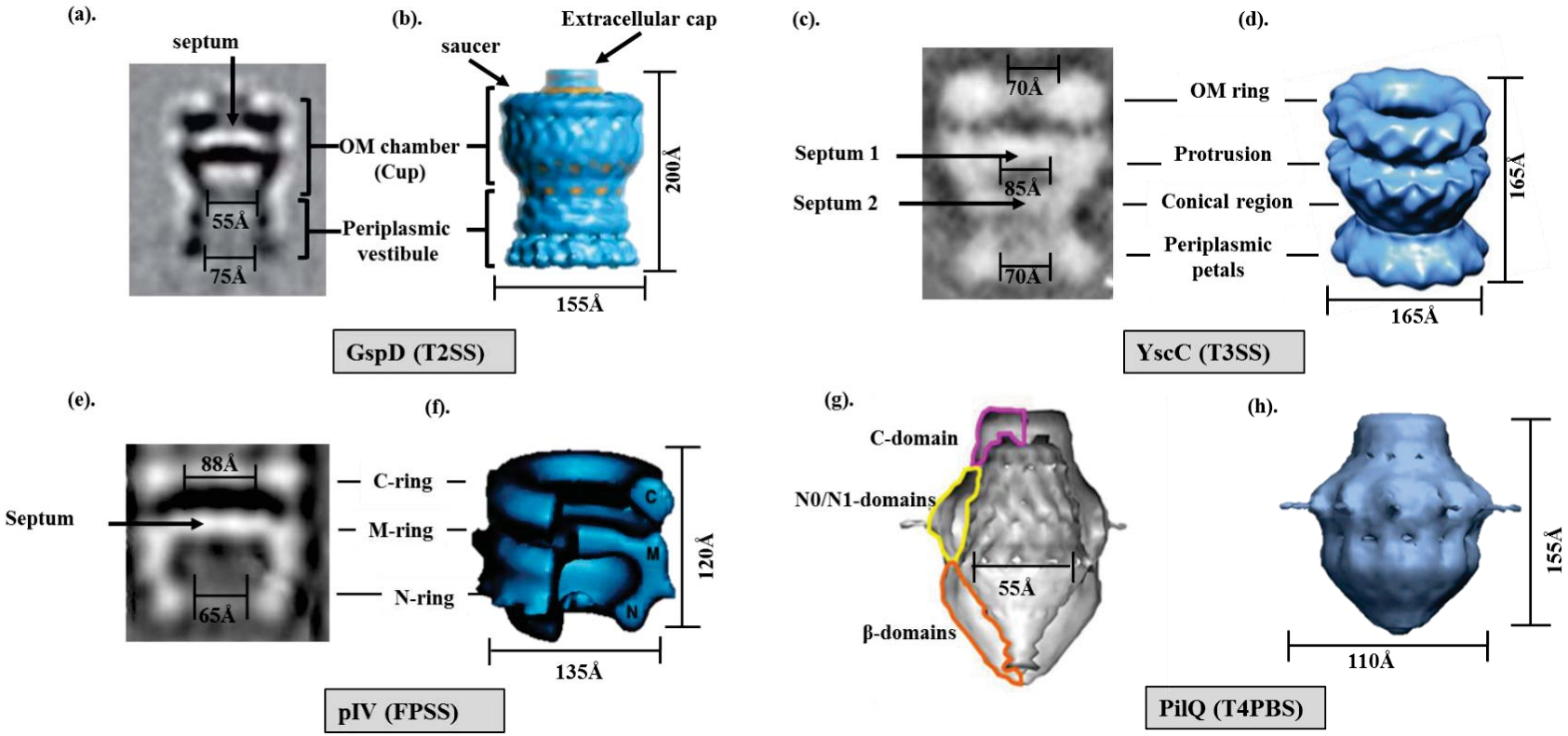

Figure 1.6 Comparison of the secretin three dimensional structures obtained by cryo-EM and single particle analyses.

(a-b). GspD (EpsD) from *Vibrio cholerae* at 19 Å resolution. The section along the length of the channel shows striated structure with strong central electron density presenting septum/plug (indicated with an arrow) that divides the channel cavity in the centre (a); GspD side view showing outer membrane lid-like chamber with saucer and periplasmic vestibule (b) (Reichow et al., 2010). **(c-d)**. YscC from *Yersinia enterocolitica* at 12 Å resolution. The section along the length of the channel reveals a conical ladder-like structure with two septums (indicated with arrows), one close to the outer membrane (analogous to the one in GspD) and other at the periplasmic end (c)

side view of YscC reveals compact outer membrane ring, protrusion, conical region and periplasmic "petals" (d); (Kowal et al., 2013). **(e-f)**. pIV from Ff filamentous phage assembly system at 22 Å resolution. The section along the pIV channel reveals three rings of electron density (e); three dimensional model of pIV showing the side view, featuring C, M and N ring. A wedge is removed to expose the structure of the septum that blocks the channel at the M-ring (f) (Opalka et al., 2003). **(g-h)**. PilQ at 19 Å resolution. Section along the secretin channel reveals central cavity which is sealed at the bottom and top. Proposed boundaries of the secretin domains are indicated (g); Side view of the PilQ channel (h) (Berry et al., 2012).

1.4.5 Gating of the secretins

Electrophysiological measurements of secretin-mediated conductance through planar lipid bilayers revealed that these channels are gated (Marciano et al., 2001). This gate presumably corresponds to a septum or plug observed in the cryo-EM structures of secretins (Figure 1.6a;c;e). The role of the gate would be to protect the bacterium from harmful substances and osmotic stress prior to secretion of a cognate substrate. In T3SS this would be at the stage of basal body assembly, prior to assembly of the needle components. In the needle complex, secretin is occupied by the needle base or rod, a rod-like appendage made of multiple copies of a single subunit. Prior to assembly of the needle, the empty T3SS (the basal body) is a hollow structure, sealed across the apical side (at the level of outer membrane) by septum which is part of the secretin channel. The basal body is also closed across the base (at the level of the inner membrane) with the basal plate. Evidence for the sealing structures across the basal body comes from densities observed by cryo-EM and single particle reconstruction (Loquet et al., 2012; Schraidt and Marlovits, 2011).

However, in the secretin of T2SS and FPSS, the gate is pivotal in maintenance of the outer membrane integrity, since there is no needle structure blocking the secretin in this system. Cryo-EM/SPA of the T2SS secretins PulD and GspD and FPSS pIV revealed septum or plug region in the centre of the channel that has similar position and morphology to the one in T3SS basal body prior to the needle assembly. However, because the structure of the secretin channel embedded in the outer membrane of Gram-negative bacteria, including the septum/plug, atomic resolution has not been determined, as discussed above, the sequence identity of the gate structure is not known. In the resting state, the secretin septum/plug presumably blocks the release of secretory proteins, i.e., when proteins are not being secreted or phages are not assembled or released. Several *in vitro* studies used membrane conductance to investigate the secretins pores in lipid bilayers. In PilQ, it was difficult to interpret the data of conductance measurements, for instance high currents were measured upon reconstitution of XcpQ secretin of *Pseudomonas aeruginosa* (Brok et al., 1999). Similarly, electrophysiological measurements of PulD and pIV showed that they are normally in tightly closed conformation as fluctuating conductance was only measured when high voltage was applied across the lipid bilayer (Marciano et al., 1999; Nouwen et al., 1999). However, when PulD and pIV are mislocalized into the inner membrane,

this induces inner membrane stress (Brissette et al., 1990; Guilvout et al., 2006), which is demonstrated as high induction of the phage shock protein (Psp) response. This phenomenon suggests that both secretins form a proton-permeable pore in the inner membrane. The pore sizes for PulD was recently estimated in an *in vitro* system in which signal sequence deletion mutants were expressed, translated and inserted into the liposomes in a single reaction in the presence of fluorescence dyes of increasing sizes. The assay that monitored leakage of fluorescent dyes from the liposome determined that the cut-off size for the *in vitro* assembled wild-type PulD was ~ 340 Da (Guilvout et al., 2014). This pore size is consistent with the inner membrane stress upon insertion of wild-type PulD, which is relieved by induction of the Psp response. Given that the cut-off size of PulD secretin is smaller than that of a porin, it has no impact on passage of molecules through the outer membrane, as the cut-off size of porins (600 Da) is much larger. However, several pIV channel mutants have been isolated that rendered *E. coli* sensitive to large antibiotic Vancomycin (Van) (MW = 1449 Da) which cannot cross the outer membrane through the porins or wild-type pIV. One of these mutants (S324G) was shown in electrophysiological experiments to require much lower voltage (energy) to open in comparison to the wild-type pIV (80 vs 200 mV), implying a defect in gate that allows opening of the channel under the voltage difference present accross the inner membrane (Marciano et al., 1999). This leaky mutant also resulted in high induction of the Psp response, and also in retarded growth of *E. coli* (increased generation time). This mutant also allowed growth of a maltoporin deficient strain (*ΔlamB*$^{-}$ on maltopentaose (MW=829 Da), which is above the porin cut-off. The uptake of maltopentaose by the leaky secretins was utilised in recent work to map the gating regions of pIV, using positive selection of randomly mutagenized gIV for mutants that conferred ability to form colonies on maltopentaose to a *ΔlamB* mutant strain (Spagnuolo et al., 2010). Mutations which increased pIV permeability were clustered mainly in two regions of C-terminal domain that were named as GATE1 and GATE2, hence these regions were proposed to have a role in channel gating or gate structure itself. TMBETA predicted transmembrane β-strands that flanked these particular gate regions. Data of this study also indicated that about half of the leaky-gate mutants hypersensitised *E. coli* to antibiotics Van and Bacitracin (Bac) (MW > 1200 Da), therefore mutations in different residues had differing effect on the gate and gating functions. General significance of this finding was that, by manipulating a secretin gate, *E. coli* and presumably other Gram-negative bacteria

containing secretins can be sensitised to > 600 Da antibiotics to which they are normally resistant, decreasing the lethal doses in some mutants by over 250 fold (Spagnuolo et al., 2010).

Not all secretins have a tightly sealed gate in the resting state. For example, the 10 Å resolution cryo-EM/SPA structure of PulD determined that the channel assembled from the N3C fragment has a mesh-like structure that contains pores 1 nm in diameter, having a similar cut-off for passage of small molecules (~ 600 Da) to that of porins (Nikaido and Rosenberg, 1983; Tosi et al., 2014). Similar pore size was identified in another T2SS secretin, OutD, but not in full-length EpsD of *V. cholerae* T2SS (Reichow et al., 2010). These observations indicate that the septa in different secretins are of different porosity or that their gates are not tightly closed *in vivo*. The existence of a pore or a grid, as reported for $PulD^{N3C}$ suggests that in some secretins a relatively small variation in local conformation in the septum might be sufficient to open the secretin channel sufficiently to allow passage of > 600 Da molecules across the outer membrane.

1.5 Envelope stress responses induced by secretins

Cell envelope of Gram-negative bacteria is a complex and dynamic in its functions, and protect the cell from external hostile environmental conditions. To perceive and respond to the internal/external threats, Gram-negative bacteria have an array of stress responses. In *E. coli* there are five major envelope stress responses, including conjugative pilus expression response (Cpx), bacterial adaptive response (Bae), RpoE (the envelope stress sigma factor), Rcs, regulation of capsular synthesis response (Koves et al., 1992) and phage shock protein response (Psp). Cpx and RpoE responses are activated with the accumulation of misfolded proteins in the periplasm, while the Psp response is activated when the inner membrane is under a stress which compromises the proton motif force. Function of Bae is not well understood; it was reported that it is induced when the cells are exposed to membrane damaging compounds such as indole or antimicrobial agents. The Rcs response is induced under the conditions that cause perturbation in the outer membrane such as osmotic shock (Boor, 2006). Out of these stress responses, Psp has been reported to be induced by mislocalization of secretins (Horstman and Darwin, 2012).

1.5.1 Phage shock protein (Psp) response

Secretin mislocalization to the inner membrane induces the phage shock protein (Psp) response, which is one of the intriguing examples of the envelope stress responses (ESRs), generated in response to the stress imposed on the inner membrane. The Psp response was first identified due to extremely high accumulation of protein named PspA in *E. coli* infected with bacteriophage f1, which after 5 hrs of phage infection becomes the third-highest expressed protein in the infected cells, after the phage-encoded major coat protein pVIII and ssDNA-binding protein pV (Brissette et al., 1990). The *pspA* gene is the 5'-terminal gene of the *pspABCDE* operon whose expression is mediated by divergently transcribed activator PspF (Brissette et al., 1991; Jovanovic et al., 1996). An additional unlinked gene, *pspG*, is co-regulated with the *pspABCDE* operon and together all *psp* genes form a regulon. Subsequent studies showed that pIV secretin alone, as well as secretins of other secretion systems that are partially mistargeted to the inner membrane also induce Psp response (Guilvout et al., 2006). Stresses other than secretins that can invoke Psp response are heat, osmotic shock, organic solvents, and blockage of protein export across the inner membrane by SecYEG saturation, high ambient pH and protonophores (Darwin, 2005; Model et al., 1997). Substantial progress has been made in understanding the mechanism of the *psp* transcriptional regulation, however its onset remains elusive. One reason of its induction associated with secretin insertion into the inner membrane, is perhaps the leakage of protons across the inner membrane to cancel the gradient introduced by electron-transport chain, resulting in disturbance of the proton motive force that is the source of energy for ATP synthesis and transport across the inner membrane (Flores-Kim and Darwin, 2012).

Besides the Psp proteins it was proposed that a two-component system comprised of proteins ArcA and ArcB is also involved in sensing the secretin stress and that they are dependent on Psp proteins (Jovanovic et al., 2006). Physiological role of the Psp response and the functions of all the proteins have not yet been fully elucidated, but the regulatory processes have been characterized to some extent in *E. coli*. Transcription factor PspF positively controls the genes of the regulon by binding at the *pspA* and *pspG* promoters, whereas PspA negatively regulates these genes by sequestration of PspF. Under the inner membrane stress conditions, membrane-bound proteins PspB and PspC are activated; as a result they become competent to bind PspA

while dissociating the PspA-PspF complex (Figure 1.7). The released PspF binds to the cognate promoters and initiates the transcriptional response which leads to the increase in PspABCDEG protein concentration, most prominently that of PspA. It was proposed that PspA is the main effector protein of the Psp response, countering the stress by maintaining the proton motive force in unknown fashion (Figure 1.7) (Gueguen et al., 2009; Kobayashi et al., 2007; Weiner et al., 1991).

Other than secretins, conditions which induce the Psp response also induce other envelope stress responses, including RpoE and Cpx, while secretin production is thought to only induce the *psp* gene expression (Seo et al., 2007). The importance of the Psp response in the secretin stress is highlighted by the fact that certain secretins, like YscC, but no other inducers, are toxic to a *psp* null strain. However, when YscC is co-produced with its pilotin YscW, which reduces the YscC mislocalization to the inner membrane, the cytoplasmic membrane permeability of the *psp* null strain is nearly eliminated (Horstman and Darwin, 2012). It is unclear why pIV secretin, that is normally mistargeted to the inner membrane, is nevertheless not lethal in a *psp* null background, despite having a similar cutoff in the closed state as YscC (~ 300 Da; (Guilvout et al., 2014; Horstman and Darwin, 2012; Weiner et al., 1991). In short, all these observations suggest that mislocalization of secretins to the inner membrane induces the Psp response. However, the factors that determine severity of the secretin stress and essentiality of the Psp response are not clear.

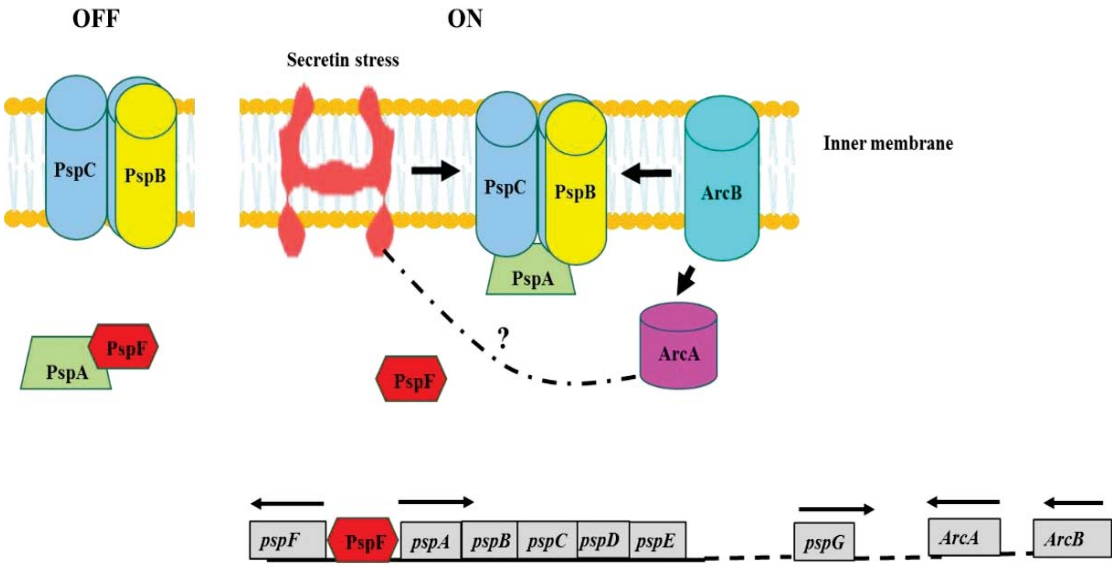

Figure 1.7 Schematic presentation of the Psp response.

In uninduced cells, PspF is sequestered by PspA in the form of inhibitory complex in the cytoplasm. Mislocalization of a secretin channel into the inner membrane, sensed by inner membrane proteins PspC/PspB, results in binding of PspA and dissociation of the PspA/F complex, releaseing PspF which then activates the transcription of the *psp* genes. It was proposed that Psp response-inducing secretin stress also activates ArcB, the sensor kinase of ArcAB system. Activated ArcB itself induces *psp* expression or activates the ArcA, which seems to be important for signal amplification (Darwin, 2013; Joly et al., 2010; Jovanovic et al., 2006).

1.5.2 The Rcs phosphorelay

The induction of Psp response by secretin mislocalization into the inner membrane is consistent with the evidence that secretins form constitutively open pores and compromise the cytoplasmic permeability barrier. Contrary to the inner membrane, outer membrane of Gram-negative bacteria tolerates the presence of secretin channels. However, insertion of severely leaky pIV mutant into the outer membrane was shown to highly induce osmotic shock response and require envelope stress response Rcs phosphorelay system for viability of expressing cultures (Spagnuolo, unpublished). This response is normally induced by variety of environmental conditions which affect the outer membrane integrity, such as osmotic shock, growth at suboptimal temperature (20 ºC), exposure to membrane-active proteins from eukaryotic host, or presence of high concentrations of zinc and glucose in the medium (Sledjeski and Gottesman, 1996). It is also induced by the overproduction of envelope proteins which affect the integrity of the outer membrane. Moreover, mutations that affect the structure of cell envelope proteins which disturb the osmolarity control and induce Rcs response. One such example are mutations in *tolQRA* (genes involved in LPS production), which destabilise outer membrane-peptidoglycan interactions and induce the Rcs response (Clavel et al., 1996).

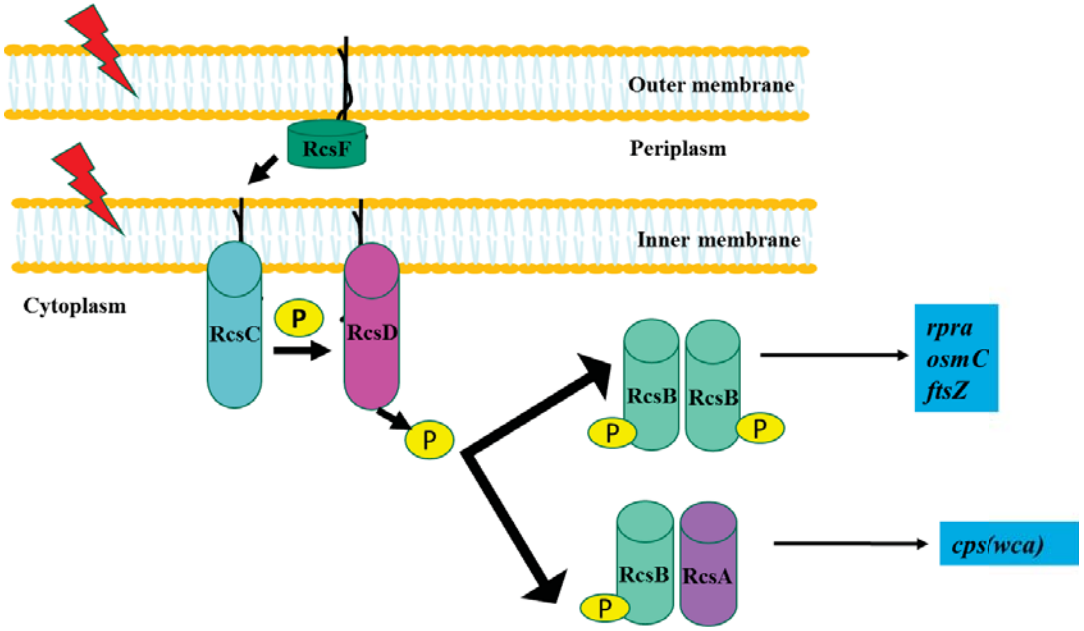

Figure 1.8 Schematic presentation of the Rcs signal transduction pathway.

Signal coming from perturbation in the outer membrane and/or periplasm is sensed by RcsF, resulting in autophosphorylation of the inner membrane protein RcsC. Phosphorylated RcsC activates RcsD by phosphorylation, followed by phosphorylation of RcsB which results in formation of RcsB homodimer, as well as RcsAB heterodimer. These dimers activate genes encoding capsular polysaccharide production and secretion proteins *cps (wca)*. In addition to capsule synthesis, RcsB in the form of homodimer activates transcription of *rprA* gene for small RNA, the cell division gene *ftsZ*, and the osmolarity inducible genes *osmB* and *osmC* (Majdalani and Gottesman, 2005).

The Rcs phosphorelay regulates the expression of the *cps* operon, which encodes the proteins of capsular polysaccharide colanic acid. In *E. coli,* the Rcs phosphorelay is composed of five proteins, including two sensor kinases, RcsC and RcsD, in the inner membrane, two response regulators, RcsB and RcsA in the cytoplasm, and the lipoprotein RcsF attached to the outer membrane from periplasmic side. After sensing the signal by RcsF, the RcsC becomes autophosphorylated. This phosphoryl group is then transferred to RcsD and finally to RcsB. Once phosphorylated, RcsB in the form of dimer binds DNA and regulates the transcription of multiple downstream genes and operons, involved in cell division and osmolarity control. Phosphorylated RcsB also forms heterodimer with another protein, RcsA. This heterodimer binds to the target DNA sequence and activates transcription of *cps* genes. RcsA is a short-lived protein and is degraded by the Lon protease (Figure 1.8) (Castanie-Cornet et al., 2006; Takeda et al., 2001).

The Rcs phosphorelay appears to be widespread in the family of Enterobacteriaceae; homologous genes to *rcsC, rcsB,rcsD, rcsA* and *rcsF* are found not only in *Escherichia*, but also in *Yersinia*, *Erwinia, Salmonella, Shigella, Klebsiella, Photorhabdus,* and *Proteus* (Flores-Kim and Darwin, 2012; Pescaretti et al., 2013; Qi et al., 2010; Szostek and Rathera, 2013). According to available genomic information it appears that the gene arrangement of *rcsC*, *rcsD* and *rcsB* within the locus is conserved. Moreover, it has been shown that Rcs phosphorelay is involved in the regulation of a variety of cellular processes like cell division, flagella biosynthesis, motility, virulence and biofilm formation. The role of the Rcs phosphorelay in the virulence of pathogenic Gram-negative bacteria was recently investigated in EHEC and *Yersinia*. It was reported that Rcs phosphorelay regulates expression of T3SS-encoding gene clusters LEE (locus for enterocyte effacement) and *Yersinia* pathogenicity island (Ysa-P1), in both positive and negative manner (Li et al., 2015; Morgan et al., 2014).

1.6 Aims of the project

Pathogenic Gram-negative bacteria such as *Klebsiella*, *Salmonella,* Enteropathogenic *Escherichia coli* (EPEC), Enterohemorrhagic *Escherichia coli* (EHEC), *Pseudomonas aeruginosa*, *Shigella* spp. or *Yersinia* spp. cause infection in humans and have been responsible for world-wide morbidity and mortality (Chiu et al., 2004; Coburn et al., 2007; Podschun and Ullmann, 1998). Antibiotics are commonly used for effective treatment of these infections. However the emergence of resistance in these microbes against existing antibiotics is alarming. Antibiotic resistance which is the consequence of mutations or acquisition of new genes by horizontal gene transfer, which alter antibiotic targets, inactivate antibiotics by chemical modification, or export antibiotics out of bacterial cells using efflux pumps. This dramatic rise of antibiotic resistance among bacterial pathogens underlies the concern that standard treatments for infectious disease will soon be largely ineffective. Resistance has evolved against nearly every clinically used antibiotic, and in the near future, this may lead us to pre-antibiotic era (World Health, 2014).

Despite a clear necessity for the development of new drugs, most large pharmaceutical companies have abandoned the field due to expensive clinical trials and low success rates which made antibiotic research unprofitable. Clearly, a renaissance in antimicrobial research is needed to combat the emergence of multidrug-resistant and untreatable resistant bacterial infections.

Gram-negative bacteria pose a particularly difficult problem because of their double membrane system (Silver, 2011). Outer membrane, which is the leaflet made of lipopolysaccharides (LPS) is not permeable to hydrophobic or hydrophilic molecules, is a real barrier for the antibiotics to reach their targets. However, small size antibiotics (< 600 Da) can pass through porins, pores (1 nm in diameter) present in the outer membrane of Gram-negative bacteria by passive diffusion. Larger antibiotics (> 600 Da), however, are ineffective against all Gram-negative bacteria that contain LPS in their OM. This means that the choice of antibiotics for the treatment of Gram-negative bacterial infections is very limited.

Moreover, development of new antibiotics for targets that have been conserved and never exploited before is also a big task. However, conserved virulence factors that are essential for colonisation and invasion of the host by pathogenic bacteria, such as the

components of their virulence factor secretion systems (T2SS or T3SS) can be the attractive targets for the development of alternative anti-bacterial drugs. One such potential target in Gram-negative bacteria are secretins, given that they are conserved and essential components of T2SS and T3SS required for colonisation and invasion of their host.

In pIV, secretin of filamentous phage, two gating regions were identified in the secretin homology domain, named GATE1 and GATE2. The GATE1/2 regions were mapped by positive selection of leaky mutants from a randomly mutagenized *gene IV* library. Findings from above study found that many of these leaky-gate mutants hypersensitised *E. coli* expressing pIV to antibiotics vancomycin and bacitracin, decreasing the lethal doses in some mutants by over 250 fold (Spagnuolo et al., 2010). Therefore, the gate of secretins could be a good target for therapeutic molecules that can hypersensitise the toxin-secreting pathogens to antibiotics. Alternatively, a new attenuated live vaccine could be developed based on attenuated bacterial strains that express a leaky non-functional secretin mutant, while retaining the desired antigenic properties of the pathogenic parent. This type of vaccine will be attenuated due to increased sensitivity of pathogens to bile salts and lack of secretion of virulence factors, yet will contain the chief immunogen, the secretion system.

Besides pIV, gate regions of T2SS secretin PulD have been determined with the same selection and screening method used for pIV by (Whitaker., 2012). However, the leaky gate mutants of PulD were not functionally characterized. Furthermore, the interactions between the N-terminal and secretin homology domains required for secretin function and the roles of GATE segments in the secretion of cognate substrate and assembly of secretins are not clear. This study focuses on investigation of GATE region roles in secretin function and sensitisation of bacteria to a range of > 600 Da antibiotics. It also looks at functional interdependence of secretin domains as well as the GATE regions and the rest of the secretin. The findings presented here will ultimately contribute to the development of molecules that could target the secretins and open these channels for the antibiotics which are > 600 Da to cross the outer membrane barrier and reach their targets, and/or block the secretion of toxins and virulence factors.

In the scenario of above discussion, current study was designed with three specific aims:

1) To functionally characterize leaky mutants of T2SS secretin PulD (Chapter 3).
2) To determine functional interdependence of secretin domains in substrate secretion, by constructing chimeras between the FPSS and T2SS secretins pIV and PulD (Chapter 4).
3) To identify the GATE regions of the T3SS secretins EscC and InvG (Chapter 5).

Chapter 2: Materials and Methods

2.1 Media

Minimal medium M63 (Miller, 1972; Neidhardt et al., 1974) was supplemented with thiamine (15 µg ml^{-1}) and biotin (2 µg ml^{-1}). Maltopentaose or maltoheptaose (Sigma-Aldrich) (0.2%) was used as a sole carbon source in the leaky mutant selection experiments, or maltose monosaccharide (0.2%) as a control carbon source minimal medium. Rich media 2xYT and SOC (Sambrook et al., 1989) were prepared using ingredients purchased from Becton Dickinson, USA. All media were supplemented with appropriate antibiotics: Chloramphenicol (Cm; 25 µg ml^{-1}), Kanamycin (Kn, 50 µg ml^{-1} in 2xYT; 25 µg ml^{-1} in M63 minimal medium), Ampicillin (Amp, 100 µg ml^{-1}) and Tetracycline (Tet, 10 µg ml^{-1}).

2.2 Bacterial Strains

All the strains used in this work were *E. coli* K12 strains except *Salmonella* Typhimurium (LT2 strain) and are listed in Table 2.1.

Strains K2359, K2360, K2361 and K2362 were obtained by removing the FRT-flanked Kn^R cassette from strains JW1935-1, JW2205-2, JW1297-1 and JW1296-5, respectively, using the FLP recombinase expressed from plasmid pCP20, which has a temperature-sensitive origin of replication (Baba et al., 2006; Cherepanov and Wackernagel, 1995). The colonies that have lost the Kn^R marker were incubated at 43ºC and the colonies that have lost the pCP20 plasmid (became Amp^S) were used for further work.

2.3 Plasmids and phage

All plasmids with their brief description are given in Table 2.2 and phages are listed in Table 2.3.

2.4 Construction of plasmids

2.4.1 Construction of phagemid pYMK01 and pIV-PulD chimeric secretins

Phagemid pYMK01 that encodes pIV was constructed by ligating fragment of pYW01(Gagic et al., 2013) containing f1 origin of replication and Cm^R into the HindIII-NcoI-cleaved vector pWW01 (derived from pPMR132 by replacing XbaI-SalI fragment with a PCR-amplified corresponding sequence of the wild-type *gIV*) (W. Wen, unpublished data). Plasmids encoding pIV-PulD chimeras were constructed by overlap-extension PCR (Ho et al., 1989). Polymerase PRIMESTAR (Takara, Japan) was used for all PCR amplifications. Briefly, two sections of the chimera N0(pIV)N3CS(PulD) were amplified using two PCR reactions with primers: i) Sk060/SK061 and ii) SK062/SK063. The template for reaction i) was pYMK01 and for reaction ii) pCHAP362. The two PCR products were purified, mixed in equimolar amounts and the chimeric product was amplified with flanking primers SK060/SK063. Amplified chimeric product was gel-purified and ligated into the linear blunt end pCR-Blunt vector followed by transformation into the chemically competent TOP10 cells. Plasmid DNA of the selected colonies was purified and sequenced using two primers, M13f and M13r (complementary to the pCR-Blunt sequences flanking the insert). A construct with the confirmed correct sequence of N0(pIV)N3CS(PulD) was further cleaved with EcoRI and HindIII restriction enzymes and the small fragment (corresponding to the chimera-coding sequence) was purified and ligated into the cleaved EcoRI-HindIII-pYMK01 to generate pYMK01$_{C1}$. Similarly, primer pairs (SK060/SK066, SK067/SK063) and (SK060/SK068, SK069/SK063) were used for amplification of different sections of N0N3(pIV)CS(PulD) and N0N3(pIV)347-429*del*CS(PulD) chimeras, respectively. Amplified PCR products were processed in the same way as described in the construction of N0(pIV)N3CS(PulD) to generate phagemids pYMK01$_{C2}$ and pYMK01$_{C3}$. Oligonucleotides with description are listed in Table 2.4.

Chimera pIV$_{(PulDGATE1)}$ was also constructed by overlap-extension PCR amplifying three sections in three PCR reactions with primer pairs: i) SK060/SK075, ii) SK076/SK070 and iii) SK079/SK080. The template for reactions i) and ii) was pYMK01 and for reaction iii) pCHAP362. The three PCR products were purified, mixed in equimolar amounts and the chimeric product was amplified using the

flanking primers SK060 and SK063. The chimeric product was ligated first into the linear pCR-Blunt vector and transformed into the chemically competent TOP10 cells. The subsequent steps were carried out in the similar fashion as described for the construction of pYMK01$_{C1}$. Likewise, for the PulD$_{(pIVGATE1)}$ construction, three sections of the chimera were amplified by setting three PCR reactions with primer pairs: i) SK086/SK084, ii) SK063/SK085 and iii) SK088/SK087. The template for reactions i) and ii) was pCHAP362 and for reaction iii) pYMK01. The three PCR products were purified, mixed in equimolar amount and the chimeric product was amplified using the flanking primers SK086 and SK063, followed by ligation into the linear blunt end pCR-Blunt vector and sub-cloned into the pCHAP362 using HindIII and ClaI restriction sites.

2.4.2 Construction of plasmids expressing type III secretins (InvG and EscC)

The *escC* gene was amplified using primers SK010 and SK011 and Enterohaemorrhagic *Escherichia coli* (EHEC 0157) genomic DNA (Supplied by N. French, Hopkirk Institute, Massey University) as a template. Amplified *escC* CDS was ligated to linear pCR-Blunt (Invitrogen). Several transformants were analysed by sequencing; the clone with the insert in the same direction as the *lac* promoter in the cloning cassette was named pCR-Blunt$_{escC}$ and used in all experiments. To amplify *escV* and *escN* genes, which are next to each other in the operon, primers SK012 and SK013 with BamHI and SalI restriction sites respectively were used to amplify both genes in one fragment, using *Enterohaemorrhagic Escherichia coli* (EHEC O157) genomic DNA as a template. Amplified PCR product was cleaved and ligated into the BamHI-SalI digested pJARA220 vector.

Two expression vectors, carrying genes encoding secretin InvG and its pilotin InvH, each under the control of T7 promoters, were obtained from the C. E. Stebbins lab (Rockefeller U., USA). Sequence analysis of the InvG plasmid received from the Rockefeller University showed a deletion near the 3´ end of the *invG* gene, which resulted in a frame-shift that eliminated 80 C-terminal residues and therefore expressed truncated InvG. To obtain the wild-type InvG protein, *invG* gene was amplified from genomic DNA of *Salmonella enterica* sv. Typhimurium (LT2 strain) using SK029 and SK030 primers containing EcoRI and BamHI restriction sites, respectively. Amplified PCR product was cleaved with EcoRI and BamHI restriction enzymes and ligated into

EcoRI-BamHI-cut pGZ119EH. Vector obtained from Rockefeller U., USA, for InvH expression had *invH* gene under the control of T7 promoter. Gene expression from this vector requires the co-expression of the T7 polymerase gene, which is normally supplied at a single copy from the chromosomally-integrated recombinant λ::T7*pol* phage (DE3). In order to introduce T7 RNA polymerase gene into an *E. coli* host, infection and lysogenizing by the DE3 (λ::T7pol) bacteriophage is required. The receptor for λ::T7pol bacteriophage is the maltoporin (LamB) in the outer membrane. As *lamB* gene is deleted in the *E. coli* K12 strain K1508 and DE3 could not be introduced into this strain, *invH* expression was placed under the *tac* promoter regulation by replacing T7 promoter of pCOLADuet-1 carrying *invH* gene with the *tac* promoter of pGZ119EH. Briefly, pGZ119EH promoter was amplified using SK018 and SK019 primers with NdeI and HpaI restriction sites, cleaved the amplified PCR product with respective restriction enzymes and ligated in to the NdeI-HpaI digested pCOLADuet-1 vector carrying *invH* gene.

To generate N-terminal GST fusion of InvG N-terminal domain, sequence encoding this portion of the CDS was PCR amplified using primers SK048 and SK049, containing BamHI and XhoI restriction sites. The PCR product was digested with BamHI and XhoI restriction enzymes and ligated into the BamHI-XhoI-cleaved expression vector pGEX-6P-2 to generate pGEX-6P-2$_{InvG(N)}$.

Table 2.1 List of strains used in this study.

Strain		Genotype	Reference
E. coli	TG1	*K-12 supE44* Δ*(hsdM-mcrB)5* (rk$^-$ mk$^-$ McrB$^-$) *thi* Δ*(lac-proAB)* F' [*traΔ36 lacI^q* Δ*(lacZ)M15 proAB*]	(Sambrook and Russell, 2001)
	TOP10	*F- mcrA* Δ*(mrr-hsdRMS-mcrBC)* ϕ80*lacZΔM15* Δ*lacX74 recA1 araD139* Δ*(ara-leu)7697 galU galK rpsL (Str^R) endA1 nupG*	Invitrogen, California, USA.
	XL1-Red	F$^-$ *endA1 gyraA96 (nalR) thi-1 relA^{1}lac glnV44 hsdR17 (rK$^-$ mK$^+$) mutS mutT mutD5 Tn10*	Stratagene
	K2204	TG1 Δ*lamB106*	(J.Spagnuolo unpublished data)
	PAP7460	MC4100 *ΔmalE444 malG501* pAPIP501 [*F´ (lac^q ΔlacZM15 proAB Tn10*] *Tc^R*	(Possot et al., 2000)
	K1508	MC4100 Δ*lamB106*	(Marciano et al., 1999)

Table 2.1 Continued

Strain		Genotype	Reference
	BW25113	F-, *Δ(araD-araB)567 ΔlacZ4787(::rrnB-3) λ- rph-1 Δ(rhaD-rhaB)568 hsdR514*	(Baba et al., 2006)
	JW2549-1	BW25113 *ΔrecO737::kan*	(Baba et al., 2006)
	K2245	JW2549-1 *ΔrecO737; F'* [*proAB lacI*^{q} *ZΔM15 Tn10* (Tet^{R})]	This study
	JW1935-1	BW25113 *ΔrcsA726::kan*	(Baba et al., 2006)
	JW2205-2	BW25113 *ΔrcsB770::kan*	(Baba et al., 2006)
	JW1297-1	BW25113 *ΔpspA740::kan*	(Baba et al., 2006)
	JW1296-5	BW25113 *ΔpspF739::kan*	(Baba et al., 2006)
	K2359	BW25113 *ΔrcsA726*	This study
	K2360	BW25113 *ΔrcsB770*	This study

Table 2.1 Continued

Strain		Genotype	Reference
	K2361	BW25113 *ΔpspA740*	This study
	K2362	BW25113 *ΔpspF739*	This study
Salmonella enterica sv. Typhimurium	LT2 strain	ATCC700720	

Table 2.2 List of plasmids

Name	Protein expressed	Expression promoter	Resistance	Origin of replication	Reference
pCHAP362	PulD	*lac*	Cm	ColD	(d'Enfert et al., 1989)
CHAP362$_{G365C}$	PulD$_{(G365C)}$	*lac*	Cm	ColD	(Whitaker., 2012)
pCHAP362$_{A369T}$	PulD$_{(A369T)}$	*lac*	Cm	ColD	(Whitaker., 2012)
pCHAP362$_{L431F}$	PulD$_{(L431F)}$	*lac*	Cm	ColD	(Whitaker., 2012)
pCHAP362$_{G458A}$	PulD$_{(G458A)}$	*lac*	Cm	ColD	(Whitaker., 2012)
pCHAP362$_{G458S}$	PulD$_{(G458S)}$	*lac*	Cm	ColD	(Whitaker., 2012)
pCHAP362$_{G466C}$	PulD$_{(G466C)}$	*lac*	Cm	ColD	(Whitaker., 2012)

Table 2.2 Continued

Name	Protein expressed	Expression promoter	Resistance	Origin of replication	Reference
pCHAP362$_{T469A}$	PulD$_{(T469A)}$	*lac*	Cm	ColD	(Whitaker., 2012)
pCHAP362$_{I475T}$	PulD$_{(I475T)}$	*lac*	Cm	ColD	(Whitaker., 2012)
pCHAP362$_{\Delta 477-481}$	PulD$_{(\Delta 477-481)}$	*lac*	Cm	ColD	(Whitaker., 2012)
pCHAP362$_{R529L}$	PulD$_{(R529L)}$	*lac*	Cm	ColD	(Whitaker., 2012)
pCHAP362$_{A534T}$	PulD$_{(A534T)}$	*lac*	Cm	ColD	(Whitaker., 2012)
pCHAP362$_{G547S}$	PulD$_{(G547S)}$	*lac*	Cm	ColD	(Whitaker., 2012)
pAH181	PulS	*ppulS*	Kn	pA15	(Daefler et al., 1997a)
pCHAP8243	Pul T2SS except PulD	*mal*	Amp	ColE1	(Francetic and Pugsley, 2005)

Table 2.2 Continued

Name	Protein expressed	Expression promoter	Resistance	Origin of replication	Reference
pGZ119EH	No protein	*tac*	Cm	ColD	(Lessl et al., 1992)
pGZ119EH$_{invG}$	InvG	*tac*	Cm	ColD	This study
pCOLADuet-1	No protein	*T7*	Kn	ColA	Novagen, Germany
pMK01$_{invH}$	InvH	*tac*	Kn	ColA	This study
pPMR132	pIV	*tac*	Cm	ColD	(Russel, 1994)
pPMR132$_{S324G}$	pIV$_{(S324G)}$	*tac*	Cm	ColD	(Russel, 1994)
pYMK01	pIV	*tac*	Cm	ColD, f1	This study
pYMK01$_{C1}$	N0(pIV)N3CS(PulD)	*tac*	Cm	ColD, f1	This study

Table 2.2 Continued

Name	Protein expressed	Expression promoter	Resistance	Origin of replication	Reference
pYMK01$_{C2}$	N0N3(pIV)CS(PulD)	*tac*	Cm	ColD, f1	This study
pYMK01$_{C3}$	N0N3(pIV)347-429*del*CS(PulD)	*tac*	Cm	ColD, f1	This study
pYMK01$_{C4}$	pIV$_{(PulDGATE1)}$	*tac*	Cm	ColD, f1	This study
pCHAP362$_{C5}$	PulD$_{(pIVGATE1)}$	*lac*	Cm	ColD	This study
pCR-Blunt	No protein	*lac*	Kn	pUC	Invitrogen, USA
pCR-Blunt$_{escC}$	EscC	*lac*	Kn	pUC	This study
pWW01	pIV	*tac*	Cm	ColD	(W. Wen, unpublished data)
pCP20	Flp	λ	Amp	Rep101^{ts}	(Cherepanov and Wackernagel, 1995)

Table 2.2 Continued

Name	Protein expressed	Expression promoter	Resistance	Origin of replication	Reference
pGEX-6P-2	Glutathione S-transferase (GST)	*lac*	Amp	ColD	(Kaelin et al., 1992)
pGEX-6P-2$_{InvG(N)}$	Fused InvG N-terminal domain with GST	*lac*	Amp	ColD	This study
pJARA220	No protein	*psp*	Cm	ColD	(J. Rakonjac unpublished data)
pJARA220$_{escVN}$	EscVN	*psp*	Cm	ColD	This study

Table 2.3 List of phages

Phage	Details	Reference
f1	Wild type	(Loeb, 1960)
R484	f1 ΔpIV	(Brissette and Russel, 1990)

Table 2.4 List of oligonucleotides

PRIMER	SEQUENCE	DETAILS
SK010	ACACACTTGTTTTCTGATATAGGAC	*escC*, forward, cloning
SK011	GAGAGCTAAATTTCCTGCTCATAAA	*escC*, reverse, cloning
M13F	GTAAAACGACGGCCAG	pCR-Blunt, forward, sequencing
M13R	CAGGAAACAGCTATGAC	pCR-Blunt, reverse, sequencing
SK012	CGC**GGATCC**TATTGAGCGCGTTCGCAGGATG	*escV*, forward, **BamHI**, cloning
SK013	ACGC**GTCGAC**CGAATAGATAAAATTCTGTCCAACAT	*escN*, reverse, **SalI,** cloning
SK014	CTTCTGCGTTCTGATTTAATCT	pJARA220, reverse, sequencing
SK015	AAGAGGACAACATTATGGGTAT	pJARA220, forward, sequencing
SK016	CGCGGATCCTTGGGAATAATATCGAACTTAAAG	*escN*, internal forward primer, sequencing
SK017	ACGCGTCGACTCATGCTCTGAAATCATTTACCG	escV, internal reverse primer, sequencing
SK029	CCG**GAATTC**ATGAAGACACATATTCTTTTGGCCA	*invG*, forward, **EcoRI**, cloning
SK030	CGCGGATCCTTGAGCCAGGAATCATTTAATTGC	*invG*, reverse, **BamHI**, cloning
SS05	TGTTGACAATTAATCATCGGCTCG	pGZ119EH, forward, sequencing
SS12	ATTCTGTTTTATCAGACC	pGZ119EH, reverse, sequencing
R1	TCACTCATTAGGCACCCCAGGCT	pCHAP362, reverse, sequencing
R2	GGCGTCCTGAAAGTGGTGCGT	*pulD*, reverse, sequencing

Table 2.4 Continued

PRIMER	SEQUENCE	DETAILS
R3	AGCGAAAAGCAGGCCGCGAA	*pulD*, reverse, sequencing
R4	AGGCCTGGCGGTACTCGTCG	*pulD*, forward, sequencing
SK018	GGGAATTC**CATATG**TATATCTCCTGTGTGAAATTGTTA	pGZ119EH, reverse, **NdeI**, cloning
SK019	AATCCTGTTTGCTGGTG**GTTAAC**	pGZ119EH, forward, **HpaI**, cloning
SK028	TAGTTATTGCTCAGCGGTGG	PCOLADuet-1, reverse, sequencing
SK048	CGC**GGATCC**CCTGGTTATTCTAGTGAAAAAATAC	$invG_{N\text{-}terminal\ domain}$, forward, **BamHI**, cloning
SK049	CCG**CTCGAG**TCATTACAGCTCAATACCATCGTTTTGCT	$invG_{N\text{-}terminal\ domain}$, reverse, **XhoI**, cloning
SK050	GGGCTGGCAAGCCACGTTTGGTGGTG	pGEX-6P-2, forward, sequencing
SK051	CCGGGAGCTGCATGTGTCAGAGG	pGEX-6P-2, forward, sequencing
SK060	GTGGTATGGCTGTGCAGGT	pYMK01, forward
SK063	CCCAA**GCTTG**GGGCGGTAACGGCGAGGCAGAA	pCHAP362, reverse, **HindIII**, cloning
SK070	AAGGGAAGAAAGCGAAAGGAG	pYMK01, reverse
SK086	GGAATTCCATATGCACAGATGAAAACGGT	*pulD*, reverse, $PulD_{(pIVGATE1)}$ cloning

Table 2.4 Continued (Overlap extension PCR primers)

PRIMER	SEQUENCE	DETAILS
SK061	GGAGGCTTTAGCGTATTTCAGGTAGATGACTTTGGTATTGCCCTG AACAAAGAAACCACCAGAAGGA	*gIV*, reverse, N0(pIV)N3CS(PulD) cloning
SK062	TCAGGAATATGATGATAATTCCGCTCCTTCTGGTGGTTTCTTTGTT CAGGGCAATACCAAAGTCATC	pulD, forward, N0(pIV)N3CS(PulD) cloning
SK066	TTCAGGCCGTCAGCGTCCTGCACTTCGGCGATAATCGCCTCGACC AGCACTGGCAAATCAACAGTTGAAAG	*gIV*, reverse, N0N3(pIV)CS(PulD) cloning
SK067	AAGATATTTTAGATAACCTTCCTCAATTCCTTTCAACTGTTGATTT GCCAGTGCTGGTCGAGGCGATTA	*pulD*, forward, N0N3(pIV)CS(PulD) cloning
SK068	AACGATGCTCGGCGTGGCGAGAATATCGTTCTTGGTGCTGCTGGA GAGGGCCTGGTCAGTTGGCAAATCAAC	*gIV*, reverse, N0N3(pIV)347-429*del*CS(PulD) cloning
SK069	AGATAACCTTCCTCAATTCCTTTCAACTGTTGATTTGCCAACTGAC CAGGCCCTCTCCAGCAGCACC	*pulD*, forward, N0N3(pIV)347-429*del*CS(PulD) cloning
SK075	TAAAGGTGGCTTCCATGTTGTCGAGGGTAACGATGCTCGGCACA GACAATATTTTTGAAT	*gIV*, reverse, $pIV_{(PulDGATE1)}$cloning
SK076	GGCGATAACATCTTCAATACCGTCGAGCGCAAAACCGTCGGCAT TTCCATGAGCGTTTTT	*gIV*, forward, $pIV_{(PulDGATE1)}$cloning

Table 2.4 Continued (Overlap extension PCR primers)

PRIMER	SEQUENCE	DETAILS
SK079	CGCATTAAAGACTAATAGCCATTCAAAAATATTGTCTGTGCCGAG CATCGTTACCCTCGA	*pulD*, forward, $pIV_{(PulDGATE1)}$cloning
SK080	TACCGCCAGCCATTGCAACAGGAAAAACGCTCATGGAAATGCCG ACGGTTTTGCGCTCGA	*pulD*, reverse, $pIV_{(PulDGATE1)}$cloning
SK084	AAATAGAACCCTTCTGACCTGAAAGCGTAAGAATACGCGGCGTG GCGAGAATATCGTTCT	*pulD*, forward, $PulD_{(pIVGATE1)}$ cloning
SK085	AAATAATCCATTTCAGACGATTGAGCGTCAAAATGTAGGTATCA AGCTAAAGGTGAAGCC	*pulD*, reverse, $PulD_{(pIVGATE1)}$ cloning
SK087	AATCGCCTTCGTTGATTTGCGGCTTCACCTTTAGCTTGATACCTAC ATTTTGACGCTCAA	*gIV*, forward, $PulD_{(pIVGATE1)}$ cloning
SK088	CGCCCTCTCCAGCAGCACCAAGAACGATATTCTCGCCACGCCGCG TATTCTTACGCTTTC	*gIV*, reverse, $PulD_{(pIVGATE1)}$ cloning

Primer sequence complementary to *gIV* has been underlined, SS05 and SS012 provided by (S. Sattar, unpublished work) and R1, R2, R3 and R4 provided by (Whitaker., 2012).

2.5 Mutagenesis

2.5.1 *In vivo* random mutagenesis of gene *escC*

To generate the mutant library of gene *escC*, plasmid pCR-Blunt carrying the *escC* gene of Enterohaemorrhagic *Escherichia coli* (EHEC 0157) was transformed into *E. coli* mutator strain XL1-Red (Stratagene, La Jolla, CA). This strain has chromosomal mutations in three of its primary DNA repair pathways, hence the mutation frequency is several orders of magnitude higher than the repair-positive strains during plasmid replication (Greener and Callahan, 1994; Greener et al., 1997). The transformed cells were recovered in 1 ml of SOC medium (Sambrook et al., 1989) for 1 h at 37°C. Transformation mixture was diluted into 2 ml of 2xYT medium containing Kn for selection of transformed cells containing the EscC-encoding plasmid. An aliquot of diluted transformation was plated onto the selective plates for enumeration and the remaining liquid culture was divided into 10 pools and incubated at 37°C overnight. Plasmid DNA was purified separately from each of the transformation pools. The resulting plasmid DNA samples corresponded to libraries of randomly mutagenized plasmids (Spagnuolo et al., 2010).

2.5.2 *In vitro* random mutagenesis of gene *escC*

In vitro error-prone amplification of gene *escC* was achieved using ϕ-29 DNA polymerase and hexameric NNNNNN primers (Templiphi kit; GE, Amersham) in the presence of 10 mM $MnCl_2$ at 30°C for 24 h. The concentration of $MnCl_2$ and other reaction conditions were experimentally adjusted, by mutagenizing pUC18 and monitoring the frequency of *lacZ*-negative colonies. The conditions used in the polymerisation (the concentration of $MnCl_2$) was adjusted to match the mutation frequency obtained by *in vivo* mutagenesis of *lacZ* (11 %) (Spagnuolo et al., 2010). After the polymerization reaction was completed, the amplified DNA of pCR-Blunt$_{escC}$ was purified using a PCR purification kit (Roche). Product of ϕ-29DNA polymerase was a large branched dendromer of many products linked together. To obtain a single-length circular plasmid, the DNA was digested with the BamHI restriction enzyme that has a single recognition site in the plasmid, purified and re-circularised by self-ligation (Fujii et al., 2004; Fujii et al., 2014). The mutagenesis reaction was carried out in ten

aliquots; each was processed separately and transformed into a separate competent cell vial of the selection host K1508.

2.5.3 Selection of leaky *escC* mutants

Mutant plasmid libraries (*in vitro* or *in vivo*) were electroporated into the selection strain K1508 (MC4100 Δ*lamB*106) and subjected to positive selection for leaky mutants. Absence of LamB, the maltooligosaccharide-specific porin, from K1508 makes the outer membrane of this strain impermeable for maltooligosaccharides such as maltoheptaose, which is too large to pass through the general porins (Marciano et al., 1999). Ten aliquots of *in vitro* and two *in vivo* mutagenized libraries were transformed separately and plated each on a separate selection plate. Briefly, transformed cells were incubated in the SOC medium containing Kn (Sambrook and Russell, 2001) for 3 h, followed by two washes in 0.9% saline to remove all nutrients. The washed cells were spread onto the selection plates that contained M63 minimal medium, supplemented with Kn (25 μg ml^{-1}), thiamine (5 μg ml^{-1}), biotin (2 μg ml^{-1}), and IPTG (50 μM). All plates also contained maltoheptaose (0.2 %) as the sole carbon source. To monitor viability of the cells and determine the selection efficiency, dilutions of the same culture were also plated on minimal M63 plates containing all supplements listed above apart from maltoheptaose; instead the carbon source was maltose monosaccharide. The dilutions were also plated on 2xYT medium, containing appropriate antibiotics and IPTG (Spagnuolo et al., 2010). Six colonies from two plates containing the *in vivo* mutant libraries and sixteen colonies from the 10 plates containing the *in vitro* libraries were colony-purified by streaking onto the M63-maltoheptaose selective plate. Plasmid DNA was prepared from individual colonies and sequenced at the Massey University Genome Service, using M13 forward and reverse primers complementary to the flanking sequences in the pCR-Blunt vector. Sequence data was analysed using sequence analysis package Vector NTI (Invitrogen).

2.6 Antibiotic sensitivity assays

Tests on solid media using E-strips (Van) were used to determine the Minimal Inhibitory Concentration (MIC) required to inhibit growth of mutant-expressing *E. coli* strains. E-test Van strips (AB Biodisk) provided an antibiotic gradient ranging from 0.2 to 256 μg. Each plate contained 100 μl of 100-fold diluted overnight culture of a

mutant on 2xYT agar plate containing Cm, Kn and 0.1 mM of IPTG. Plates containing the Van E-test strips were incubated at 37°C for 18 h. The minimal inhibitory concentration (MIC) was measured by reading the E-test strip value at the point at which the region of "halo" or "clearing" intersects with the E-test strip scale.

Dose-response growth-inhibition assays in liquid medium were used to determine the MIC of the PulD/PulS-expressing cultures for multiple antibiotics: Van, lincomycin, fusidic acid, novobiocin, rifamycin SV, Bac, daptomycin, and DeOxyCholate (DOC). Strains used in these assays were K1508 expressing PulD wild-type or mutants in combination with either PulS or the whole Pul T2SS (including PulS). These assays were carried out in 384-well plates (Corning, Sigma-Aldrich). Serial dilutions of each antibiotic were mixed with bacterial cultures to achieve the starting cell numbers of 10^5 cells/ml. Plates were incubated for 14 h at 30 °C. Growth was monitored by determining Optical Density of the wells at 630 nm wavelength (OD_{630}). Plates were read at time points 0 and 14 h; the OD values were obtained by subtracting the 0 h readings from the 14 h readings. Triplicates of each antibiotic concentration have been assessed. The Z'-test value, measuring the reliability of assay (Campbell, 2010) was calculated from four columns on each plate, two for negative control (2xYT containing Cm and Km) and two for positive control (2xYT containing Cm and Kn and Tet at concentration of 10 μg ml^{-1}).

Besides the MIC assays, efficiency of plating (EOP) at a fixed concentration of Van, Bac or DOC was used to compare the sensitivity to these molecules of the strains expressing secretins. Plating efficiencies were determined by plating serial dilutions of overnight cultures on the agar plates containing antibiotics that are selection for retaining the plasmid markers, 0.1 mM IPTG and one of the each large molecular weight antibiotics: Van (100 μg ml^{-1}), Bac (50 μg ml^{-1}) and detergent DOC; (0.4%). Cells expressing wild-type secretin pIV (of the filamentous phage assembly system) or a derived leaky mutant were used as a control in this experiment.

2.7 Protein extraction, electrophoresis and detection

Overnight cultures were used as starting material in preparing total or fractionated cell extracts. For fractionation into water-soluble, inner membrane, outer membrane and aggregate fractions, the overnight cultures were diluted 1:100 into 5 ml of 2xYT

medium supplemented with appropriate antibiotics. The gene expression was induced with 0.1 mM IPTG when OD_{600} reached 0.2 and incubated at 37 °C until the OD_{600} has reached 0.6. Cells were chilled, then harvested by centrifugation for at 4 °C and re-suspended at a density of 1.2 OD_{600} units ml^{-1} in Tris-EDTA buffer (200 mM Tris, 2 mM EDTA, pH 8.0) containing protease inhibitor cocktail (Complete, without EDTA, Roche). Resuspended cells were exposed to lysozyme treatment and two freeze-thaw cycles, to lyse the cells and release water-soluble (cytoplasmic and periplasmic) cell fraction, which was separated from the water-insoluble fraction by centrifugation for 5 min at room temperature. After removing the supernatant (soluble fraction), the pellet was subjected to further fractionation. The inner membrane was first extracted by resuspending pellet in a Tris-triton-$MgCl_2$ buffer (50 mM Tris, 1 % triton, 10 mM $MgCl_2$, pH 8.0), $MgCl_2$ precipitates the outer membrane, followed by centrifugation under the same conditions as above (Russel and Kazmierczak, 1993). The supernatant containing extracted inner membrane was collected, whereas the pellet containing the outer membrane was resuspended in the Tris-triton-EDTA buffer (50mM Tris, 1% triton, 10mM EDTA, pH 8.0) in order to chelate Mg^{+2} and thereby solubilise the outer membrane, followed by centrifugation. The supernatant containing the outer membrane fraction was collected, whereas the remaining pellet, representing insoluble protein aggregates and remnants of cell wall debris, was resuspended in 4% SDS (Russel and Kazmierczak, 1993). For analyses of the native proteins and secretin multimers, aliquots of the samples were mixed with 1/3 volumes of either native or denaturing sample buffer (4x) and analysed by agarose or SDS-PAGE electrophoresis, respectively. The 4x native sample buffer contained 125 mM TrisHCl pH 6.8, 10 % β-mercaptoethanol, 0.01 % bromophenol blue and 20 % glycerol, whereas the equivalent denaturing buffer also contained 4 % SDS) (Laemmli, 1970). Some of the sample aliquots were precipitated with equal volume of 10% TCA, followed by incubation on ice for 30 min and centrifugation at 4 °C at 17000 x g for 5 min. Pellets were washed with 100 % acetone, air-dried for 10 min and re-suspended in 4 % SDS. After denaturing sample buffer was added as described above, the mixtures for denaturing SDS-PAGE were subjected to boiling for 5 min prior to loading onto the gel. SDS-PAGE gels contained 10 % acrylamide, whereas the agarose gels contained 2 % NuSieve GTG agarose (Lonza). The Tris-glycine buffer (25 mM Tris, 192 mM glycine, pH 8.3) system was used; denaturing gel electrophoresis buffer included 0.1 % SDS. After electrophoresis, separated proteins were blotted from the agarose or

PAGE gels onto nitrocellulose membranes in the Tris-glycine buffer containing 0.1 % SDS, and proteins of interest were detected by western blotting using specific antibodies.

For urea-treated samples, cells from the same cultures used for cell fractionation were pelleted by centrifugation and then re-suspended in 25 mM Tris (pH 7.2). Urea was added at 4 M final concentration and the extract was incubated for 1h at room temperature (Guilvout et al., 2014). Samples with or without urea treatment were analysed by SDS-PAGE and immunoblotting as described above.

2.7.1 Protein extraction, electrophoresis and detection

Western blotting was performed as previously described (Sambrook and Russell, 2001). Primary antibodies were used in dilution of 1:1000 to 1:10,000, while the secondary anti-rabbit IgG, horseradish peroxidase-conjugated secondary antibody (GE Healthcare) was used at 1:20,000 for ECL detection and anti-Rabbit IgG–alkaline phosphatase-conjugated secondary antibody (Sigma) was used at 1:10,000 for detection of primary antibodies. Affinity-purified primary antibodies specific for PulD were custom-generated against 18 and 19 residues long peptides of GATE1 (CSQTTSGDNIFNTVERKT) and GATE2 (CDAASSTSSDLGATFNTRT), respectively, by ProteoGenix, France, whereas the polyclonal EscC-specific antibodies were generated against two 12 residues long peptides of EscC N-terminal domain by Abmart, China. The PulA antibodies were a gift from O. Francetic, Institut Pasteur, France. The OmpA-specific antibodies were purchased from Antibody Research, USA. The InvG-specific polyclonal antibodies were generated in rabbits against purified N-terminal domain of InvG by Abmart, China. The PspA antibodies are gifted by M. Russel, Rockefeller University, USA.

2.8 Pulullanase secretion assays

To test the functionality of leaky PulD variants in secretion of Pullulanase, *E. coli* strain PAP7460 carrying pCHAP8243 (encoding proteins of the whole Pul T2SS except PulD (Francetic and Pugsley, 2005; Tikhonova et al., 2002) complemented with PulD wild type or mutants expressed from pCHAP362 or by mutated derivatives were grown under well-aerated conditions at 30°C in mixed medium containing 2xYT and M63 minimal media (9:1) and appropriate antibiotics for plasmid maintenance. The

PulA encoded by pCHAP8243 was a non-acylated mutant that is secreted efficiently into the media (the wild-type PulA is a lipoprotein anchored in the outer membrane via covalently attached acyl group). Expression of *pul* operon (from its own promoter) was induced with 0.4 % maltose and *pulD* from the *tac* promoter with 0.1 mM IPTG. Induced cultures were incubated until OD_{600} has reached 1.0, followed by separation of cells from supernatant by centrifugation (Francetic and Pugsley, 2005). Proteins were precipitated from both the cell and supernatant fractions with TCA, separated by denaturing SDS-PAGE and analysed by western blotting as described in the protein extraction section. Besides PulA, amount of PulD was also analysed in each sample. Protein bands on western blots were scanned either in the intelligent dark box (for the HRP chemiluminescent detection) or a computer scanner (for alkaline phosphatase colorimetric detection). The scanned bands were quantified using the ImageGauge and ImageQuant software.

For enzymatic quantification of PulA, an aliquot of the supernatant from the above cultures was filtered through a 0.45 µm filter to eliminate bacteria and subjected PulA-specific enzymatic assay described by (Hope and Dean, 1974; Michaelis et al., 1985). Briefly, pullulan (Sigma) was added at 10 mg ml^{-1} final concentration to 1ml of the supernatant sample, and incubated at 30°C. Samples (100 µl) were removed at 30 min intervals, followed by centrifugation at 13000 x g for 1 min. After centrifugation, the amount of product, the maltotriose, was quantified by a chromogenic reaction. To each sample, 300 µl of dinitrosalicylic acid reagent (DNS; 3,5-dinitrosalicylic acid (1%), 2M-NaOH, sodium potassium tartrate (30%)) was added to and boiled for 10 min, followed by addition of 1.6 ml of ice-cold water for final quenching and measuring absorbance at 520 nm. Total protein concentration in the samples was determined by (Lowry et al., 1951) method. The specific pullulanase activity was expressed as nanomoles of maltotriose liberated per minute per milligram of protein.

2.9 Phage assembly and secretion assay

To investigate functionality of pIV and the engineered chimeras for phage assembly and secretion, complementation of the *gIV* deletion mutant phage R484 (Russel, 1994) was tested in the strain carrying phagemid expressing pIV-PulD chimeric secretins. Phagemids expressing wild-type pIV or no pIV were used as positive or negative controls, respectively. Overnight cultures of the assayed strains (K2245 carrying

phagemids expressing pIV-PulD chimeric secretins, pIV or no pIV) were diluted 100-fold into the 2xYT medium containing appropriate antibiotics and incubated with aeration. When diluted cultures reached density of OD_{600} 0.2, they were infected with phage R484 at a multiplicity of infection (m.o.i.) of 50 phage per cell, followed by induction of *gIV* expression with IPTG (0.1 mM). The infected cultures were incubated for 20 min without shaking. The remaining unabsorbed phage were removed by pelleting the cells (at room temperature), followed by resuspension in the fresh 2xYT medium containing Cm and IPTG. Cells resuspended in the fresh medium were incubated for 2 h at 37°C with aeration and then sedimented by centrifugation. The supernatant was collected and the remaining cells were removed by filtering through a 0.45-µm-pore filter. The assembled phagemids (phagemid particles or PPs) and phage were enumerated by titration as described (Bennett et al., 2011). Host for titration of PPs was TG1, whereas the hosts for titration of phage were the pIV complementing strain (TG1 transformed with plasmid pPMR132 expressing wild-type pIV) (Russel, 1994) or non-complementing strain (TG1 transformed with the vector pGZ119EH; not expressing pIV). The wild type phage f1 was used as a control.

2.10 Protein purification for antibody production

Overnight culture of the cells containing pGEX-6P-$2_{InvG(N)}$ was diluted 100-fold into the 2xYT medium containing 0.2% glucose and Amp (100 µg ml^{-1}). Expression of the GST fused N-terminal domain of InvG was induced when OD_{600} reached to 0.6 with 0.3 mM IPTG. After 2 h of growth under inducing conditions, the cells were harvested by centrifugation at 4000 x g for 10 min, and resuspended in PBS (pH 7.3), then lysed by mild sonication. Cellular debris remaining after sonication was sedimented by centrifugation at 9000 x g at 4°C for 20 min. Cleared lysate was directly applied to Glutathione Sepharose 4B to affinity-purify the GST-$InvG_N$ fusion according to the GST gene fusion system manual (GE Healthcare Life Sciences). Briefly, after the binding step, non-specifically bound proteins were removed by washing three times with PBS (pH 7.3). Bound GST-$InvG_N$ fusion was eluted with elution buffer (10 mM reduced glutathione in 50 mM Tris-HCl (pH 8.0). Purified protein was lyophilized and sent to Abmart, China, for production of polyclonal antibodies.

2.11 Synthetic lethality assays

To determine the synthetic lethality of secretin expression in the null mutants of Δ*rcsA*, Δ*rcsB*, Δ*pspA* and Δ*pspF* strains, efficiencies of plating (EOP) of strains induced to produce a secretin in the strains containing these stress response gene mutations. Chemically competent cells of null mutants K2359, K2360, K2361 and K2362 and the wild type strain K2241 were transformed each with plasmids expressing the assayed secretins, EscC, PulD/PulS or InvG/InvH. Overnight cultures of transformed cells were serially diluted and 25 µl of each dilution of each culture were spread on 2xYTagar with appropriate antibiotics and with/without 0.1 mM IPTG. The EOPs were calculated by dividing the number of colony forming unit (CFU) of a given mutant expressing a secretin by the number of CFU of the same mutant expressing vector only on 2xYT plates containing appropriate antibiotics and 0.1 mM IPTG. The EOP for each host/plasmid combination was determined from three cultures of three independent transformants. Alternatively, 10 µl drops per each dilution were placed on the same plate to visually compare the plating of each host/plasmid combination (Chin-Yi et al., 2003).

2.12 Statistical analysis

All the experimental data were expressed as mean ± standard deviation of three technical/biological replicates. Differences were tested by two-tailed t-test and the values $P < 0.05$ were considered statistically significant.

Chapter 3: Characterization of PulD leaky mutants

The GATE regions were previously identified in the pIV secretin of the filamentous phage assembly system, using random mutagenesis and positive selection for leaky gate phenotype (Spagnuolo et al., 2010). These regions corresponded to loops between the β-strands predicted by TMBETA, an algorithm that predicts transmembrane β strands in the outer membrane proteins (Gromiha et al., 2005); based on porin structures). Characterization of the leaky point mutants in pIV showed that 29 out of 30 point mutations causing the leaky phenotype allowed filamentous phage assembly (Spagnuolo et al., 2010). The question, however, remained whether the gating regions and their roles in assembly/secretion are conserved between the secretins of different secretion systems. To address this question, PulD, a T2SS secretin from *Klebsiella oxytoca*, was subjected to the mutagenesis and selection in order to map the gating regions (Whitaker., 2012). In this thesis, the leaky PulD mutants were analysed to determine the roles of mutated residues in the channel function and the secretion of the cognate T2SS substrate, PulA.

3.1 PulD leaky mutations correspond to those in pIV

In his MSc work Whitaker (2012; unpublished data) identified regions involved in gating of the secretin PulD using random mutagenesis and positive selection for the leaky-gate mutants that acquired ability to utilise maltopentaose as a sole carbon source, as described for secretin pIV in Spagnuolo et al. (2010). However, these mutations were not characterized. This thesis work focused on characterization of mutants, including formation of multimeric channel and secretion of the cognate substrate, enzyme pullulanase (PulA), an amylolytic glucanase that degrades pullulan, a branched polysaccharide of glucose.

Briefly, PulD leaky-gate mutants were identified after *in vivo* or *in vitro* random mutagenesis (as described in section 2.5.2 for EscC; except that mutated plasmid encoded *pulD*). The mutagenized plasmid library was transformed into a Δ*lamB* strain containing a PulS-expressing plasmid pAH181 (Table 2.2). PulS is a specific

chaperone, or pilotin, that is required for folding and targeting of PulD to the outer membrane. The leaky mutants were selected on plates containing maltopentaose as the sole carbon source (as described for pIV; Spagnuolo et al, 2010). Besides the *in vivo* and *in vitro* mutagenesis, colonies of several spontaneous mutants were isolated by plating of PulD/PulS-expressing Δ*lamB* strain on the maltopentaose selective media (without prior mutagenesis). Sequencing of *pulD* gene from spontaneous maltopentaose-permissive colonies identified three missense mutations (G458A, G466C and I475T) and one 5-residue in-frame deletion (Δ477-481) in PulD. Out of 64 maltopentaose-permissive mutants selected from the *in vivo* mutagenesis, 8 missense mutations: E334K, A359V, L431F, G458S, S467L, T469A, R529L and G547S, and one deletion (Δ513-522) were identified (Figure 3.1). Point mutation G458S was the most frequently isolated mutant, occurring in 9 maltopentaose-permissive mutants. All mutants from *in vivo* mutagenesis contained only a single mutation per gene. In contrast, most of the mutants from *in vitro* mutagenesis contained multiple missense mutations. Out of 30 sequenced *in vitro* mutants only three contained a single amino acid substitution (G365C, A369T and A534T) combined with a silent mutation, whereas others contained multiple missense mutations in the PulD coding sequence and were eliminated from further analysis (this work was done by R. Whitaker).

Mapping of mutations to the primary amino acid sequence of PulD revealed that most were clustered in two regions of the secretin homology domain corresponding to previously defined GATE1 and GATE2 regions of pIV, based on the clustering of leaky-gate mutants in that secretin (Figure 3.1; (Spagnuolo et al., 2010)). Mutations G458A/S, G466C, S467L, T469A, I475T and Δ477-481 were mapped to the GATE1 region, whereas Δ513-522, R529L and A534T were mapped to GATE2 region. These GATE regions are less conserved in the secretin family than the flanking sequences. While GATE1 was predicted to have propensity to form helix-loop-helix structure (Buchan et al., 2013; Mullan and Bleasby, 2002), GATE2 was predicted to be unstructured, as it is Ser-Gly-rich (Guilvout et al., 2014). In addition to GATE1 and GATE2 mutation clusters, a minor cluster of mutations was identified at the very N-terminus of the secretin homology domain (A359V, G365C and A369T). This is in contrast to just one mutation in this segment in pIV (Spagnuolo et al., 2010). Two additional mutations were identified downstream of GATE2, including one of a highly conserved Gly residue, which matched with the residue in pIV, whose missense

mutation was reported to cause leaky phenotype in pIV (Russel, 1994). All the work described in section 3.1 was done by R. Whitaker (2012).

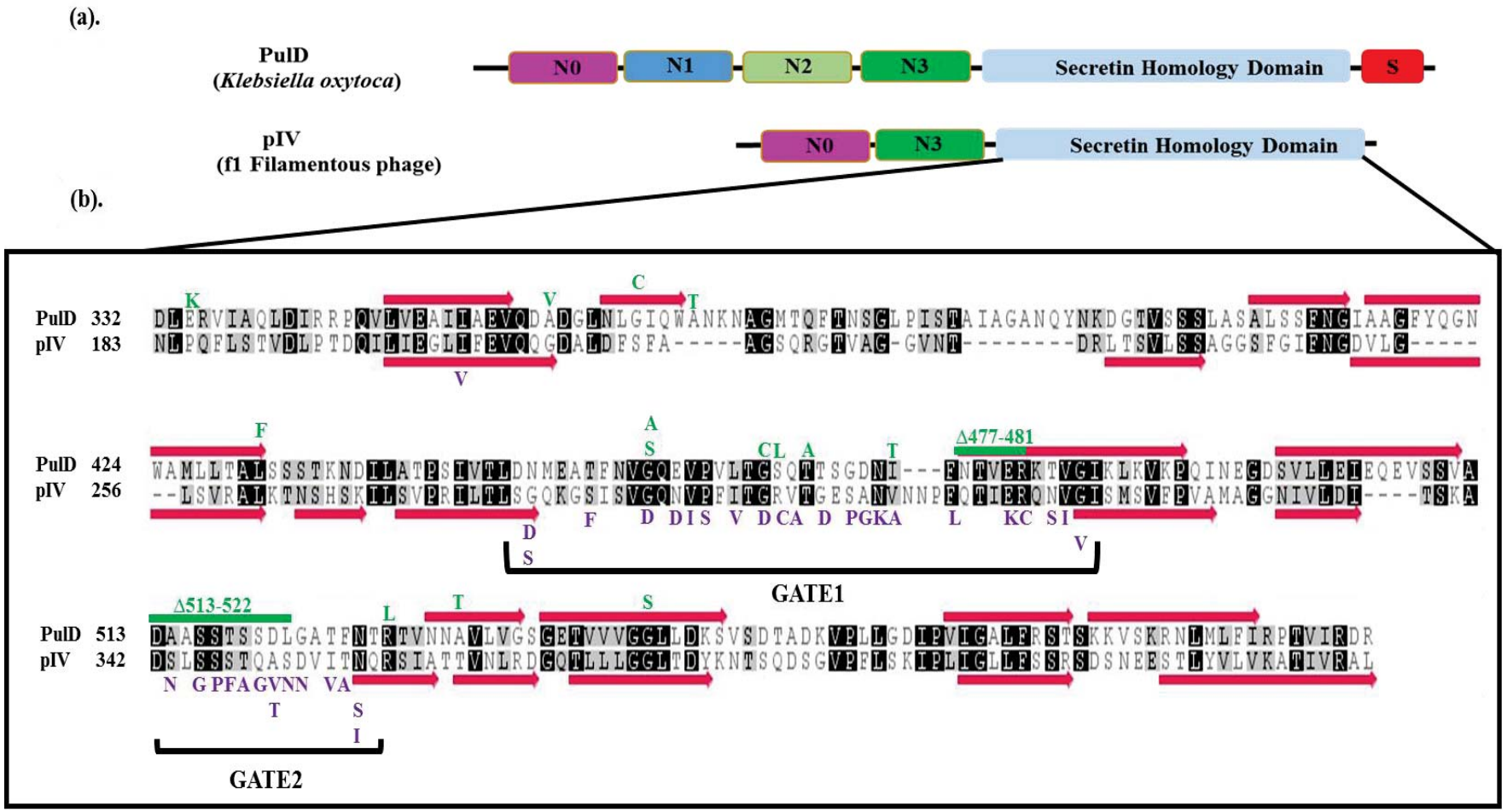

Figure 3.1 Alignment of PulD and pIV leaky mutations.

(a). Schematic presentation of PulD and pIV domain organization. Purple rectangle, N0; dark blue rectangle, N1; light green rectangle, N2; dark green rectangle, N3; light blue rectangle, secretin homology domain; red rectangle, S (pilotin binding domain) (Chami et al.,

2005; Korotkov et al., 2009). **(b).** Alignment of secretin homology domain of PulD and pIV (bottom) with predicted trans-membrane β strands (pink) using the TMBETA algorithm (Gromiha et al., 2005), and with leaky mutations of PulD (green) and pIV (purple) highlighted. GATE1 and GATE2 regions are marked with square brackets (Marciano et al., 1999, 2001; Russel et al., 1997; Spagnuolo et al., 2010; Whitaker., 2012).

3.2 Characterization of leaky mutants

Maltopentaose, whose uptake was the selection criterion for leaky mutants, has molecular weight of 828 Da, and is too large to pass through the porins or wild-type PulD (Disconzi et al., 2014). In order to determine whether larger molecules can pass through the PulD leaky mutant pores, a set of 12 mutants was further characterized for sensitivity to a larger molecule, glycopeptide antibiotic Van (Mw 1449 Da; Table 3.1). An assay using the E-test strips was carried out for the cultures that co-expressed PulD with PulS (Table 1, data column 1) or PulD with all other genes of the *pul* operon (Table 1, data column 2). The cells expressing PulD demonstrated a wide range of sensitivities to Van, when expressed in the presence of PulS, from highly sensitive (MIC = 2 μg ml^{-1}) to completely resistant (MIC > 256 μg ml^{-1}). Mutants upstream of the GATE1 (G365C, A369T and L431F) were resistant to Van. All but two mutants (G466C and A543T) in the GATE regions and the conserved Gly547 (G547S) mutant at the end of C-terminal domain showed various levels of sensitivities toward Van (Table 1). Within the GATE1 region, mutations at the extremities of the segment caused higher sensitivity (lower MIC) in comparison to those in the central portion. Cultures co-expressing PulD/PulS and those expressing PulD in combination with the rest of the Pul T2SS showed the same MIC based on the zone of inhibition (apart from G547S). However, the cultures expressing the complete T2SS showed very thin growth that corresponded to zones of complete clearance in the PulS/PulD-co-expressing cells (not shown). The cells in this zone of poor growth were not revertants, but rather the cells that have lost the *pul* operon-encoding plasmid pCHAP8243 (Amp^R), including PulS which is required for targeting and assembly of PulD leaky channels in the outer membrane. The plasmid loss was possible due to the protection of Amp^S segregants that lost pCHAP8243 by the β-lactamase that typically leaks from the periplasm of the cells that retained the plasmid before their death, and a number of cell divisions before death that is typical of the cell wall synthesis inhibitors (both ampicillin and Van). These factors allowed cross-protection of Amp^S cells by growth of Amp^R cells before their lysis. The selection for loss of pCHAP8243 was in turn due to the selective pressure of PulD leaky mutant toxicity which was manifested as very slow growth of cultures co-expressing the whole *pul* operon. The toxic effect was only observed in the cultures expressing the complete T2SS but not those co-expressing

PulS (data not shown), suggesting that the complete trans-envelope complex is required for toxicity.

To test the effect of the leaky-gate mutations on PulD function, secretion of the T2SS secretion substrate, pullulanase (PulA) was assayed. PulA is normally anchored in the outer leaflet of outer membrane after secretion, however pCHAP8234 *pulA* is a mutant that is secreted into the medium (Francetic and Pugsley, 2005) and was therefore easily separated from the non-secreted cell-associated fraction. Two different assays were used: detection of protein secreted into the culture supernatant vs. cell-associated by western blotting and densitometry, and enzymatic assay of secreted PulA in the supernatant. All PulD point mutants were found to be active in secretion of PulA, secreting between 20% and 98% of PulA (relative to the wild-type PulD expressing cells) into the supernatant (Figure 3.2, Table 1). In contrast, the five-residue deletion mutant (Δ477-481) at the C-terminal end of GATE1 did not secrete PulA. Consistent results were obtained with both the PulA protein detection and enzymatic assay. The two assays are somewhat different in that the western blot assessed the ratio of secreted vs. cell-associated PulA, whereas the enzymatic assay only determined the activity that depends on the secreted fraction of PulA (Figure 3.3; Table 1).

For the Δ477-481 mutant that did not mediate secretion of PulA above the background observed in cells not expressing PulD at all, the question was whether the protein was produced at all. To determine the amount of PulD protein produced by the leaky mutants, all PulD mutants were detected by western blotting. All but one were present at a level of 65% or higher relative to the wild-type PulD. The low-abundance mutant G547S was produced at about one-third of the wild-type PulD. Interestingly, the five-residue deletion PulD mutant, Δ477-481, which was not functional in PulA secretion, was present at a relatively high level, 65 % that of the wild-type, and caused relatively high sensitivity to Van (16 μg ml^{-1} in the E-test)

. From these findings it appears that the leaky point mutants were all active in secretion of PulA, hence all their functions in secretion have been preserved. In contrast, the five-residue deletion mutant Δ477-481 was not functional despite assembling a (leaky) channel and presence in relatively high amount in the cell.

Table 3.1 Summary of PulD mutants and their phenotypes.

		PulS+PulD	Whole *pul* operon + PulD			
Region	PulD mutant	Van MIC (μg ml^{-1}) [a]	Van MIC (μg ml^{-1}) [a]	PulA secretion (mutant vs WT PulD) [c]	PulA activity (mutant vs. WT PulD) [d]	PulD amount (relative to WT) [e]
	G365C	R	R	71%	91%±0.5	145%
	A369T	R	R	78%	94%±0.6	135%
	L431F	R	R	113%	102%±0.6	95%
GATE1	G458A	2.5±0.7	2±0.01 [b]	98%	94%±0.4	115%
	G458S	7±1.4	9±1.4 [b]	43%	49%±0.3	75%
	G466C	R	R	44%	46%±0.2	100%
	T469A	56±1.1	56±1.1 [b]	20%	37%±0.5	38%
	I475T	16±4.5	80±2.2 [b]	46%	49%±0.5	68%
	Δ477-481	16±0.01	12±5.6 [b]	0.2%	8%±0.1	65%
GATE2	R529L	1.5±0.0	7±1.4 [b]	76%	80%±0.4	113%
	A534T	R	R	44%	48%±0.5	83%
	G547S	3.5±0.7	96±4.5 [b]	49%	41%±0.3	31%
	WT	R	R	100%	100%±0.6	100%
	ΔPulD	R	R	0.02%	9%±0.04	0.01%

[a.] Minimal inhibitory concentrations of Van as measured by concentration gradient strips (μgml^{-1})are indicated. R, completely resistant at the highest concentration tested (256 μgml^{-1}); each value was obtained as a mean of the triplicate; standard error is indicated.

[b.] Refers to a zone of partial clearance.

[c.] Amount of PulA protein was quantified by densitometry of the western blots of the supernatant vs. total produced by the cell. The numbers represent % of secreted PulA in each mutant relative to the amount secreted by the wild-type PulD.

[d.] Specific activity of PulA secreted in the supernatant was measured by enzymatic assay described by (Hope and Dean, 1974). The number represent % of PulA specific activity secreted by mutants relative to wild-type PulD.

[e.] The amount of PulD expressed by a particular mutant relative to the wild-type by densitometry of western blots, detected in the cell extract samples of the same cultures analysed for PulA secretion.

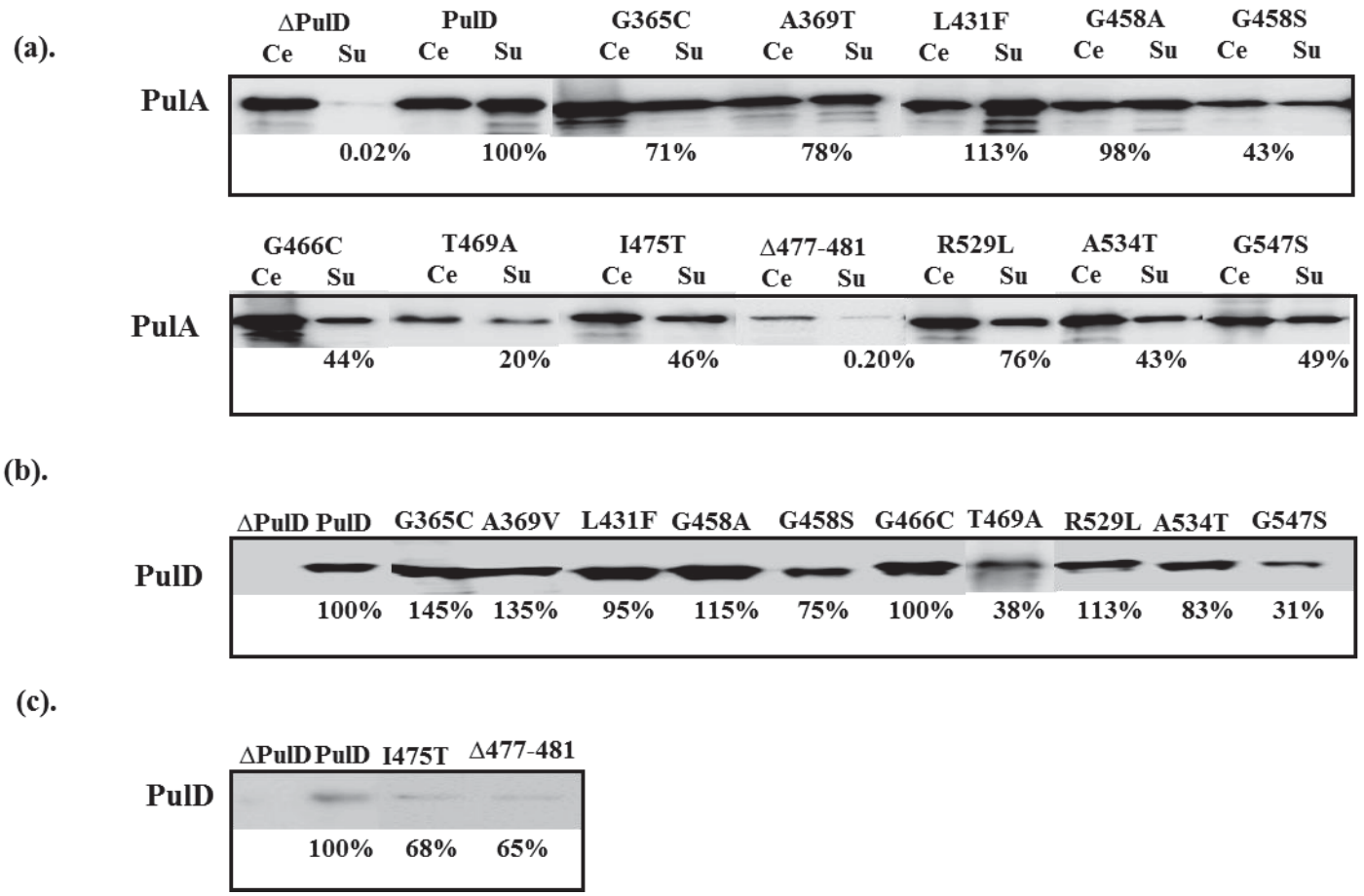

Figure 3.2 Detection of PulA and PulD by western blotting.

The amounts were determined by densitometry. **(a).** PulA detected in the TCA-precipitated proteins from the Cellular (Ce) and Supernatant (Gromiha et al.) fractions of the cultures expressing PulD wild-type (labelled PulD) or PulD mutants (position and change indicated above each lane) complemented with *pul* operon. For PulA, the amount of secreted protein (detected in the supernatant fraction) relative to the

total amount (the sum of secreted and cellular) was determined. The values shown below each lane were obtained by dividing the relative mount of secreted of PulA for each PulD mutant with the number calculated for the wild-type PulD-expressing cells. **(b);(c),** PulD in the cellular fraction of the same samples analysed in (a). Antibodies used for detection were raised against the GATE1 C-terminal peptide (CSQTTSGDNIFNTVERKT); (b)) and a peptide corresponding to GATE2 (CDAASSTSSDLGATFNTRT); (c)). The mutants analysed in (c) were not recognised by the anti-GATE1 antibody due to the missing epitope. The numbers below the lanes represent the amount of each PulD mutant relative to the amount of the wild-type PulD lane obtained using the same antibody (note that the intensity of bands for the wild-type PulD were different in (b) and (c).

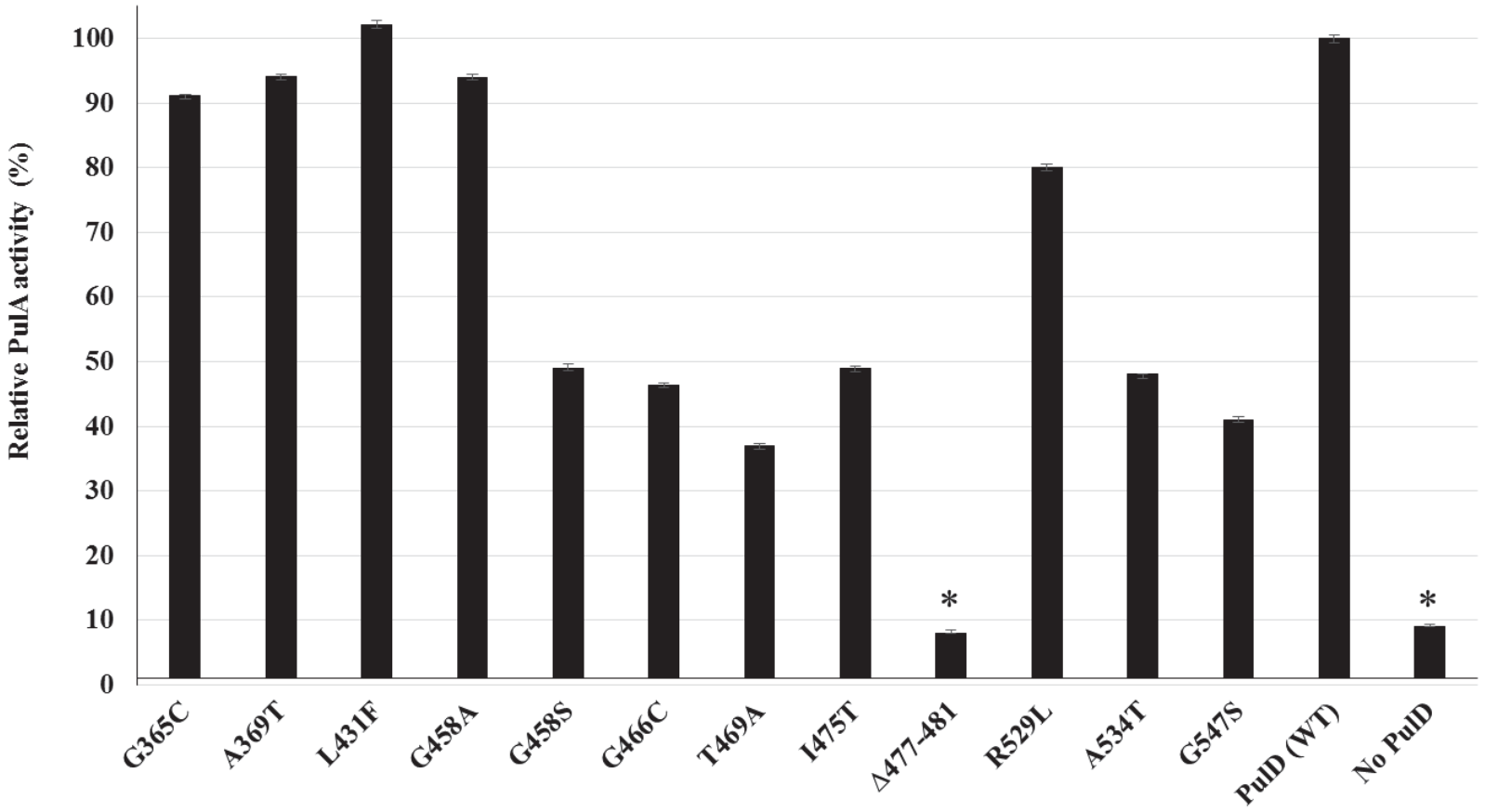

Figure 3.3 Secreted pullulanase (PulA) enzymatic activity.

Enzymatic assays of aliquots from the culture supernatants (the same cultures that have been analysed by western blotting, showed in Figure 3.2). The specific activity of PulA was determined from initial rate of reaction (amount of product maltotriose in µmol, liberated

from the pullulan per min) per mg of protein in the culture (Hope and Dean, 1974). Activity of cells expressing each PulD mutant was calculated relative to that of the activity secreted from cells expressing the wild-type PulD. All cultures co-expressed the *pul* operon (apart from *pulD*) from a separate plasmid, pCHAP8243. * =P-value > 0.05 (two-tailed t-test). Error bars indicate the standard deviation from three technical replicates.

3.3 Sensitization of GATE1 leaky mutants G458S and Δ477-481 to antibacterials

Two mutants near the borders of GATE1 region, and the most frequently isolated mutant G458S and an in-frame deletion mutant (Δ477-481). Both mutants showed high sensitivity to Van and therefore were likely to have relatively large pores, were further analysed to estimate the pore size using dose-response assay against seven antibiotics ranging in size from 461 to 1621 Da and detergent sodium DeOxyCholate (DOC) whose average micelle size is 2000 Da (Figure 3.). The cells co-expressed PulS pilotin to allow folding, targeting and multimerization of PulD. The dose-response growth inhibition curves were compared between the cells expressing two leaky mutants and the wild-type PulD (Figure 3.4). No difference in the inhibition between the cells expressing the leaky mutant and the wild-type was detected for lyncomycin (MW = 461 Da). This is expected, as lyncomycin is sufficiently small to pass through both the general porins (Pages et al., 2008) and wild-type PulD pore (Disconzi et al., 2014), both about 1 nm in diameter, with a cut-off about 600 Da, hence its entry into the cell is not obstructed. However, some difference in the MIC50 (inhibitory concentration required for 50% growth inhibition) between the leaky mutants and the wild-type was detected for fusidic acid (539 Da) and novobiocin (635 Da) which are at the borderline molecular weight with respect to the cut-off for general porins and wild-type PulD (~ 600 Da). More pronounced differences were noted for the larger molecules: rifamycin SV (720 Da), Bac (1423 Da), Van (1449 Da) and daptomycin (1621 Da). Cells expressing wild-type PulD were completely resistant to low concentrations of DOC (415 Da), however the leaky mutants become sensitive once the critical micellar concentration range was reached, indicating that the micelles, which can pass through the leaky mutant channels, but not the wild-type PulD, are the toxic form of DOC.

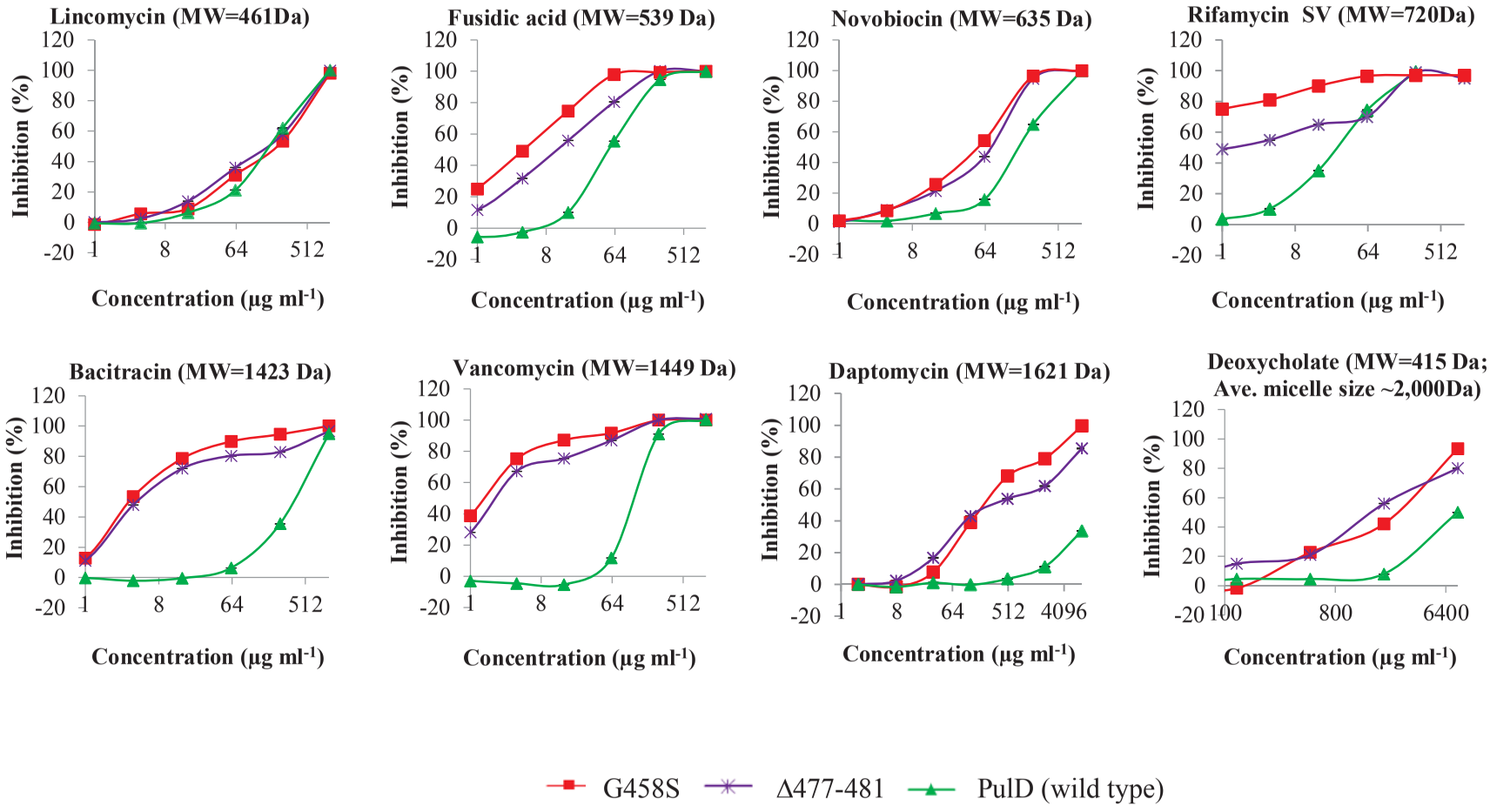

Figure 3.4 GATE1 mutants sensitise *E. coli* to high molecular weight antibiotics and detergent deoxycholate (DOC).

Dose-response growth assay in liquid PulD/PulS-co-expressing culture, starting with 10^5 cells per well. The Critical Micelle Concentration (CMC) of DOC is 830 to 2490 μg ml^{-1} and the average micelle size is 2,000 Da. Error bars indicate the standard deviation from three technical replicates.

3.4 Outer membrane targeting and multimerization of leaky GATE1 mutants G458S and Δ477-481

The observations of size-dependent growth inhibition by large antibacterials could be explained by the enlarged opening of the pores in the PulD septum of properly targeted multimers; however, Δ477-481, which is not functional in secretion of the substrate, could also cause the leaky phenotype by disturbing bacterial envelope by a mechanism independent of channel assembly. To examine targeting of PulD, cell fractionation experiments were first undertaken for the cells used in the growth inhibition experiments, to determine whether PulD mutants were targeted to outer membrane. Proteins were precipitated using trichloroacetic acid (TCA) which breaks apart the otherwise SDS-resistant PulD multimers, hence only monomers are observed in the SDS-PAGE (Figure 3.5a, top panel). Both leaky mutants, like the wild-type PulD, were targeted to the outer membrane. However, an increased fraction of mutant protein Δ477-481 was found in the inner membrane, consistent with somewhat increased amount of the phage shock protein A (PspA) identified in the cells expressing this mutant in comparison to the wild-type PulD (Figure 3.5a, middle panel). Induction of PspA has been reported when the fraction of PulD or other secretins are inserted into the inner membrane (Daefler et al., 1997a). The G458S mutant was more strongly detectable in the soluble fraction (corresponding to the combined periplasm and cytoplasm) in comparison to the wild-type and Δ477-481. Therefore, this mutant may exhibit delayed folding and insertion into the membranes.

To test multimerization of G458S and Δ477-481 mutants, inner and outer membrane fractions (native triton X-100 extracts) were analysed by native agarose gel electrophoresis, using Tris-glycine buffer without SDS (Spagnuolo et al., 2010) and western blotting (Figure 3.5b). Bands that correspond in size to the wild-type PulD multimer and the two mutants were detected in the outer membrane, showing that both mutants form multimeric channels. Interestingly, whereas PulD wild-type and Δ477-481 mutant migrated as a smear of multiple bands, the G458S migrated as a single band on the native gel (Figure 3.5b).

The wild-type PulD multimer was reported to be partially resistant to SDS and urea (Guilvout et al., 2011), hence equal resistance of the leaky mutants would argue that there is no defect in multimer formation in the leaky mutants (Guilvout et al., 2014).

To compare the stability of the leaky mutant multimers, their resistance to urea was examined (Figure 3.6). Wild-type PulD and Δ477-481 mutant contained each a multimer band after SDS-PAGE electrophoresis in samples with and without urea (Figure 3.6a), while no urea-resistant multimer bands were detected for the G458S mutant, indicating decreased stability (Figure 3.6b). Given that G458S mutant is functional in secreting PulA, the somewhat lower stability of the multimer apparently does not have functional implications. In conclusion, despite forming a multimer of similar stability to wild-type PulD, the leaky deletion mutant Δ477-481 multimer were not functional in PulA secretion. Therefore, the missing residues are important for substrate secretion, but not in assembly of a stable multimer.

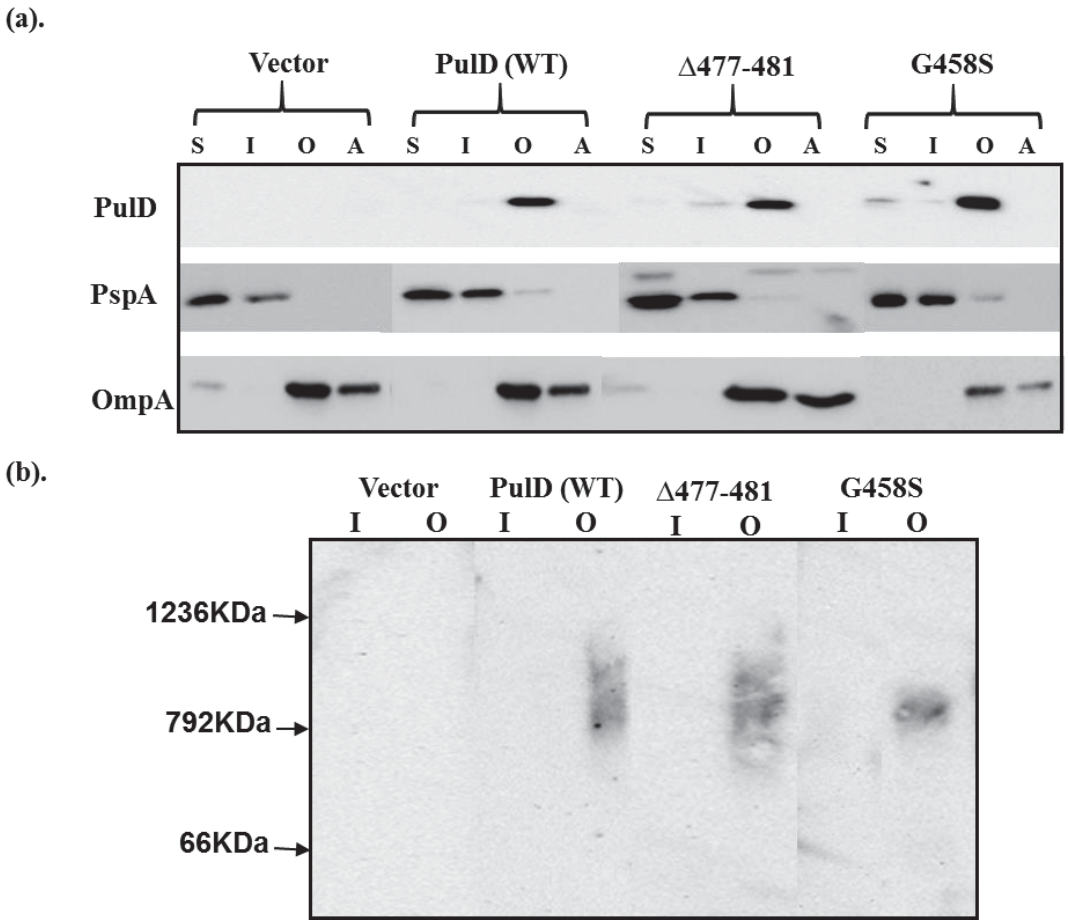

Figure 3.5 Outer membrane targeting and multimerization of PulD mutants.

(a). Subcellular fractions of the cultures expressing PulD GATE1 mutants (Δ477-481 and G458S), wild-type PulD and no PulD (vector) were subjected to a TCA precipitation to dissociate the PulD multimers and separated by SDS-PAGE. Proteins of interest were detected by western blotting. OmpA (outer membrane porin) and PspA (peripheral inner membrane / cytoplasmic protein) were used to monitor fractionation. S, soluble fraction (periplasm and cytoplasm); I, inner membrane fraction; O, outer membrane fraction, A, insoluble aggregates. **(b).** Native agarose gel electrophoresis of the inner (I) and outer (O) membrane fractions of cells producing no PulD (vector), wild-type PulD, PulD GATE1 mutants (Δ477-481 and G458S). The fractions were obtained from the same cultures used in (a). PulD was detected by western blotting.

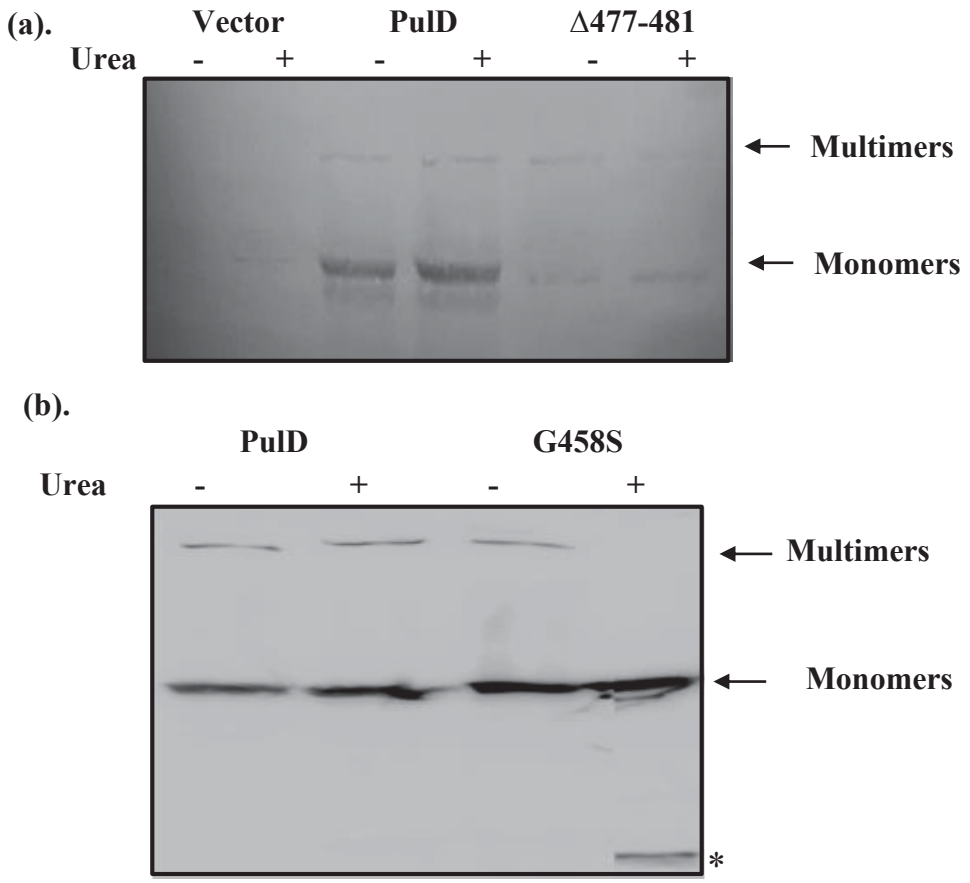

Figure 3.6 Characterization of the multimers formed by the PulD GATE1 leaky mutants Δ477-481 and G458S.

SDS-PAGE and immunoblot analysis of the PulD wild-type and mutant multimer urea resistance. Total cell lysates of the cells expressing PulD wild-type and mutants (Δ477-481 and G458S) *in trans* with PulS were re-suspended in 25 mM Tris (pH 7.2) containing 4M urea and incubated at room temperature for 1 h (as described in section 2.7) and subjected to SDS-PAGE followed by blotting and visualisation using PulD-specific antibodies. Asterisk * indicates PulD degradation product. Antibodies specific to GATE2 and GATE1 were used in A and B, respectively.

3.5 Conclusions

In this chapter, twelve PulD leaky mutants were characterized to examine the effect of mutations on this secretin's properties. All mutants produced PulD and all apart from one secreted the substrate, PulA. The PulD leaky mutations at the N-terminal portion of the secretin homology domain and the central portion of GATE1 allowed passage of maltopentaose (828 Da), but not Van (1449 Da). These mutations probably resulted in increased diameter of the PulD pore present in the resting or "closed-gate" channel in the absence of the secretion substrate (Tosi et al., 2014). Mutants located at the borders of GATE1, including G458S and Δ477-481, sensitised bacteria to Van. These two mutations allow entry of even larger molecules, including daptomycin (1621 Da) and deoxycholate micelle (2000 Da), suggesting that the affected residues are central to keeping the integrity of PulD gate or septum.

The toxicity of leaky mutants that depends on the presence of complete assembled T2SS indicates that the PulD gate or septum region of the wild-type channel likely provides additional protection to the cells from environmental stress.

In summary, severely leaky mutants can result in sensitivity to a battery of large antibiotics to which the Gram-negative bacteria are normally resistant, and are toxic to the host cell. The secretins could therefore be good targets for development of molecules that open the gate permanently, sensitising cells expressing the secretins to previously ineffective antibiotics, and/or killing the cells containing the secretion system. Moreover, given that a five-residue in-frame deletion mutation in GATE1 (Δ477-481) results in non-functional PulD channel, the gate-targeting molecules could also have an inhibitory effect on secretion of the substrates which are generally toxins or virulence factors that contribute to pathogenicity.

Chapter 4:

Probing the functional compartmentalisation and domain-domain interactions of secretins pIV and PulD

In this chapter engineered chimeras between secretins pIV and PulD were used to probe functional compartmentalisation among the secretin domains and the segments involved in gating. Construction of chimeras is expected to provide information on independent folding and/or cooperative function of domains within secretins, through analysis of multimerisation and functionality in secretion of cognate substrates, pullulanase and f1 phage. A past study that analysed pIV and PulD chimeras resulted in non-functional proteins (Daefler et al., 1997b) apart from pIV that contained the pilotin-binding S-domain of PulD at the very C terminus, without disturbing the rest of pIV. The chimeric secretins in Daefler et al. (1997) work were designed before the structural information about the N-terminal sub-domains and data on the gating and assembly was available. Upon re-examination it was evident that in Daefler et al. (1997) the borders of swapped sequences mostly fell within the domains, resulting in chimeric domain sequences that were unlikely to fold due to disrupted secondary structure elements and lack of interactions between chimeric counterparts required for domain folding. It was therefore not surprising that these pIV-PulD chimeras did not fold into functional proteins. With the new information on domain structure of secretins, as well as the gating regions that were hypothesised to correspond to loops or minidomains in the periplasm, interacting with each other, but not with the rest of the sequence, precise domain swaps between the two proteins became possible. The chimeras were designed with the aim to investigate the interdependence of these domains or sequences from each other in the assembly and function of pIV and PulD.

4.1 Approach to identify the exchangeable domains

Secretins PulD and pIV have overall 54% amino acid identity (Figure 4.1); however they are much more divergent in the N-terminal moiety and more conserved in the secretin homology domain. Differences between the two proteins include different number of N-terminal subdomains (two in pIV and four in PulD) and different number of subunits per channel (14 in pIV and 12 fold in PulD). However, the gating regions in these proteins are functionally conserved, and the framework of the C-terminal secretin homology domain has high conservation (Figure. 4.1), hence it was expectable that domain swap chimeras would fold and multimerise. The functionality of the chimeras, however, was uncertain and it would depend on whether longitudinal cooperation between the N-terminal secretin-specificity domains and the C-terminal secretin homology domain is critical for opening of the channel, given that the C-terminal domain was not found to be involved in the interactions with the substrate or other components of the T2SS. Chimeras between highly conserved secretins of the same secretion system (T2SS OutD homologues from *Erwinia chrysanthemi* and *Erwinia carotovora*) were found to be functional (Bouley et al 2001). Chimeras of more distant secretin homologues, pIV proteins of phage f1 and Ike, were not functional, but the strong selection pressure for plaque formation allowed the chimeras to "evolve" by acquiring spontaneous compensatory mutations and becoming functional in f1 phage assembly (Daefler et al., 1997b).

In this thesis , two types of chimeras were constructed using overlap-extension PCR. First type was constructed to interrogate the ability of the periplasmic N-terminal specificity domains of one secretin to function in conjunction with the membrane-spanning C domain (secretin homology domain including the pilotin domain if applicable) of other secretin. Three such pIV-PulD domain-swapped chimeras were constructed (Figure 4.2). The first chimera, named N0(pIV)N3CS(PulD), combined the pIV N0 domain with the fragment of PulD comprising complete N3, C and S domains. Second and third chimera, N0N3(pIV)CS(PulD) and N0N3(pIV)347-429*del*CS(PulD), combined N0 and N3 subdomains of pIV with the C (secretin homology) and S domains of PulD. The difference between the two chimeras was in that the N-terminal 83 residues of the C domain (secretin homology domain) were deleted in the third chimera in order to determine the role of this sequence in folding and multimerisation (Gokhale and Khosla, 2000; Robinson and Sauer, 1998). In order to swap domains between pIV and PulD with minimal possible interference, the design

was based on the findings from high-resolution structural studies of N-terminal domains that determined the boundaries of N-terminal sub-domains in T2SS secretins (Korotkov et al., 2009). All chimeras were confirmed by sequencing. It was noted that the N0(pIV)N3CS(PulD) chimera, for which obtaining the recombinant plasmid was difficult, always had an L409→I missense mutation. Given the conservative nature of this mutation, this construct was included in further analyses.

The second type of chimeras were constructed in order to investigate whether the homologous GATE regions; identified earlier in both pIV and PulD at their primary sequence level in their C-terminal trans-membrane domains (Spagnuolo et al., 2010; Whitaker., 2012) are functionally autonomous. Two chimeras were constructed: $pIV_{(PulDGATE1)}$, corresponding to pIV whose GATE1 was replaced with the one from PulD and the reverse chimera $PulD_{(pIVGATE1)}$, corresponding to PulD whose GATE1 region was replaced by the one from pIV (Figure 4.2). The swapped sequences were designed based on the sequence homology and the positions of predicted trans-membrane β strands by TMBETA. Schematic representations of the GATE regions of both pIV and PulD and GATE1 swap chimeras with residue numbers are given in Figure 4.3.

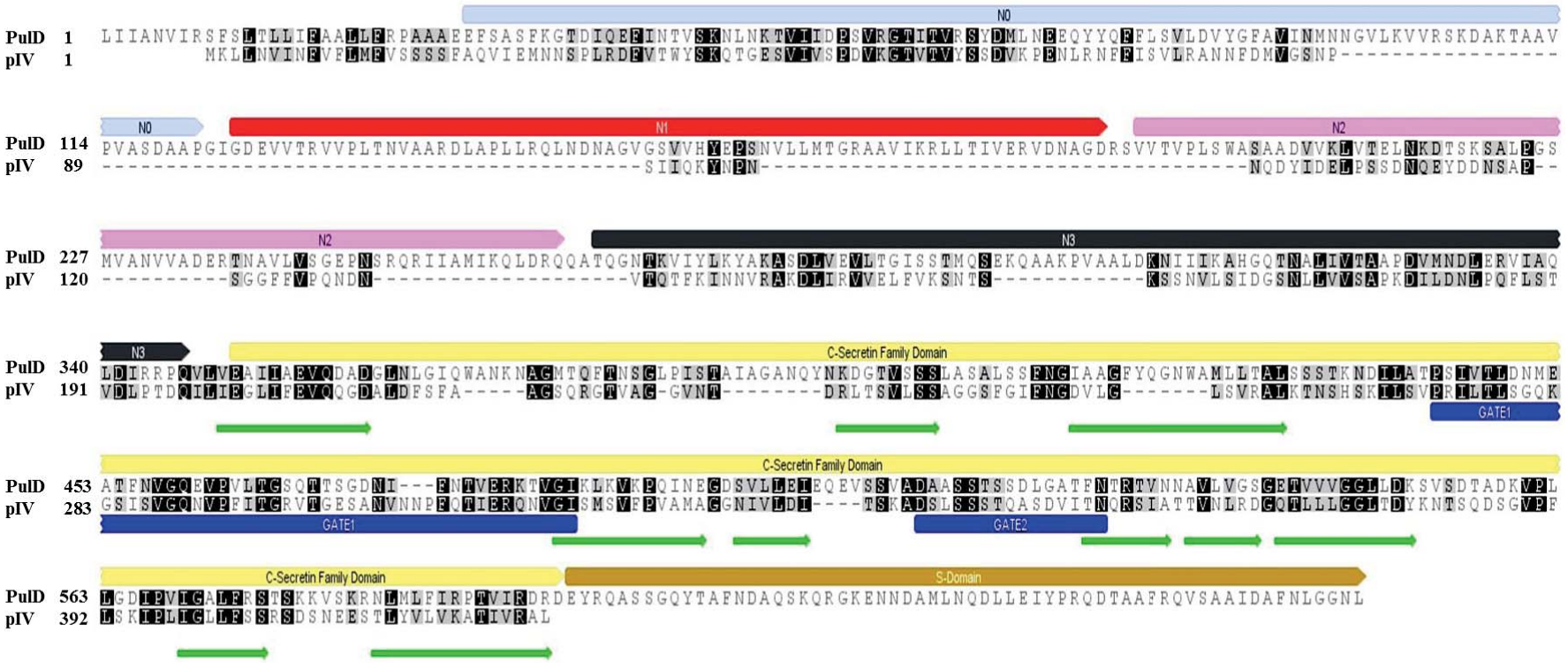

Figure 4.1 Alignment of pIV and PulD.

Protein sequences of PulD and pIV (bottom) were aligned using ClustalW with Blosum 62 matrix, highlighting the domains N0 (light blue), N1 (red), N2 (pink), N3 (black), secretin homology domain (yellow) and S domain. GATE1 and GATE2 regions are highlighted with dark blue rectangles. Green arrow, trans-membrane β-strands predicted in the C-terminal secretin homology domain using TMBETA algorithm (Gromiha et al., 2005). Numbers correspond to the residue numbers of the source secretins (Korotkov et al., 2009). Please note that the numbering is for pre-proteins. Coordinates will be different for pIV here than in most of publications, where the numbering was set based on the mature protein. The numbering was adjusted with the PulD literature that uses the pre-protein numbering.

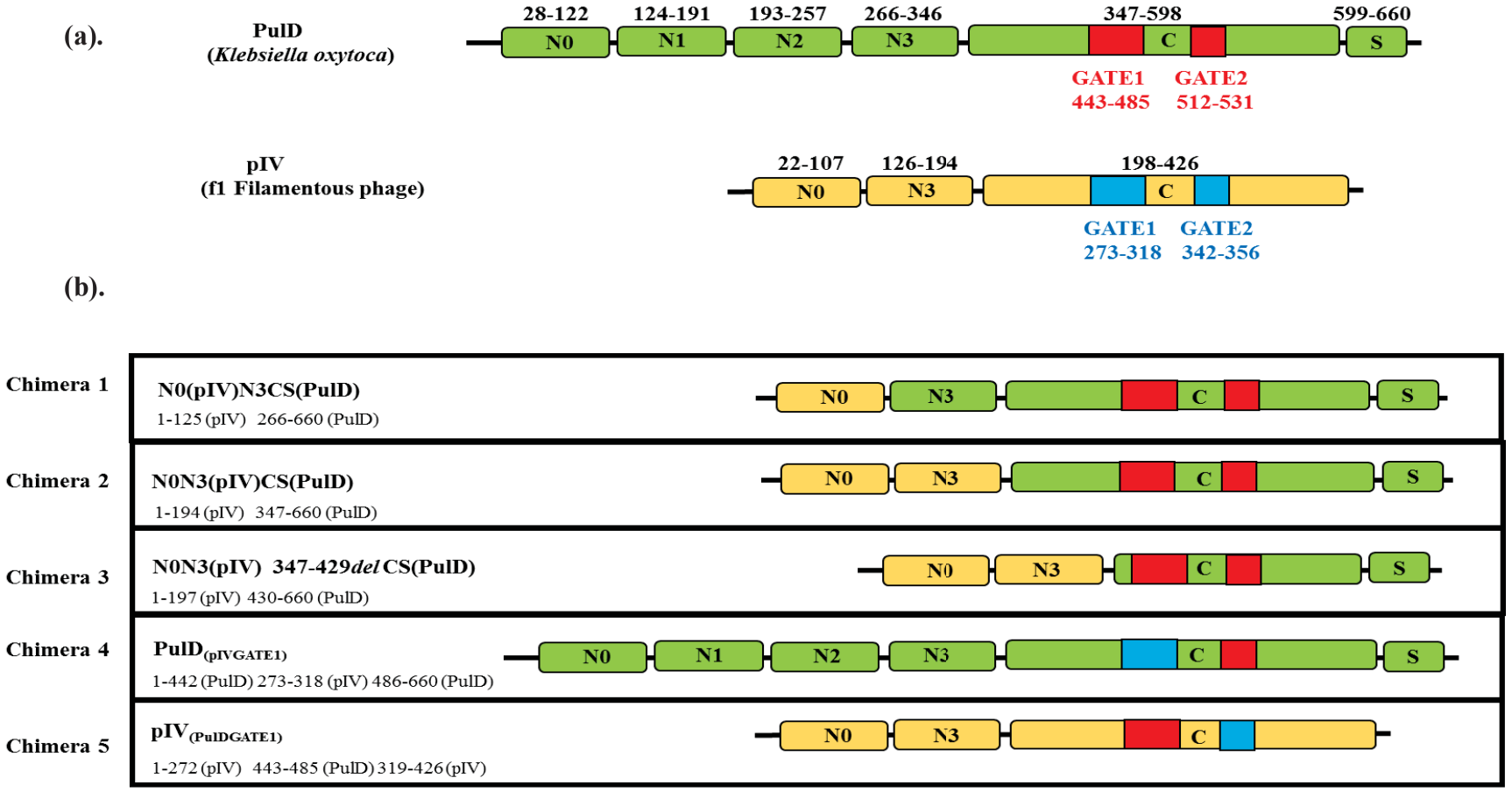

Figure 4.2 Schematic presentation of PulD and pIV domain organization and pIV-PulD chimeras.

(a). N0, N1, N2 and N3 correspond to the N-terminal subdomains; C, the secretin homology domain; S, pilotin-binding domain; PulD is green and pIV orange. red and black boxes correspond to the GATE regions of PulD and pIV, respectively (Spagnuolo et al., 2010;

Whitaker., 2012). **(b). pIV-PulD chimeras**; exact point of fusion in these chimeras is indicated on the left hand side under the names of the chimeras. Numbering corresponds to the source secretin (Chami et al., 2005; Korotkov et al., 2009).

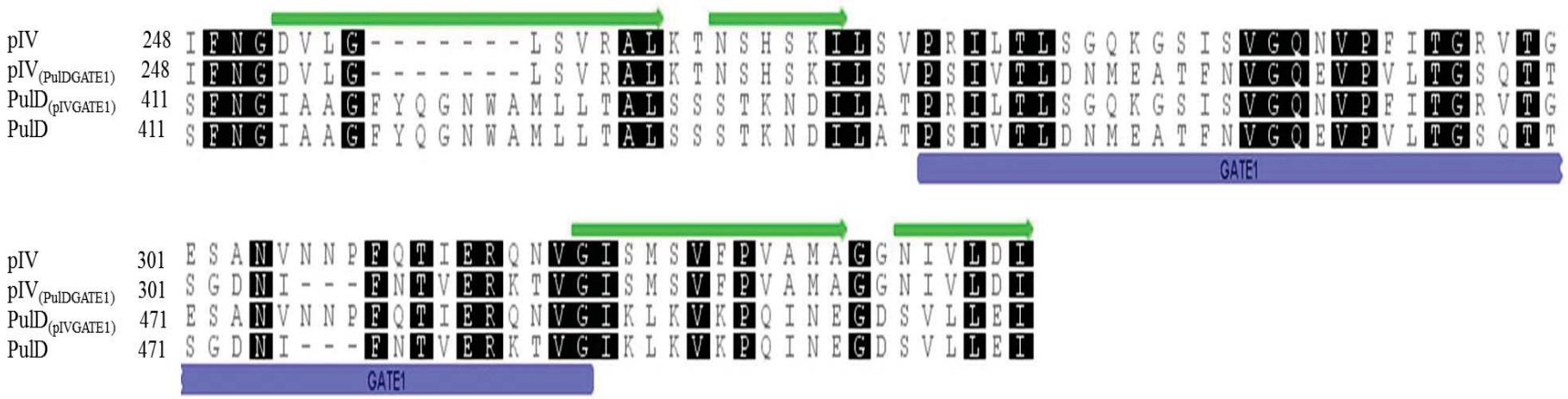

Figure 4.3 Alignment of GATE1 region of pIV, pIV(PulDGATE1), PulD(pIVGATE1) and PulD.

Protein sequences were aligned using ClustalW with Blosum 62 matrix, highlighting GATE1 region (blue) (Spagnuolo et al., 2010; Whitaker., 2012). Green arrow, trans-membrane β-strands predicted using TMBETA algorithm (Gromiha et al., 2005). Numbering corresponds to the source secretin.

4.2 Phagemid-based complementation assay for assessing the functionality of pIV and derived chimeras

Complementation assays are a standard for measuring the function of proteins. In the case of Ff phage, a *gene IV* deletion (*ΔgIV*) mutant phage R484 in conjunction with pIV produced from a plasmid has been using for this purpose in the past (Marciano et al., 2001). However, this system can measure a relatively small functionality range, since the cultures infected with the phage always have a reasonably high background of input phage from the stock, hence low-efficiency complementation cannot be detected. Furthermore, in the plasmid complementation, the *gene IV* sequence does not become assembled into the phage, so there is no possibility to select for mutants with improved activity. Construction of mutants in the phage is prohibited because low functionality would not allow replication in the absence of a wild-type copy and in turn would prevent analysis of stability, assembly and targeting of the non-functional chimeric channels due to the cell killing phenomenon by phage infection in the absence of pIV (Rakonjac et al., 2011). For these reasons, a phagemid system (Figure. 4.4) was constructed that would allow not only the phage-independent expression of pIV and the derived chimeras, but also selection for phagemid-containing phage-like particles (PPs) containing *gene IV* sequence, whose production would depend on the functionality of the particular pIV mutant or chimera in a complementation assay. A phagemid pYMK01 (containing the f1 origin of replication in addition to the plasmid *ori*) expressing wild-type pIV from a *tac* promoter, was used in conjunction with *ΔgIV* phage R484 (Figure 4.4). Phagemid pYMK01 was constructed (Chapter 2) by inserting f1 origin of replication into the pIV-expression plasmid pWW01 (W. Wen and J. Rakonjac, unpublished; derived from pPMR132) that also contains chloramphenicol resistance (Cm^R) marker gene and *colD* plasmid origin of replication.

To avoid homologous recombination, a strain with deletion of *recO* gene (K2245) was used to prepare stocks of phage and in complementation experiments. K2245 strain was constructed starting from the Keio collection *ΔrecO*::Kn^R mutant (JW2549-1) by removing the Kn resistance cassette that replaced *recO* gene and by mating with the F' donor strain XL1- blue (see Chapter 2 for details). The *recO* deletion mutant was used because this mutation has been shown to decrease recombination frequency between a *gIII* deletion mutant Ff phage and a complementing plasmid (Deng and Perham,

2002). Strain K2245 (*ΔrecO*) was co-transformed with phagemid pYMK01 expressing wild-type pIV or pIV-PulD chimeras constructed as described in Chapter 2, and the second plasmid (pAH181) expressing the PulS pilotin under its native promoter; PulS is required for the folding and targeting of pIV-PulD chimeras to the outer membrane (Daefler et al., 1997b).

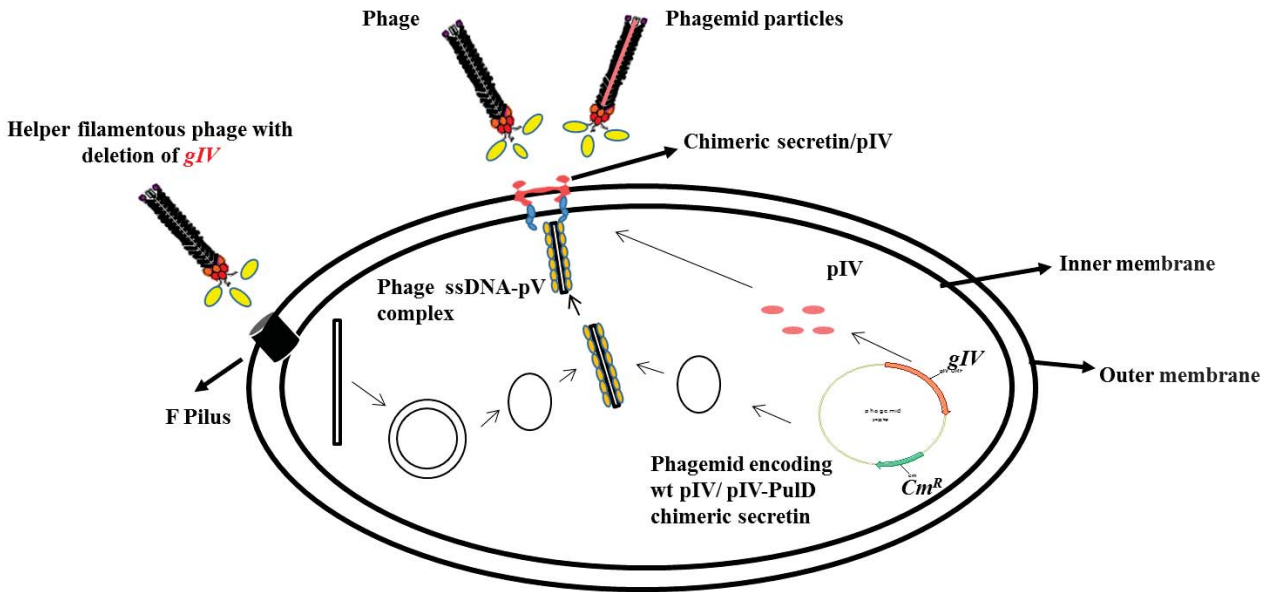

Figure 4.4 Schematic presentation of "phagemid-phage" complementation system for testing the function of pIV-PulD chimeras.

Cells expressing pIV or pIV-PulD chimeric secretin from a phagemid was infected with *ΔgIV* phage R484. Inside the bacterial cell, ssDNA of phage was first converted into double stranded replicative form (RF). This phage encodes all proteins required for replication of phagemid from the f1 origin and packaging into phagemid particles, apart from pIV, which is encoded by the phagemid. During assembly, ssDNA of phage and phagemid genomes first form complexes with phage protein pV, which are targeted to the assembly machinery which is composed of the inner membrane complex of pI/pXI and phagemid-encoded outer membrane channel pIV (or pIV-PulD chimera) encoded by the phagemid. Two types of particles are formed in this phage-phagemid complementation system, first carrying the *gIV*-

deleted helper phage genome and the second carrying the phagemid genome encoding pIV (or chimera) and the Cm^R marker, the latter used for enumeration of produced phagemids.

The complementation assay was performed by infecting the cells producing pIV or a chimera with *ΔgIV* phage R484, which was produced in a complementing host containing wild-type pIV-expressing plasmid pYW01 and therefore only contained phage particles (no Cm^R phagemid particles). After infection the input phage from the original infecting stock was removed by washing the cells in the fresh medium. The culture was further incubated to produce novel particles. Two types of particles were formed in the phagemid-phage complementation system, one carrying *ΔgIV* phage genome (phage) and the second type carrying the phagemid genome (phagemid particles or PPs). After the cells were removed and supernatant filtered to remove any remaining viable *E. coli*, the PPs were titrated based on their ability to confer (transduce) Cm resistance (encoded by the phagemid genome) to the indicator strain (untransformed strain TG1) upon infection (i.e. each infected indicator cell forms a Cm^R resistant colony on a titration plate). Besides the PPs, the *ΔgIV* phage R484 was also titrated on the indicator complementing strain (TG1 containing complementing plasmid pPMR132) that expressed pIV . Ff phage recombine with other episomes in the same cell in a non-RecA-dependent manner (Deng and Perham, 2002). As recombinants carried over from the stock or selected for during the complementation assay would form an undesirable population of gIV^+ phage that would allow assembly of PPs even by the phagemids expressing non-functional chimeras, the frequency of these gIV^+ phage was determined from the plaque titres on the non-complementing strain TG1.

Titres of the phagemid particles released by pIV-PulD chimeric secretins were much lower than those by wild-type pIV (five to six orders of magnitude), indicating that all these chimeras had functionality much below the wild-type pIV (Figure 4.5a). However, one of the fusions, $pIV_{(PulDGATE1)}$, had titres of phagemid particles about 10-fold over the negative control where no pIV was encoded by the phagemid in the host cells. The phagemid production mediated by $pIV_{(PulDGATE1)}$ was nevertheless quite low in comparison to the wild-type pIV, whose titre was eight orders of magnitude above the negative control. The phage titration showed the expected background titres of 10^6-10^7, which represent carried-over phage from the infecting stock remaining after washing of the cells. As expected, this high background prevented identification of phage released by the low-efficiency chimeric proteins. The phage titration of the positive control, the wild-type pIV complementation, showed that the ratio of PPs to

the ΔgIV phage is 1:100, consistent with the fact that R484 is not a "professional" helper phage. Given the low titre of the $pIV_{(PulDGATE1)}$-produced particles (10^3) and the negative control (10^2), it was not possible to correlate these with the much higher background of unwashed phage from the R484 infecting stock. The major concern for the interpretation of the low PP titres are potential gIV^+ recombinant phage in the stock of *ΔgIV* phage R484 that are typically generated during growth of stock on complementing strain at low frequencies. To determine the titres of gIV^+ recombinants at the end of experiment, the phage were titrated on non-complementing host (TG1). The titre of the phage from the $pIV_{(PulDGATE1)}$ expressing cells was about 10-fold higher than that of the PPs. This would indicate that PPs were derived from the cells infected with gIV^+ recombinants from the phage stock, however given that the ratio of PPs to R484 phage in the cells expressing the wild-type pIV was deternmined to be 1:100 (see above), the 1:10 ratio for the $pIV_{(PulDGATE1)}$ mutant was consistent with a 10-fold increase of phagemid production over the background. Therefore it appears that the GATE1 swap chimera $pIV_{(PulDGATE1)}$ showed very low but detecctable function in phage assembly. In contrast, other three chimeras, between the N-domains of pIV and the secretin homology domain of PulD, did not demonstrate increase of PP production over the background, showing that the specificty-determining N-terminal subdomain N0 or both N0 and N3 of pIV are not exchangeable with the corresponding domain of PulD.

In addition to complementation of pIV function in phage assembly, the chimearas were assayed for complementation of PulA secretion as described in Chapter 3, using an enzymatic assay (Figure 4.6). This analysis showed that the chimeras were inactive in PulA secretion. This was expected, as the N-terminal specificity domain of pIV was not expected to interact with the inner membrane components of the Pul T2SS (which are very different from the inner membrane components of the phage assembly system). The reverse GATE1 swap chimera, $PulD_{(pIVGATE1)}$, was also tested for PulA secretion and shown to be inactive. The sensitivity range of the PulA complementation assay is only two orders of magnitude (in contrast to seven orders of magnitute for the f1 assembly assay), as the release of PulA into the supernatant from dead and lysed cells sets a high background. Therefore, the reverse swap, which has the complete PulD apart from the GATE1 segment, could have had a low activity that is below the background value of the assay due to the PulA release by cell lysis/death.

(a).

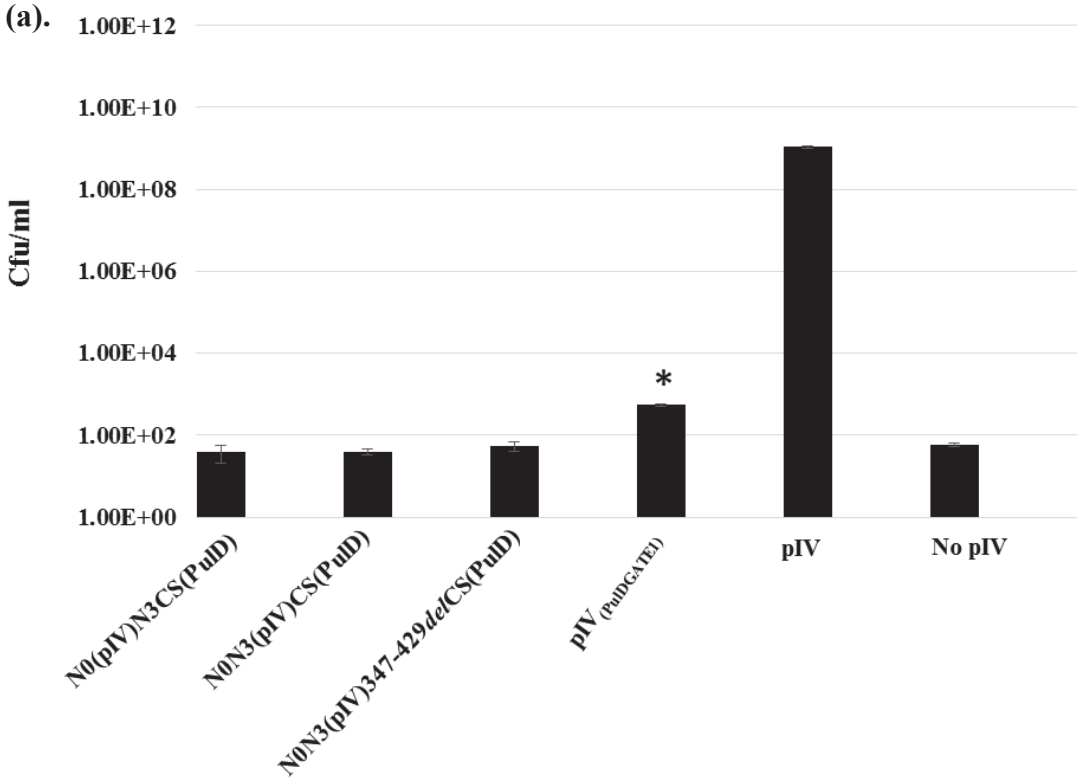
1.00E+12
1.00E+10
1.00E+08
1.00E+06
1.00E+04
1.00E+02
1.00E+00
Cfu/ml
*
N0(pIV)N3CS(PulD)
N0N3(pIV)CS(PulD)
N0N3(pIV)347-429delCS(PulD)
pIV (PulDGATEI)
pIV
No pIV

(b).

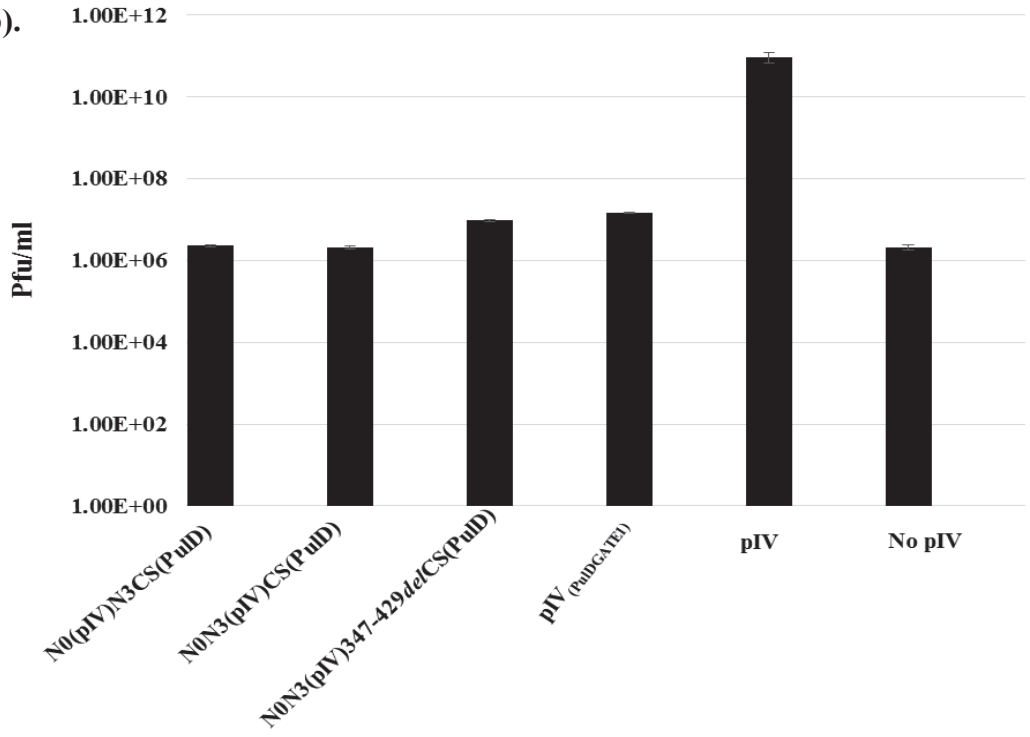
1.00E+12
1.00E+10
1.00E+08
1.00E+06
1.00E+04
1.00E+02
1.00E+00
Pfu/ml
N0(pIV)N3CS(PulD)
N0N3(pIV)CS(PulD)
N0N3(pIV)347-429delCS(PulD)
pIV (PulDGATEI)
pIV
No pIV

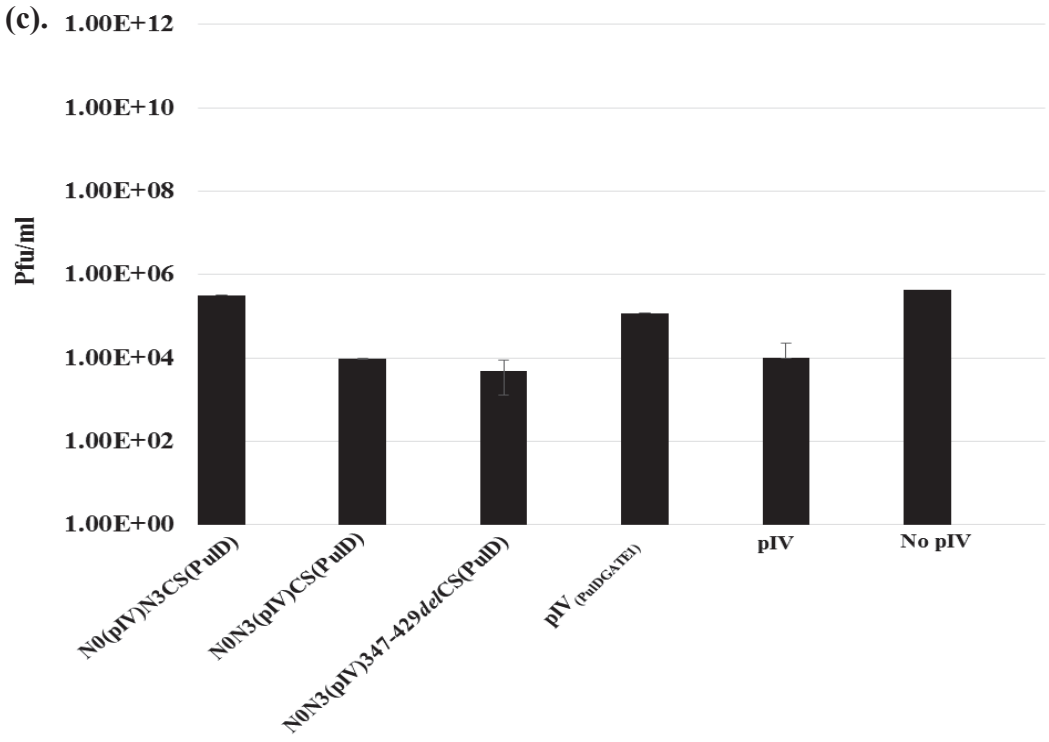

Figure 4.5 R484 (helper phage) and phagemid titers.

(a). Phagemid titers on TG1 cells: Phagemid particles (PPs) were titrated by counting Cm^R colonies formed on the lawn of TG1 strain after infection with dilutions of filtered culture supernatant from the complementation experiment. * =P-value < 0.05 (two-tailed t-test).

(b). R484 (helper phage) titers on complementing host (TG1 cells expressing pIV). The same dilutions as above, except that plaques were counted and the indicator strain expressed pIV from the complementing plasmid (pPMR132).

(c). Titres of the *gIV*$^+$ recombinant phage. The same samples as above, except that the indicator strain was untransformed TG1 (no pIV available for complementation), hence only the phage that were *gIV*$^+$ could form the plaques.

Error bars indicate the standard deviation from three technical replicates.

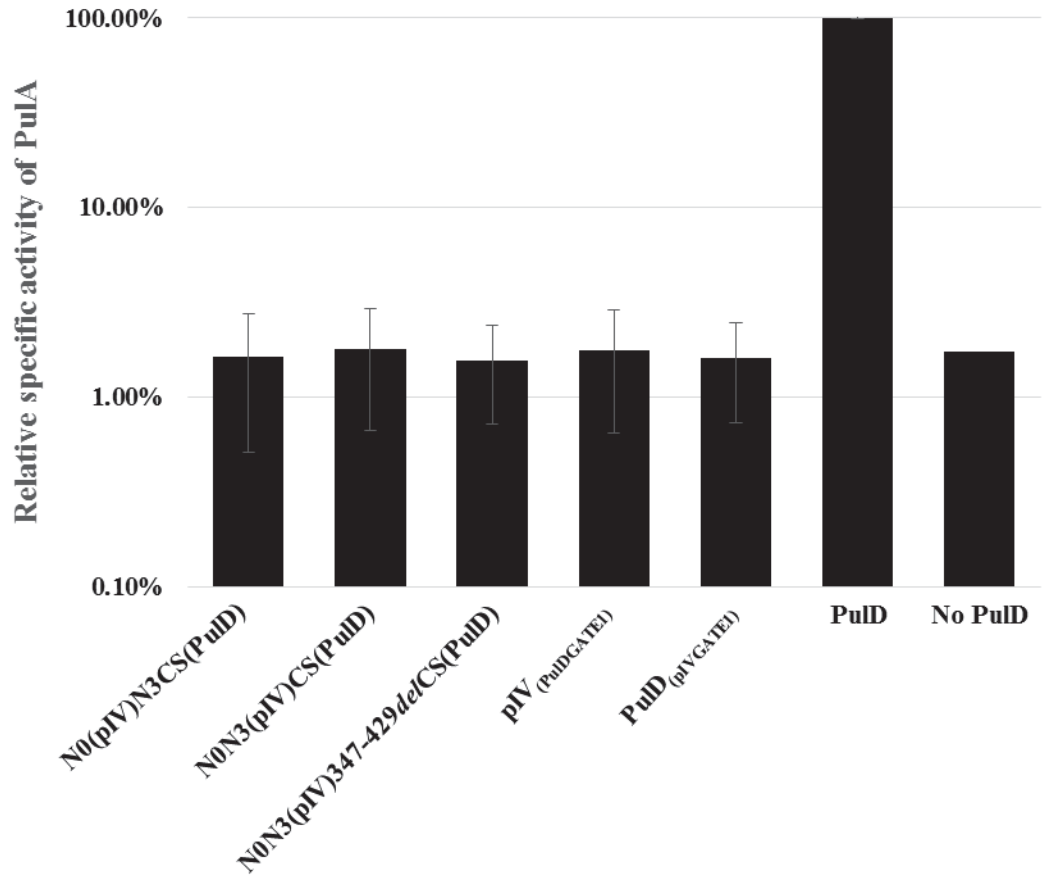

Figure 4.6 PulA secretion by pIV-PulD chimeras.

Enzymatic assays of aliquots from the culture supernatants of complementation experiment conducted with cells co-expressing the pIV-PulD chimeras and the remaining *pul* genes. The specific activity of PulA was determined from initial rate of reaction (amount of product maltotriose in µmol, liberated from the pullulan per min) per mg of protein in the culture (Hope and Dean, 1974). Activity of cells expressing each PulD mutant was calculated relative to that of the activity secreted from cells expressing the wild-type PulD. All cultures co-expressed the *pul* operon (apart from pulD) from a separate plasmid, pCHAP8243. Error bars indicate the standard deviations from three technical replicates.

4.3 Stability, targeting and multimerisation of pIV-PulD N-C chimeras.

Structural analyses using TEM and cryo-EM coupled with single particle analysis have shown that the PulD core region was composed of N3,C and S domains. This core region was shown to be required for multimerization in order to form a channel and insertion into the outer membrane in the presence of PulS. The chimeras constructed between the N-terminal subdomains of pIV and the complete and incomplete secretin homology domain of PulD were found not to be functional in phage assembly. The reason for a lack of function could be as simple as failure of a protein to fold, which would lead to rapid degradation in the periplasm, and/or failure to be targeted to the outer membrane and to form a functional channel. It was therefore of interest to determine whether the chimeric proteins were detectable in the cells and if so whether they were targeted to the outer membrane and whether they form multimers.

Periplasmic folding intermediates of secretins are degraded by periplasmic proteases such as DegP if they remain unfolded, hence the overal amount is typically proportional to the ability of the protein to fold and form multimers in the membranes (Spagnuolo et al., 2010). In the case of chimeras analysed here, all three were expressed from the same vector (and same promoter), hence the amount of protein detected in the extracts derived from the same number of cells is expected to reflect the protein degradation which in turn is triggered by failure to fold. Therefore, the total amount of chimeras in the cells was first analysed (using the antibodies specific to the GATE1 sequence from PulD). Two pIV-PulD chimeric secretins, N0N3(pIV)CS(PulD) and N0N3(pIV)347-429*del*CS(PulD), although they had N3 domain of pIV and the secretin homology domain of PulD, were detectable in the cell extract in similar or larger amounts as the wild-type PulD (Figure 4.7). This suggests that the two chimeras fold in a manner that prevents their degradation in the periplasm. PulD multimer is extremely stable; upon TCA precipitation (that dissociates pIV multimers) and boiling in SDS it still shows a faint multimer band, in addition to the monomer band on SDS-PAGE (Figure 4.7). Multimer band was detectable not only for the wild-type PulD, but also the chimera N0N3(pIV)CS(PulD), whereas no multimer band was detected for N0N3(pIV)347-429*del*CS(PulD) chimera, which has a deletion of the N-terminal 83 residues of the C (secretin homology) domain. This

finding suggests that, if any, its multimer is less stable during TCA precipitation and boiling in the presence of SDS than was the intact chimera. The third N-C chimera, N0(pIV)N3CS(PulD), was not detectable in the cell extracts, suggesting that either individual domains or complete polypeptide has failed to fold, resulting in degradation in the periplasm.

To examine the subcellular targetting cells expressing the detectable chimeras, N0N3(pIV)CS(PulD) and N0N3(pIV)347-429*del*CS(PulD), were fractionated into the inner membrane, outer membrane, soluble fraction (cytosolic and periplasmic) and aggregates (material that is insoluble afer extracting the above fractions). The pIV-PulD chimera that is stable like the wild type PulD, N0N3(pIV)CS(PulD)**,** was, unexpectedly, targeted not only to the outer membrane, but also to the inner membrane, despite PulS pilotin being co-expressed in the same cell. Furthermore, the majority of this protein was found in the aggregate fraction (Figure 4.8). Besides the dominant full-length protein band, the N0N3(pIV)CS(PulD) chimera in the aggregate fraction was presented as by a ladder of shorter bands, corresponding to degradation products that contain the antibody epitope (in GATE2). The second pIV-PulD chimera, N0N3(pIV)Δ347-429*del*CS(PulD) was present in a much lower amount, indicating slower folding and decreased stability and present in aggregate fraction. No protein was found in the inner membrane fraction; however this could be due to the overall much smaller amount of protein. Dominant localisation of both N0N3(pIV)CS(PulD) and N0N3(pIV)347-429*del*CS(PulD) chimeras in the aggregate fraction indicates that these chimeric proteins are either strongly associated with peptidoglycan or are for some reason delayed in targeting to the SecYEG system, resulting in formation of inclusion bodies in the cytoplasm, or both. Strong fractionation to the inner membrane, however, suggests that the former is probably the case. Interestingly, multimer bands were not identified in the fractionated samples, despite the same processing of the samples as those in the total lysate.

As misfolding of the chimeric channels can potentially result in disturbed septum, the cells expressing these chimeras were tested for permeability to maltopentaose and Van, two molecules that cannot pass through porins or the two wild-type secretin channels. Cells expressing all N-C chimeras were impermeable to the two tested molecules (Table 4.1), This result is not surprising for the N0-N3 chimera which was

unstable and not detected in the cells. With respect to the N0N3(pIV)CS(PulD) and N0N3(pIV)347-429*del*CS(PulD) chimeras the potential multimers either do not form a channel or form a channel whose septum has pores that have a cut-off equivalent or below that allowing passage of maltopentaose (829 Da).

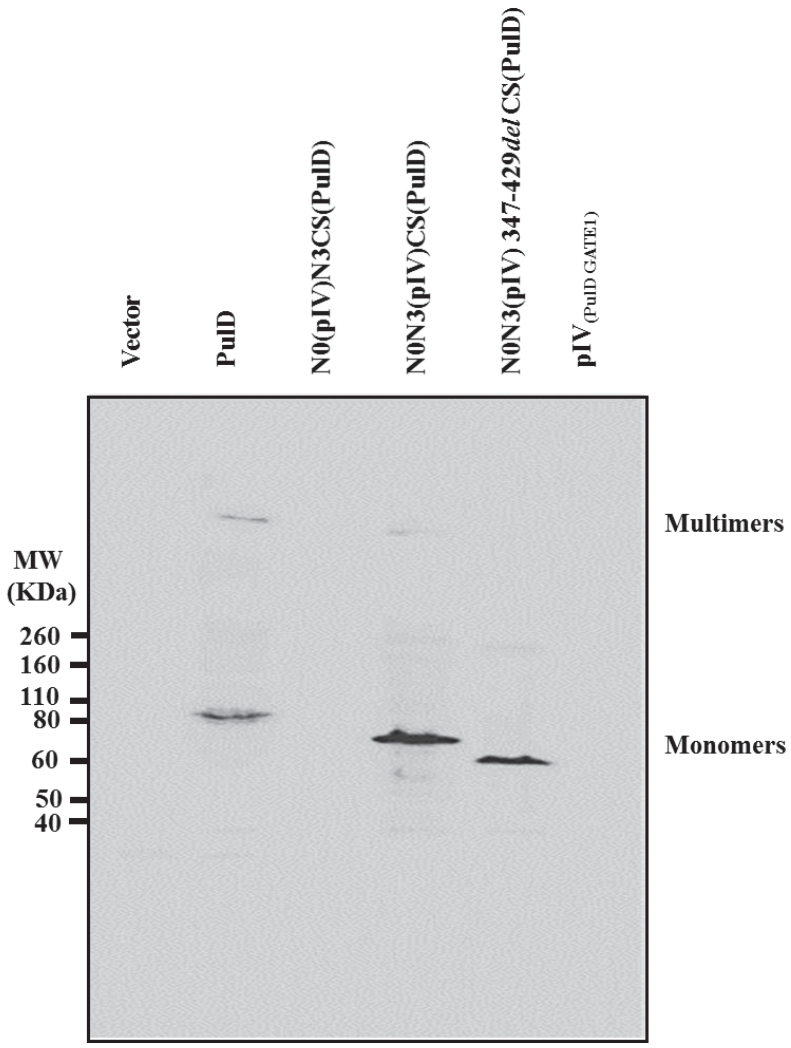

Figure 4.7 Detection of pIV-PulD chimeric secretins monomers and multimers.

Total cell extract of the cells expressing pIV-PulD chimeric secretins using 0.1 mM IPTG (co-expressed with the pilotin PulS were prepared using TCA precipation. Nitrocellulose membrane with transferred samples was blotted with PulD specific antibodies against a GATE1 peptide.

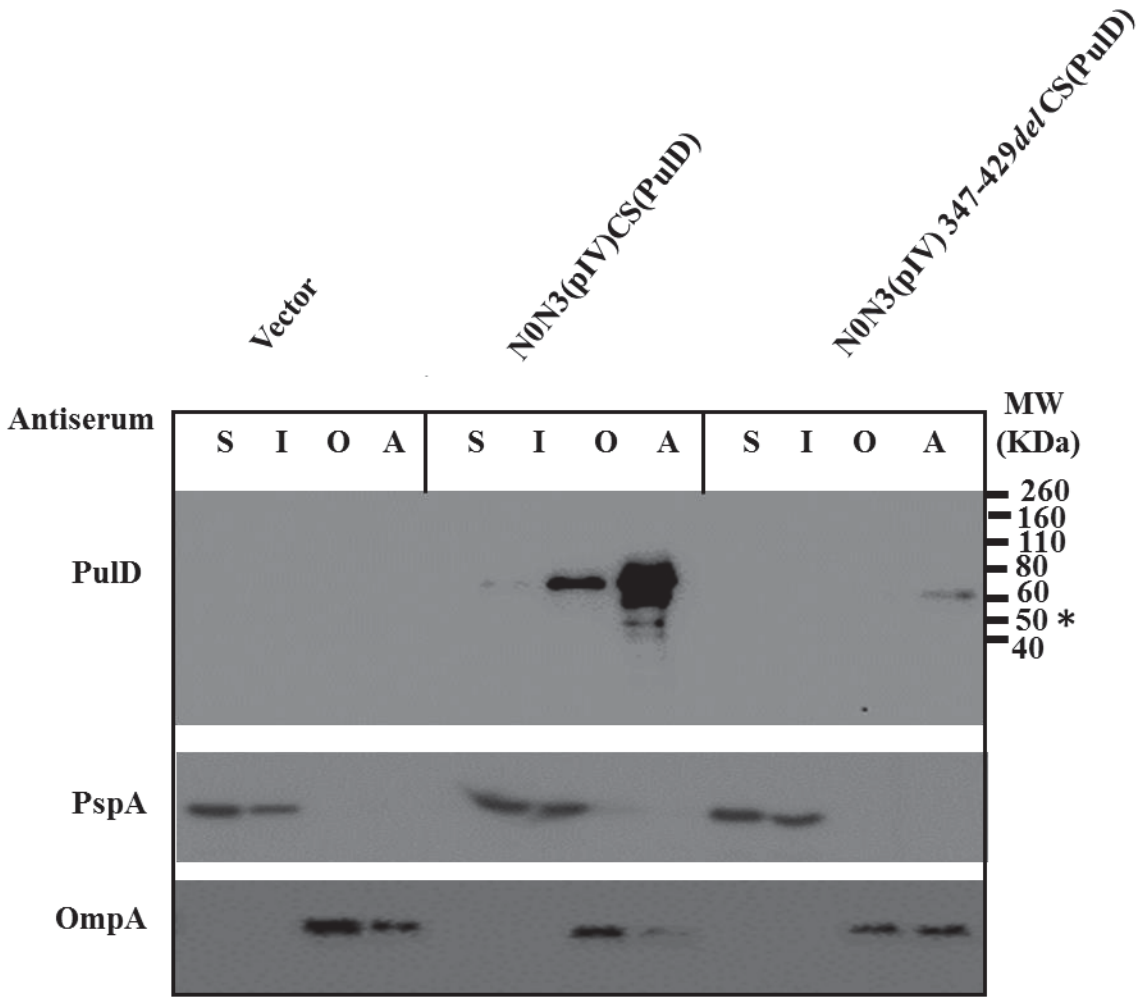

Figure 4.8 Targeting of pIV-PulD N-C chimeric secretins.

Subcellular fractions of cultures expressing pIV-PulD chimeras: N0N3(pIV)CS(PulD) and N0N3(pIV)347-429*del*CS(PulD) and no PulD (vector) were subjected to a TCA precipitation. Fractionation markers, OmpA (outer membrane porin) and PspA (peripheral inner membrane / cytoplasmic protein) were used to monitor fractionation. Proteins were detected by western blotting; PulD antibodies were specific for a GATE1 peptide (See Chapter 2). S, soluble fraction (periplasm and cytoplasm); I, inner membrane fraction; O, outer membrane fraction, A, insoluble aggregates. Asterisk * indicates the smallest PulD degradation product.

Table 4.1 Permeability of pIV-PulD chimeras to Van and maltopentaose

Secretins	Van MIC (μg ml^{-1})[a]	Ability to utilize maltopentaose[b]
pIV	R	No
PulD	R	No
N0(pIV)N3CS(PulD)	R	No
N0N3(pIV)CS(PulD)	R	No
N0N3(pIV)347-429*del* CS(PulD)	R	No
pIV$_{(PulDGATE1)}$	R	Yes[c]
PulD$_{(pIVGATE1)}$	R	No

[a.] Minimal inhibitory concentrations of Van as measured by concentration gradient strips (μg ml^{-1}) are indicated. R, completely resistant at the highest concentration tested (256 μg ml^{-1}).

[b.] Minimal media containing maltopentaose as sole carbon source.

[c.] Weak growth detected after 48 h of incubation.

4.4 Stability, targeting and multimerisation the PulD-pIV GATE1 swap chimeras

The $pIV_{(PulDGATE1)}$ chimera constructed by replacing the 46-residue GATE1 (pIV residues 273-318) with the 43-residue equivalent from PulD. This chimera was the only one demonstrating a low activity in f1 assembly (Figure 4.5), hence it was of interest to determine whether it forms a multimer. However, this protein was not detectable in the whole cell extracts of the expressing cells (Figure 4.7). It could therefore be concluded that the low activity of this protein may have been carried out by very small number of assembled secretion-active multimers. This possibility could be confirmed by isolating an "evolved" stable mutant of this chimera through mutagenesis and selection for efficient assembly of chimera-encoding phagemid.

The reverse chimera, $PulD_{(pIVGATE1)}$, in which 43 residues corresponding to PulD GATE1 segment (residues 443-485) were replaced by the predicted GATE1 region of pIV (46 residues) was not active above the background in the PulA secretion assay (Figure 4.6), albeit the background leakage of PulA in this assay made it impossible to detect a low activity such as that of the reverse chimera in the much more sensitive phagemids assembly assay. Interestingly $PulD_{(pIVGATE1)}$ chimera was readily detectable in the cell extract in a similar amount as was the wild-type PulD, suggesting that the swapped GATE1 region did not have a major effect on protein folding (data not shown). Furthermore, fractionation experiments showed that the $PulD_{(pIVGATE1)}$ chimera was targeted to the outer membrane (Figure 4.9a), albeit a reasonable fraction was mistargeted to the inner membrane, despite the co-expression of the pilotin PulS. As expected, no wild-type PulD could be detected in the inner membrane in the same fractionation experiment (Figure 4.9a). The presence of multimer was analysed in the native outer and inner membrane fractions by native protein agarose electrophoresis (Figure 4.9b). This experiment showed that the $PulD_{(pIVGATE1)}$ chimera is a multimer. Interestingly, the outer membrane multimer of the chimera migrated as two distinct bands, similarly as the wild-type PulD. In contrast, the inner membrane multimer migrated as a single band equivalent to the faster-migrating outer membrane band (Figure 4.9b).

Given that the gate of pIV, despite conservation with that of PulD, has numerous mismatches (Fig. 4.3), it was possible that the assembled channel may be leaky. The

cells expressing both chimeras were assayed for sensitivity to Van using the E-test strips and for permissivity to maltopentaose. Whereas the stable $PulD_{(pIVGATE1)}$, chimera was not permeable to either of the molecules, the cells expressing the $pIV_{(PulDGATE1)}$ chimera showed limited growth on the plates containing maltopentaose as a sole carbon source, indicating marginal permissivity to this molecule (MW = 829 Da). This was surprising given that the $pIV_{(PulDGATE1)}$ chimera was not detectable by western blotting; however it is consistent with formation of a small number of active channels, as indicated by the low level of activity in the phagemids complementation assay.

Given that the $PulD_{(pIVGATE1)}$, chimera is folded and stable, it was assayed for sensitivity to a range of antibiotics that include some that have a molecular weight lower than maltopentaose, such as rifampicin (MW = 720 Da), using a dose-response growth inhibition assay that allows more precise comparisons between different strains than the E-strip assay (Figure 4.10). The dose-response assay has shown that the cultures expressing $PulD_{(pIVGATE1)}$ chimera demonstrated similar resistance to all tested antibiotics as did the cultures expressing wild-type . Furthremore, cultures expressing $PulD_{(pIVGATE1)}$ were less sensitive to rifampicin and bacitracin than cells expressing the wild-type PulD, suggesting that the septum of the chimeric protein, in a closed state, has a smaller pore size than that proposed for the wild-type PulD (1 nm). Decreased pore size was reported for some inappropriately folded but multimerised GATE1 mutants (Guilvout et al., 2014).

In conclusion, the GATE1 swap chimeras have different properties. While the GATE1 of PulD in pIV impairs folding, it appears that the small amount of folded channels result in a functional and leaky channel. In contrast, GATE1 of pIV in the PulD secretin framework does not prevent folding and multimerisation of the channel, however the multimer appears not to be functional and to have a pore that is of slightly smaller diameter than that of the wild-type PulD. Given that GATE1 residues (470, 472, 473, 474, 475,476), that were shown by Guilvout et al (2014) to be required for the PulD multimer to assume the channel properties in an *in vitro* liposome system, and that the critical residues are different in pIV GATE1 to those in the equivalent positions in PulD, perhaps the swap resulted in the similar properties of the multimer formed by the $PulD_{(pIVGATE1)}$ chimera.

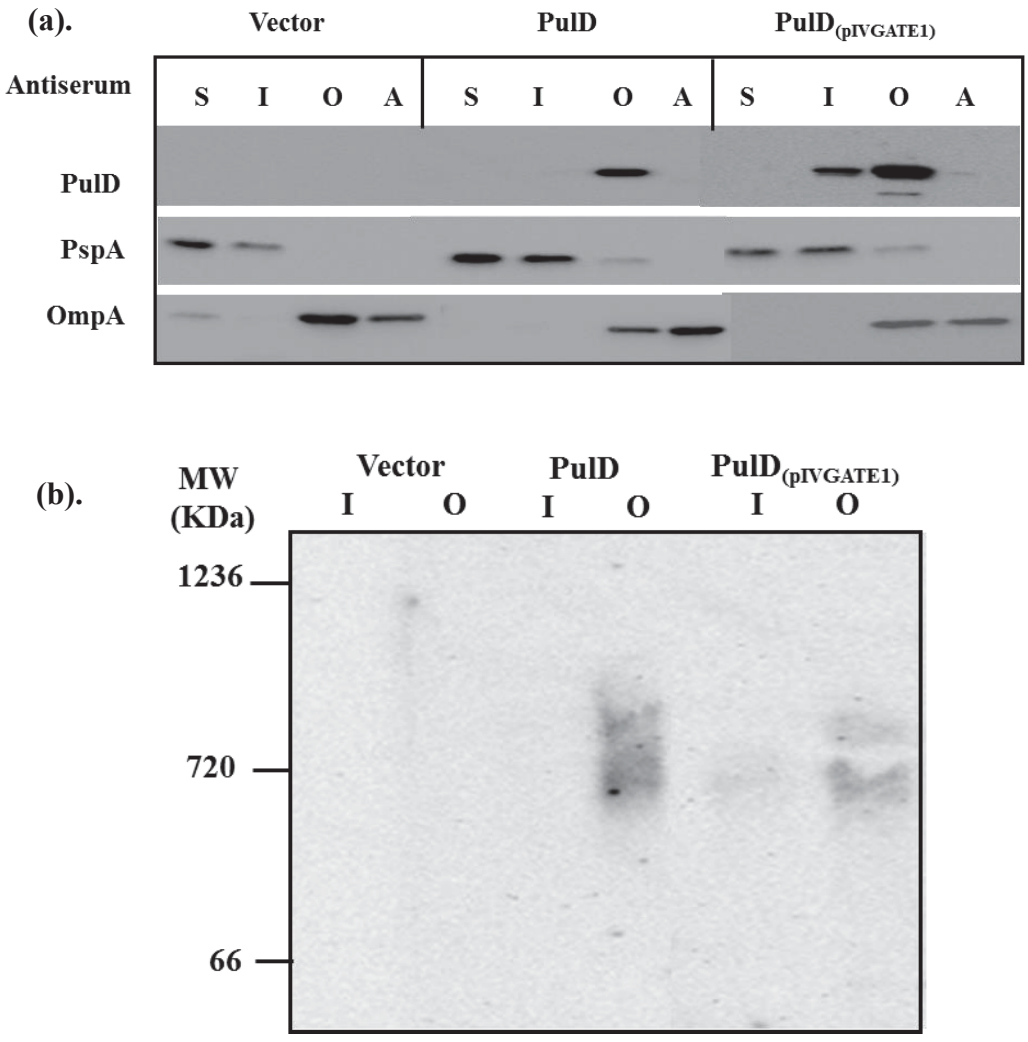

Figure 4.9 Outer membrane targeting and multimerization of PulD mutants.

(a). Subcellular fractions of the cultures expressing $PulD_{(pIVGATE1)}$, wild-type PulD and no PulD (vector) were subjected to a TCA precipitation and separated by SDS-PAGE. Fractionation markers OmpA (outer membrane porin) and PspA (peripheral inner membrane / cytoplasmic protein) were used to monitor fractionation. S, soluble fraction (periplasm and cytoplasm); I, inner membrane fraction; O, outer membrane fraction, A, insoluble aggregates. **(b)** Native agarose gel electrophoresis of the native (Triton X-100)inner (I) and outer (O) membrane fractions of cells producing no PulD (vector), wild-type PulD, $PulD_{(pIVGATE1)}$.The fractions were obtained from the same

cultures used in (a). Proteins were detected by western blotting; PulD antibodies were specific for a GATE2 peptide.

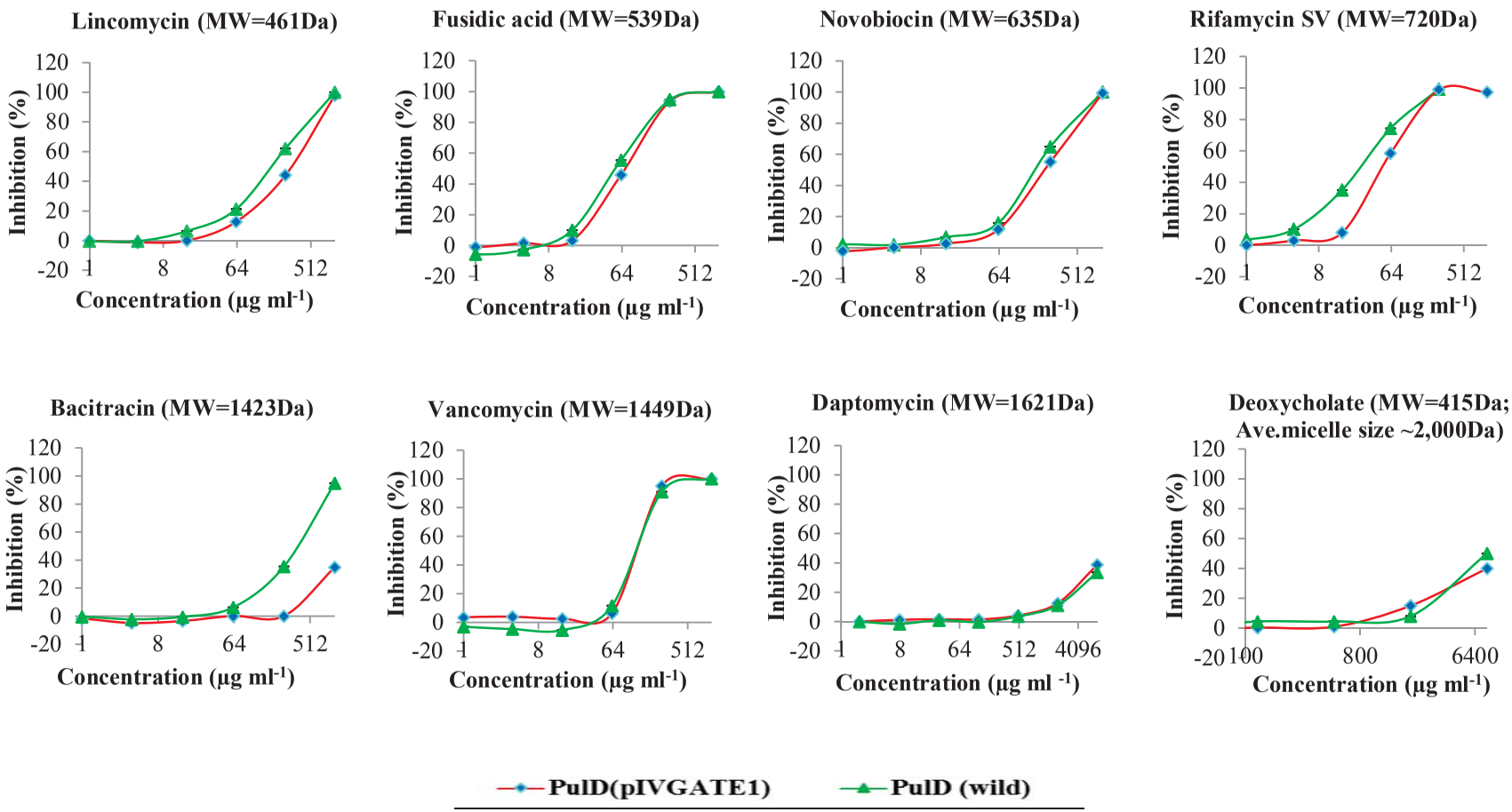

Figure 4.10 PulD$_{(pIVGATE1)}$ chimeric secretins failed to sensitise E. *coli* to high molecular weight antibiotics and detergent deoxycholate (DOC).

Dose-response growth assay in liquid culture, starting 105 cells per ml (PulD variants are co-expressed with PulS *in trans*). The Critical Micelle Concentration (CMC) of DOC is 830 to 2490 μg ml-1 and the average micelle size is 2,000 Da. Error bars indicate the standard deviation from three technical replicates.

4.5 Conclusions

This chapter has analysed the engineered chimeras between pIV and PulD, to probe functional compartmentalisation among the secretin domains and the segments involved in gating. This was achieved by analysis of targeting, multimerisation, permeability to > 600 Da molecules and functionality in secretion of cognate substrates, pullulanase and f1 phage.

Overall, work in this chapter that analysed chimeras between N-terminal domains of pIV and C-terminal domains of PulD showed that the complete N domain of PulD is exchangeable with corresponding domain of pIV without affecting protein stability in the periplasm and targeting to the outer membrane, suggesting that folding of PulD core region has occurred. Moreover, an N3 swap that also contained a deletion of 83 residues at the N-terminus of the C-terminal secretin homology domain [N0N3(pIV)347-429*del*CS(PulD)] was found in the outer membrane, hence the deleted sequence was not required for folding of PulD and targeting to the outer membrane. Chimeric N0N3(pIV)CS(PulD), but not the N0N3(pIV)347-429*del*CS(PulD) were found to form TCA- and SDS-resistant multimers like wild type PulD. Given that N0N3(pIV)347-429*del*CS(PulD) chimera is targeted and inserted into the outer membrane, it is possible that it forms a multimer. Interestingly, some of N0N3(pIV)CS(PulD) chimera was targeted to in the inner membrane fraction. This was particularly surprising for this chimeric secretin as it contained pilotin-binding domain and was co-expressed with the cognate pilotin PulS in the same cells. Targeting profile of both N0N3(pIV)CS(PulD) and N0N3(pIV)347-429*del*CS(PulD) was unusual, in that majority of the protein was found in the aggregate fraction. This may either mean that they were associated strongly to incompletely hydrolysed insoluble, peptidoglycan or form inclusion bodies in the cytoplasm due to poor targeting for export to the SecYEG translocon upon overexpression, as it sometimes occurs for overexpressed signal sequence-containing proteins. In contrast to the complete N-domain swaps, fusion of N0 domain of pIV to the PulD N3CS was undetectable in the cell lysates, showing that the folding/stability of this chimera was severely compromised.

In addition to the N-C swaps, the GATE1 swaps between pIV and PulD were constructed to probe the role of this segment in folding, targeting, multimerisation and

function. The chimera $PulD_{(pIVGATE1)}$ was targeted to the outer membrane as a multimer of similar size to that of the wild-type, according to the native protein agarose gel electrophoresis. In contrast, the reverse chimera of pIV with PulD GATE1 was not detectable in the cell lysate, hence it had a major folding defect, resulting in degradation of most of the protein in the periplasm.

Among the engineered chimeras between pIV and PulD that contained the N-terminal domains of pIV, only the $pIV_{(PulDGATE1)}$ was found to have some functionality (10-fold over background, but six orders of magnitude below the wild-type pIV) in the phagemid assembly assay. None of the fusions had PulA secretion functionality above the background, albeit the range of the assay was only two orders of magnitude, hence it did not permit detection of low-efficiency activity as is possible in phagemids production assay, hence low-activity proteins could not be assayed. Of all mutants, only the $pIV_{(PulDGATE1)}$ was leaky to > 600 Da molecules – maltopenaose. All other mutants were impermeable to the tested molecules, including properly targeted multimer-forming $PulD_{(pIVGATE1)}$. Interestingly this latter mutant was less permeable than the wild-type PulD to the > 600 Da antibiotics rifamycin and Bac. These findings confirm that manipulation of the gating domain through GATE1 swap affects the gating properties. All these findings indicate that N and C terminal domains of the secretins may not work autonomously, but rather interact with each other and with the substrate during the secretion process and that GATE1 sequences are involved in both gating secretin function and overall folding of the secretins. Surprisingly, stability was not compromised when 83 out of a total of 230 residues that correspond to the secretin homology domain were deleted. This region contains three TMBETA-predicted transmembrane β strands (Figure 4.1) and if they were correctly predicted, their removal would result in a major defect in folding and membrane targeting. Therefore, it appears that the deleted sequence does not contain outer membrane targeting signals. It is possible that the deleted 83 residues form part of the periplasmic fold of the secretin homology domain.

Chapter 5: Gating of EscC and InvG, secretins of type III secretion systems

The gate regions of the filamentous phage secretion system secretin pIV and the T2SS system secretin PulD have been determined (Spagnuolo et al., 2010); Chapter 3). This current chapter aims to determine whether the gating regions are conserved in T3SS secretins InvG and EscC with those identified in pIV and PulD.

T3SS secretins EscC and InvG analysed in this study are encoded on pathogenicity islands of LEE and SPI-1 of pathogenic bacteria EHEC O157 and *S.* typhimurium, respectively. In their cognate organisms, these secretins are outer membrane components of the T3SS that secrete dozens of virulence factors and effectors and toxins required, respectively, for formation of special adherence structures (pedestals) and invasion of epithelial cells. Secretins have an initiator role in assembly of T3SS (Galan and Wolf-Watz, 2006; Marlovits et al., 2006) that would in principle require maintenance of a gate structure within the basal body before the needle assemble. It could also have additional roles in the assembly/secretion of the needle base subunits and assembly of the needle itself. Therefore, it was of interest to identify gating residues in these secretins and compare them to those identified in the secretins pIV and PulD.

5.1 Characterisation of the EscC secretin

5.1.1 Phenotypic effect of EscC expression in *E. coli* K12

The CDS encoding EscC was cloned into pCR-Blunt vector under the control of the *lac* promoter and expressed in *E. coli* K12 (see Chapter 2 for details). It was found that, of the two Δ*lamB* strains that can be used for selection of leaky-gate secretins, strain K2204 (TG1, Δ*lamB*) tolerated the EscC expression better than K1508 (MC4100, Δ*lamB*). Colonies of EscC-expressing cells demonstrated a peculiar phenotype. In both strains, colonies of similar size to those containing the vector only

(pCR-Blunt without an insert) were formed overnight at 37 °C on plates that contained IPTG to induce production of EscC. However, upon storage in the cold room for 48 h, these colonies became transparent, presumably due to cell lysis, in contrast to vector-containing strain K1508, whose colonies did not change the appearance under the same conditions.

5.1.2 Effect of the EscC expression on sensitivity to large antibiotics

To examine the effect of EscC expression on the integrity of the outer membrane barrier function, cells of strain K2204 expressing EscC were titrated on solid media containing Van (100 μg/ml), Bac (50 μg/ ml), and DOC (0.4%), to which *E. coli* expressing the wild-type secretins pIV and PulD/PulS are resistant. Cells expressing the wild-type pIV were used as a control in this experiment. Relative plating efficiencies of secretin-expressing vs. vector-containing cultures on Bac- and Van-containing plates were found to be almost equal for EscC and the pIV (Figure 5.1); however, the appearance of colony morphology was different. While the colonies of the wild-type pIV-expressing strain were indistinguishable from those of the cells containing an empty vector, the colonies of the EscC-expressing strain were small and transparent, presumably due to cell death/lysis or slow growth, suggesting that these antibiotic concentrations either kill a significant fraction of the cells or extend the generation time, resulting in a decreased number of bacterial cells per colony. The effect of EscC expression on plating efficiency in the presence of DOC was more prominent. The relative plating efficiency of the EscC-expressing to vector control culture on plates containing DOC was nearly 5-fold as low as that of the relative plating efficiency of the pIV-expressing culture, suggesting that the EscC expression renders outer membrane more permissive to this detergent compared to pIV. Furthermore, when plated on the maltopentaose-containing M63 minimal solid media, the EscC-expressing cells formed colonies, although their size was smaller than those formed by the cells expressing a "leaky" mutant of pIV secretin, pIV^{S324G}. The same culture failed to form colonies on the plates where maltopentaose was replaced by a longer maltooligosaccharide, maltoheptaose (MW=1153 Da). These findings indicate that the EscC contains a pore whose cut-off size is larger than that of pIV, permitting the passage of maltopentaose and DOC, but not maltoheptaose. The pore must be partially permissible to Van and Bac, given the decreased colony size in the presence of these antibiotics.

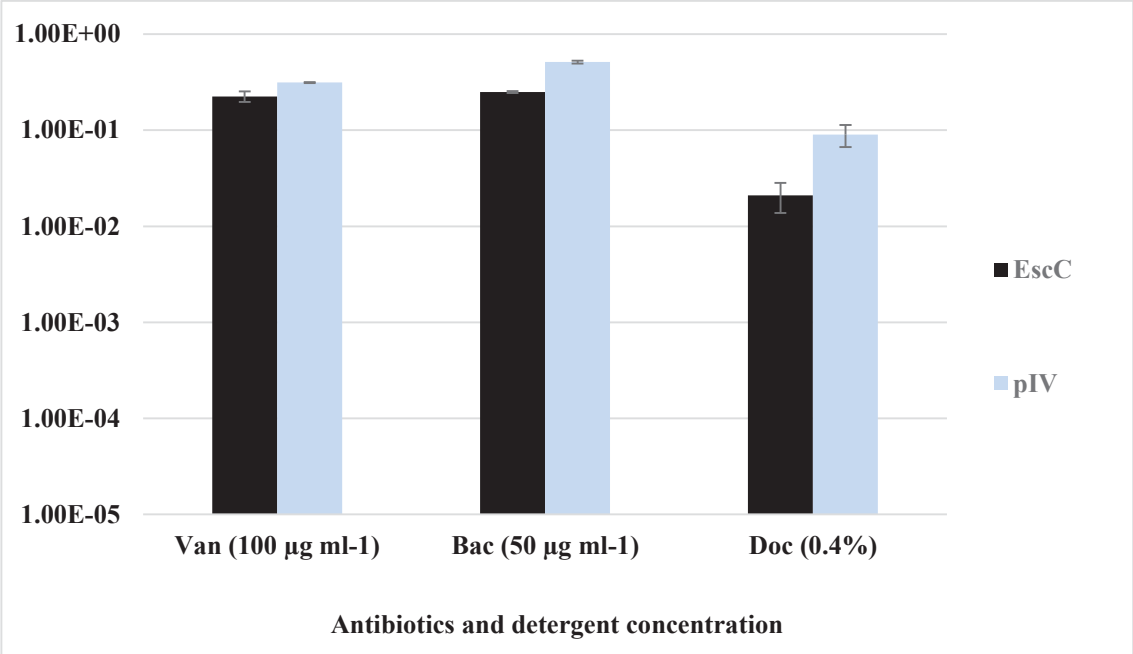

Figure 5.1 Plating efficiencies of the cells expressing EscC in the presence of large antibiotics and DOC.

Plating efficiency of strain K2204 transformed with pCR-Blunt expressing wild type EscC and pPMR132 expressing wild type pIV in the presence of antibiotics and DOC was calculated as a ratio of plating in the absence *vs*. presence of particular antibiotic/detergent. Error bars indicate the standard deviation from three technical replicates.

5.1.3 Subcellular targeting of EscC in *E. coli* K12

To investigate the subcellular targeting of EscC, K2204 cells expressing this protein were fractionated into subcellular fractions: the soluble proteins (cytoplasm and periplasm), inner membrane, outer membrane and insoluble aggregates. Distribution of EscC among these fractions (cellular compartments) was investigated by SDS-PAGE and western blotting, using EscC-specific antibodies. These antibodies were custom-made against the purified N-terminal portion of EscC (as described in Chapter 2). Inner-membrane-associated protein PspA and outer membrane protein OmpA, served as fractionation markers. These two proteins were detected by cognate antibodies (described in Chapter 2). EscC was equally targeted to both inner and outer membrane and soluble fraction. Distribution among the soluble, inner and outer membrane fractions was expected based on the similar distribution of pIV, which, like EscC, does not contain a pilotin-binding domain and has no specific pilotin to guide its precise targeting to the outer membrane. However, in contrast to pIV, most of the EscC was in the aggregate fraction, which is composed of insoluble molecules and would contain misfolded (insoluble) proteins from the cytoplasm, and/or peptidoglycan-associated proteins. Given a high expression of EscC and higher concentration in the soluble fraction relative to the membrane fractions, it is very likely that some portion of the protein in the aggregate fraction represents inclusion bodies of the cytoplasmic protein that could not be exported due to oversaturation of the SecYEG system, which is reported when signal-sequence-containing proteins are overexpressed in *E. coli* K12 (Mergulhao and Monteiro, 2004; Mergulhao et al., 2004). Interestingly, a ladder of EscC bands in the aggregate fraction pointed at the presence of stable multimers or aggregates that could not be completely separated by 5% TCA followed by boiling in 4% SDS (Figure 5.2). However, in addition to these multimers, degradation products were also identified in the aggregate fractions, most likely generated from misfolded or unfolded fraction of EscC by cytoplasmic or periplasmic chaperones whose role is to degrade misfolded proteins. The analysis used protein PspA as an inner membrane marker. This protein is also a marker of inner membrane stress; encoded by the *psp* regulon whose expression was induced by insertion of secretin channels into the inner membrane. Massive production of PspA was consistent with insertion of EscC into the inner membrane. Interestingly, PspA, which is an inner membrane marker, was found in the outer membrane fraction, in contrast to the cells

that do not express EscC, where there is very little in the outer membrane. This indicates that EscC expression affects the outer membrane assembly, resulting in contamination of the outer leaflet of outer membrane with phospholipids. Very similar fractionation pattern for both the PspA and the secretin has been observed with EspD secretin from the T2SS of *Vibrio cholerae*, upon expression in *E. coli* in the absence of its pilotin (J. Spagnuolo and J. Rakonjac, unpublished)

Like EscC expression, EspD expression also caused increased sensitivity to phospholipid-soluble detergent DOC, but not to hydrophilic molecules Van and Bac which cannot cross the phospholipid membranes and therefore remain excluded from the periplasm, despite the compromised LPS integrity in the outer leaflet of the outer membrane. As expected, fractionation of the outer membrane marker OmpA did not detect this protein in the inner membrane or soluble fractions, indicating a successful fractionation.

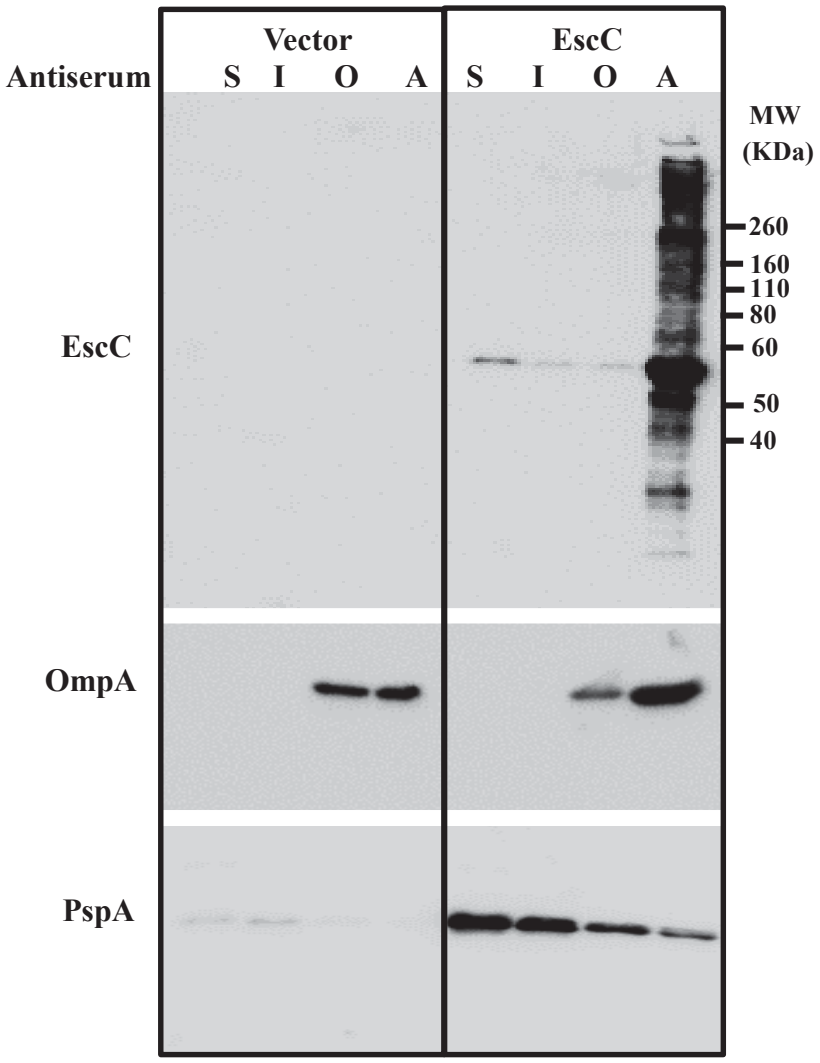

Figure 5.2 Subcellular localization of EscC.

Cultures expressing EscC (right panel) or containing the corresponding empty vector (left panel) were subjected to fractionation into the: S, soluble; I, inner membrane; O, outer membrane; A, insoluble aggregate fractions. Proteins in each fraction were precipitated using TCA, denatured by boiling in SDS, separated by SDS-PAGE and analysed by western blotting using EscC-, OmpA- and PspA-specific antibodies.

5.1.4 Effect of EscVN coexpression with EscC on *E. coli* K12

It has been reported that if secretins are mislocalized into the inner membrane, they become toxic to the cells, presumably due to the disturbance of the proton motive force across the inner membrane (Brissette et al., 1990; Guilvout et al., 2006). Given that a significant fraction of EscC is mislocalized to the inner membrane when expressed on its own, this could be the reason for observed growth retardation and in-colony lysis of the host *E. coli* K12 cells. EscC has no pilotin-binding domain or a cognate pilotin, but was reported to depend for targeting and assembly on two T3SS proteins, EscV and EscN, in gene knock-out studies of the pathogenic EHEC strains (Gauthier et al., 2003). To test whether provision of these two proteins in *E. coli* K12 had a capacity to relieve the toxicity of EscC, both EscV and EscN (whose coding sequences are adjacent within the same operon) were cloned into vector pJARA220 to be co-expressed under the control of the *psp* promoter. The *psp* promoter is highly induced by expression of EscC, as confirmed by a high increase in the amount of PspA protein in the EscC-expressing cells (Figure 5.2). EscN is a cytoplasmic, inner membrane-associated protein, which is the obligatory T3SS ATPase (Cornelis, 2006). EscV is an inner membrane protein and as yet is not fully characterized.

Co-expression of EscV and EscN with EscC failed to improve viability of cells. On the contrary, their co-expression resulted in a reduced colony size and density of overnight cultures, relative to those cells in which EscC was expressed alone (not shown), reflecting an increased toxicity of co-expression to *E. coli* K12. These results led to the conclusion that EscC might require some other proteins or factors from T3SS-encoding sequence or the remaining of the EHEC genome for better targeting to the outer membrane. These findings suggest that EscVN did not facilitate targeting of EscC to the outer membrane.

With respect to the functions of EscVN in the T3SS, a homologue of the EscV in Yersinia, YscV, was found to oligomerize and form ring-like structure in the inner membrane (Diepold et al., 2011) that, study also revealed that assembly of YscV was promoted by three other proteins of export apparatus: YscR, YscS and YscT. In the absence of these proteins (YscR, YscS and YscT), fluorescence of fusion protein YscV-EGFP in the membrane decreased dramatically, indicating the lack of targeting to the inner membrane and/or degradation. Data of the above study also indicated that

interaction of the YscV with secretin YscC is not direct, but requires a connecting protein, YscJ. This protein, a homolog of EHEC T3SS protein EscJ, forms a large inner membrane ring within the basal body of *Yersinia* T3SS (Diepold et al., 2011). This information indicates that the EHEC T3SS homologues EscR, EscS and EscT are very likely required for assembly of EscV, and EscJ is required to link EscV to EscC. In the absence of these additional proteins, the over-expression of EscV is very likely to further increase the inner membrane stress and the SecYEG translocon load instead of improving the targeting of EscC to the outer membrane.

Since the purpose of EscNV expression was prevention of EscC leaky mutant toxicity due to the inner membrane targeting, which was unlikely to the published data of *Yersinia* homologues and the observed increased toxicity, these two proteins were excluded from further work with EscC.

5.1.5 Construction of leaky gate mutant libraries of *escC*

Given that cells expressing wild-type EscC were permissive to maltopentaose, but not maltoheptaose, the larger maltooligosaccharide was used to select, from a random mutant library, those mutants that had an increased leaky phenotype relative to wild-type EscC. Given the anticipated toxicity of leaky EscC mutants, *in vitro* rather than *in vivo* mutagenesis was undertaken. For mutagenesis, Φ-29 phage polymerase that carries out rolling circle amplification (RCA) was used in the presence of increased concentrations of $MnCl_2$, which increases the error rate of polymerization (Fujii et al., 2004; Fujii et al., 2014). The RCA product, which is a highly branched dendromer containing multiple-length plasmid products, was cut with single-cutting restriction BamHI, and religated to reconstitute the plasmid monomers. Transformation of the ligation products into the selection strain K2204 resulted in the library of RCA-generated mutants. The mutagenic conditions of the RCA reaction were adjusted using inactivation of *lacZ*α of pUC19 as a gauge, to match the rate that is obtained by *in vivo* mutagenesis in the mutator strain that were successfully used in the published secretin pIV mutagenesis (0.11) (Spagnuolo et al., 2010). Plating efficiency of the mutant library on maltoheptaose-containing M63 minimal media was 0.0038 (1/263) as compared to that on maltose (Table 5.1). The lower frequency of maltoheptaose-permissive mutants relative to *lacZ*α-negative mutants was expected, as the frequency of obtaining the leaky gate mutants observed for secretin pIV was 1/2500 (0.0004),

also much lower than the simple inactivation of *lacZα*, in pUC19 (Spagnuolo et al., 2010). The frequency of 1/263 for EscC was ~10-fold higher than that for pIV; suggesting either a larger number of mutations that cause the leaky phenotype, or less stringent selection.

Table 5.1 Transformation and plating efficiency of EscC-RCA product.

DNA used for transformation	2xYT cfu/µg of DNA	M63 maltose cfu/µg of DNA	M63 maltoheptaose cfu/µg of DNA	Frequency of maltoheptaose-positive colonies[a]
100ng	7.6×10^6	8×10^5	3×10^3	0.0038

[a]Ratio of plating on maltoheptaose relative to the maltose monosaccharide.

Sixteen colonies from the maltoheptaose plate were passaged on the same medium to achieve colony-purification and sequenced their plasmid DNA. Out of 16, ten showed mutation in their DNA sequence and six had no mutations. This observation suggests that the maltoheptaose selection was not highly stringent, potentially due to contamination of the maltoheptaose with shorter-chain maltooligosaccharides, including maltopentaose, to which the cells expressing EscC are permissive.

The ten mutated *escC* CDS's contained a variable number and type of mutations (Table 5.2). Two mutants each contained a single amino acid substitution without any other mutations, while the rest had more than one mutation, including frame-shifts and silent substitutions of nucleotides, two mutants had same frame-shifts mutation. The EscC missense mutations were not localized in the regions corresponding to the clustering of pIV leaky missense mutants (Figure 5.3), apart from one of the two mutations in mutant #1, A428T, which falls in the GATE2 region. The second mutation, A447V, is within the region downstream of the GATE2 hotspot, where the leaky mutations were also identified in pIV and PulD (Spagnuolo et al., 2010). Mutation D289E corresponds to the region where two leaky mutations were identified in PulD (Chapter 3), Similarly, S328N was identified in the N-terminal segment of the secretin homology domain; in the vicinity of $PulD^{L431F}$ leaky mutation.

In mutants 7, 8 and 9 frameshift mutations in the region encoding the N-terminal portion of EscC were identified. Interestingly, additional missense mutations were

detected downstream of the frame-shift in each of these mutants. These additional missense mutations could have made a leaky phenotype, however if they were toxic they could have acquired a compensatory frameshift mutation that placed the channel-forming secretin-homology domain out of frame to overcome the toxicity.

Table 5.2 Sequence analysis of EscC-RCA mutants.

Mutants	Nucleotide changes	Amino acid change	Domain
EscC M1	C711T	-	
	C1257T	-	
	G1282A	A428T	C-terminal
	C1340T	A447V	C-terminal
EscC M2	C207T	-	
	G789A	-	
	T828C	-	
	G983A	S328N	C-terminal
EscC M3	T436C	S146P	N-terminal
EscC M4	T867A	D289E	C-terminal
EscC M5	A270C	-	
	T1039A	S347T	C-terminal
	C1352T	A451V	C-terminal
EscC M6	C252T	-	
EscC M7	C1152T	-	
	1215A	FS [a] after K405	C-terminal
EscC M8	C207T	-	
	246A	FS [a] after K82	N-terminal
EscC M9	401A	FS [a] after N133	N-terminal

[a]FS, frame-shift mutations.

,

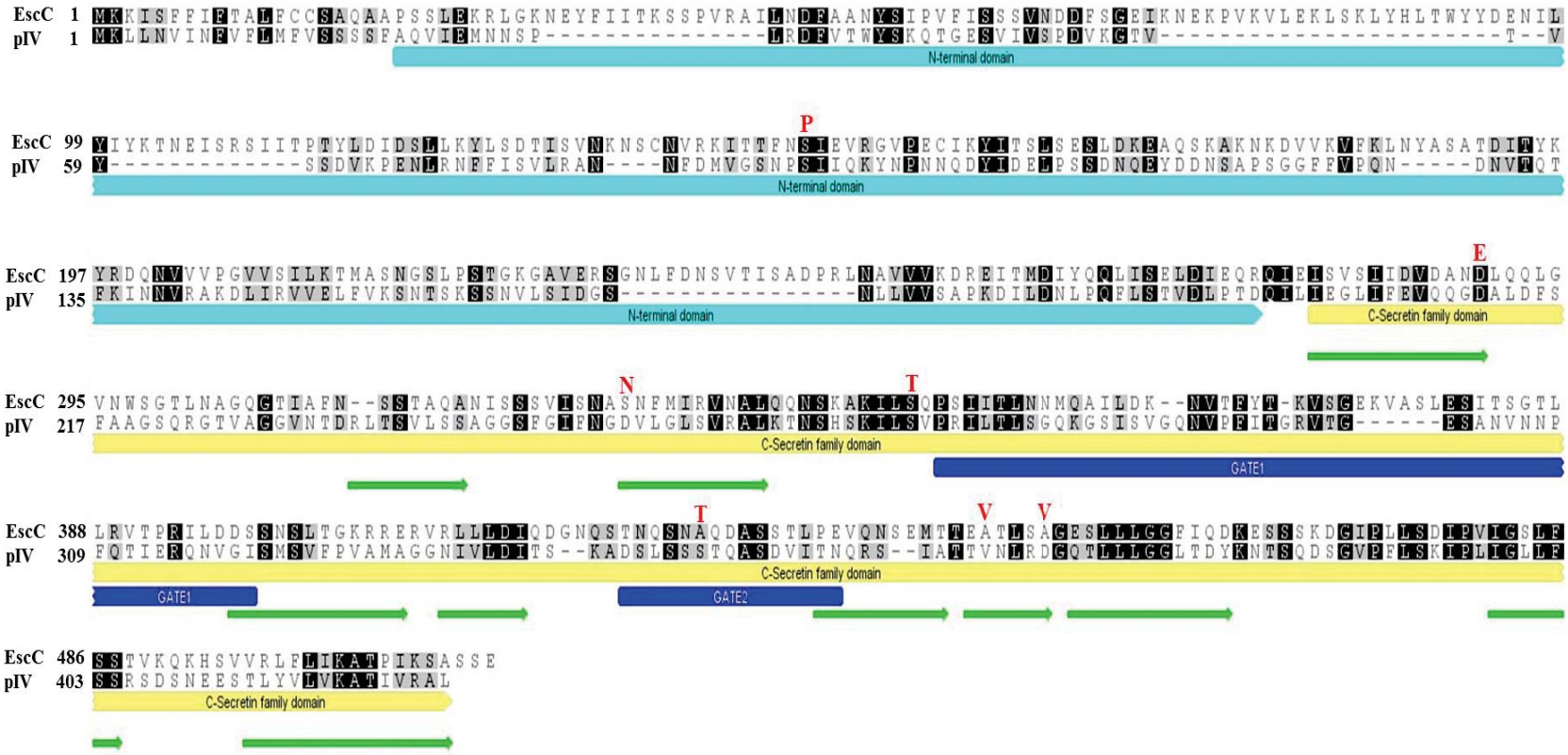

Figure 5.3 Alignment of EscC with pIV, showing the GATE regions as mapped in pIV and the newly obtained EscC mutations.

Domains are shown in different colors: cyan, N-terminal domain; yellow, Secretin homology (C-terminal) domain (pfam number PF00263). Green block arrows represent the transmembrane β strands predicted using TMBETA algorithm. Mutations in EscC (red) and pIV GATE regions (blue) are highlighted.

These findings indicate that either the gate regions of EscC are different from those in pIV and PulD or that the cells expressing EscC leaky gate mutants failed to survive due to toxicity of the leaky secretin. In the colonies containing EscC with multiple mutations, it is possible that colony-forming cells expressed the EscC variants that attained secondary or compensatory mutations that eliminated or decreased the multimeric channel assembly. Three mutants contained a frame shift that eliminated expression of the membrane-inserting secretin homology domain (Mutants 7, 8 and 9). The high frequency wild-type EscC found among mutant library and unmutated plasmid transformants on maltoheptaose are likely due to mutations in their genomes, in genes encoding the outer membrane channels such as BamA or Imp, or the F-pilus assembly system outer membrane channel that could have resulted in a leaky phenotype and growth on maltoheptaose.

Plating efficiency of missense mutants on Van, Bac and DOC was tested to determine whether they became leaky to these molecules (Figure 5.4). Whereas the wild-type EscC showed moderate sensitivity to detergent DOC (decrease in efficiency of plating by bout 20-fold on 0.4 % DOC), unexpectedly, the cells expressing the mutants showed higher plating efficiencies and therefore higher resistance to DOC than the wild-type EscC. While this is hard to rationalize, it is possible that the selective pressure of EscC toxicity in the minimal medium has led to selection of mutants that, while being more permissive for maltoheptaose, became less permissive to DOC. Another explanation is that the sensitivity to DOC that comes from destabilising effect of wild-type EscC on the outer membrane, may have been eliminated in most of the mutants, while the pore size of the EscC channel itself remained too narrow for the DOC micelle (MW=2000 Da). Selection of these mutants on maltoheptaose-containing M63 medium indicates that these mutants can use maltoheptaose (MW=1153 Da) as their sole carbon source. However, they do not allow the entry of higher molecular weight antibiotics Van (1449 Da) and Bac (1423 Da), or detergent deoxycholate (micelle size 2000 Da).

Overall, high frequency of silent and frame-shift mutants invalidated this mutagenic screen. Besides the intrinsic EscC toxicity, the RCA mutagenesis method could also have been a cause of the multiple mutations per CDS.. Multiple mutations are hard to interpret and require further work to separate in order to ascribe each a specific phenotype.

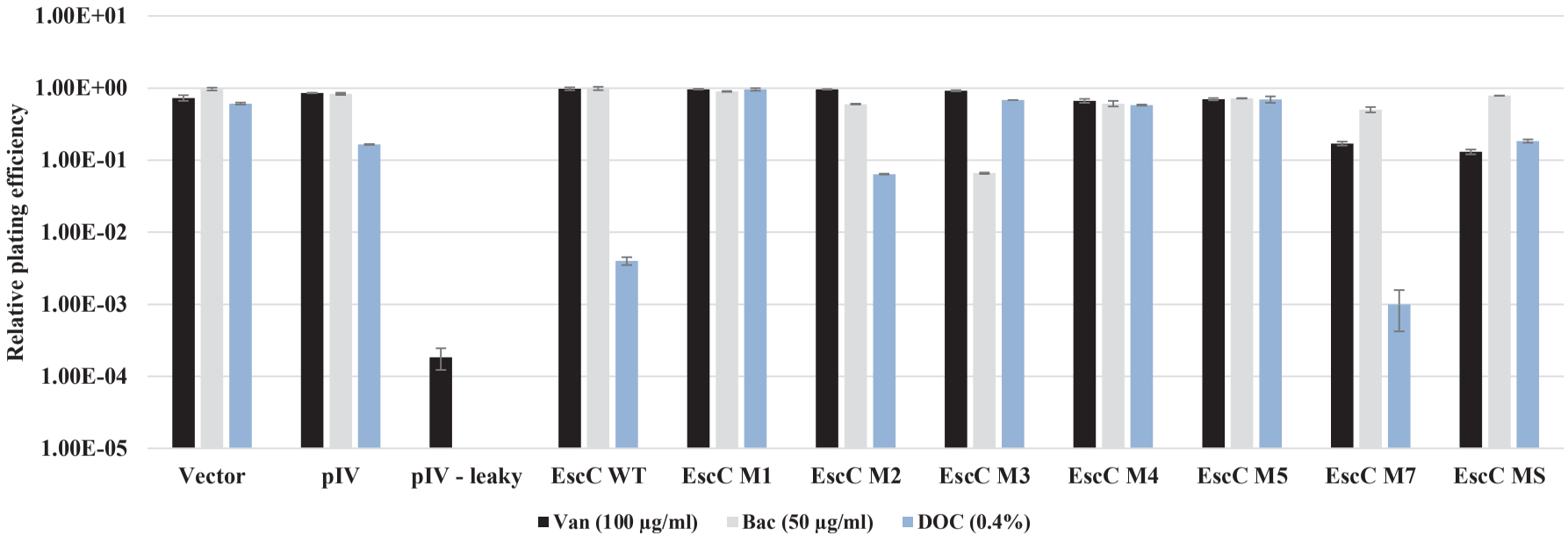

Figure 5.4 Plating efficiencies of EscC mutants in the presence of large antibiotics and DOC.

Plating efficiency of strain K2204 transformed with plasmid expressing wild type EscC and EscC-RCA mutants in the presence of antibiotics and DOC was calculated as a ratio of plating in the absence *vs*. presence of particular antibiotic/detergent Plasmids expressing wild-type pIV and a leaky mutant were used as controls. Vector, pCR-Blunt (expression vector used for cloning of EscC); pIV, pPMR132 (expressing wild-type pIV); pIV leaky, pPMR132-S324G; EscC, pCR-Blunt-EscC (WT); EscC M1, pCR-Blunt-EscC M1 etc; EscC WT-MS, colony from maltoheptaose plate expressing unmutated EscC. Error bars indicate the standard deviations from three biological replicates, each represented by three colony counts.

To overcome the problems caused by the RCA mutagenesis, *in vivo* mutagenesis was undertaken which in the case of PulD and pIV resulted in a range of single mutations, allowing mapping of their GATE regions (Chapter 3; (Spagnuolo et al., 2010; Whitaker., 2012). To mutagenize *escC*, *E. coli* XL1-Red mutator strain was transformed with plasmid expressing EscC. Mutagenized plasmids were transformed into selection strain and plated on maltoheptaose, where colonies were obtained after a seven-day incubation. These colonies were passaged on the same medium (containing maltoheptaose as a sole carbon source) to obtain the clonal lines and then used to isolate plasmid DNA. Surprisingly, sequencing of *escC* from six purified colonies all revealed the wild-type sequence. Given that the wild-type EscC expression is already toxic to *E. coli* after prolonged incubation, it is possible that toxicity of the leaky mutants was so severe that it prevented colony formation on the selection plate. Colonies which grew after seven days of incubation might have acquired undefined chromosomal mutations in other large outer membrane channels, such as general outer membrane translocator BamA or LPS translocator Imp (Ruiz et al., 2005; Ruiz et al., 2006), that could potentially allow uptake of the maltoheptaose.

5.2 InvG, type III secretion system secretin of *Salmonella* Typhimurium

The secretin InvG from *S.* Typhimurim SPI-1-encoded T3SS has been a subject of intense research within the structural and functional studies of this system. Targeting of this secretin to the outer membrane is dependent on the pilotin InvH in *E. coli*, and *S.* Typhimurium, than EscC. Therefore InvG was expressed and its gating regions identified in the primary sequence through mutagenesis.

5.2.1 Phenotypic effect of InvG or InvGH expression

To express the wild-type InvG protein, *invG* gene was amplified from genomic DNA of *S.* Typhimurium strain LT2 and cloned into the vector pGZ119EH under the control of the *tac* promoter. The pilotin InvH was expressed from a vector derived from the pCOLADuet-1, which was modified by replacing T7 promoter with the *tac* promoter (as described in Chapter 2, section 2.4.2). In contrast to PulD-expressing cells that were only slightly affected by induction of PulD expression on its own, due to rapid degradation in the absence of PulS (Chapter 3; Whitaker., 2012), InvG expression on

its own was found to be highly toxic to the *E. coli* strain K2204 (Δ*lamB*), even more toxic than EscC. "Background" expression from the vector in the absence of IPTG decreased the plating efficiency relative to empty-vector-transformed cells to 4.4×10^{-4}. Induction of InvG expression by IPTG decreased plating efficiency to 8.6×10^{-5} in InvH-coexpressing cells, and down to less than 10^{-7}-fold in the absence of InvH (no colonies were formed), showing that the specific pilotin partially rescues the plating of InvG-induced cells (Figure 5.5).

Toxicity of InvG expression to *E. coli* suggests that this secretin is naturally leaky and that in the absence of the pilotin it forms multimers in the inner membrane, resulting in the cell death. To examine whether the InvG targeted to outer membrane (when co-expressed in *E. coli* with InvH) caused a leaky outer membrane phenotype, efficiency of plating on Van, Bac and DOC was determined. The InvG/InvH co-expressing strain showed resistance to Bac and DOC but high sensitivity to Van, (Figure 5.6). These findings show that InvG is leaky when expressed in *E. coli* K12, even more than EscC which did not cause increased sensitivity to Van.

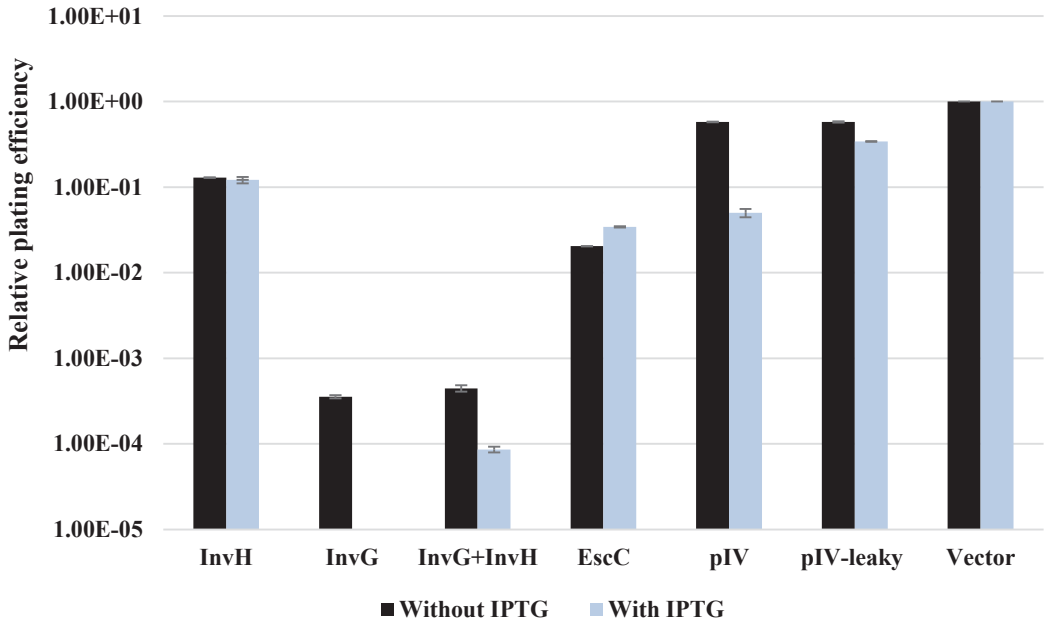

Figure 5.5 Plating efficiency of cells expressing InvG.

Plating efficiency of the strain K2204 transformed with plasmid expressing wild type InvH/InvG/InvG+InvH was calculated relative to the plating of the cells transformed with the vector control in the absence *vs*. presence of 0.1 mM IPTG. Plasmids expressing wild-type EscC, pIV and a pIV-leaky mutant were used as controls. Vector control were cells transformed with pGZ119EH (expression vector used for cloning of InvG) and pCOLADuet-1 containing *tac* promoter (expression vector used for cloning of InvH). InvG, pGZ119EH-InvG; InvH, pCOLADuet-1-InvH; pIV, pPMR132 (expressing wild-type pIV) pIV leaky, pPMR132-S324G; EscC, pCR-Blunt-EscC (WT). Error bars indicate the standard deviations from three biological replicates.

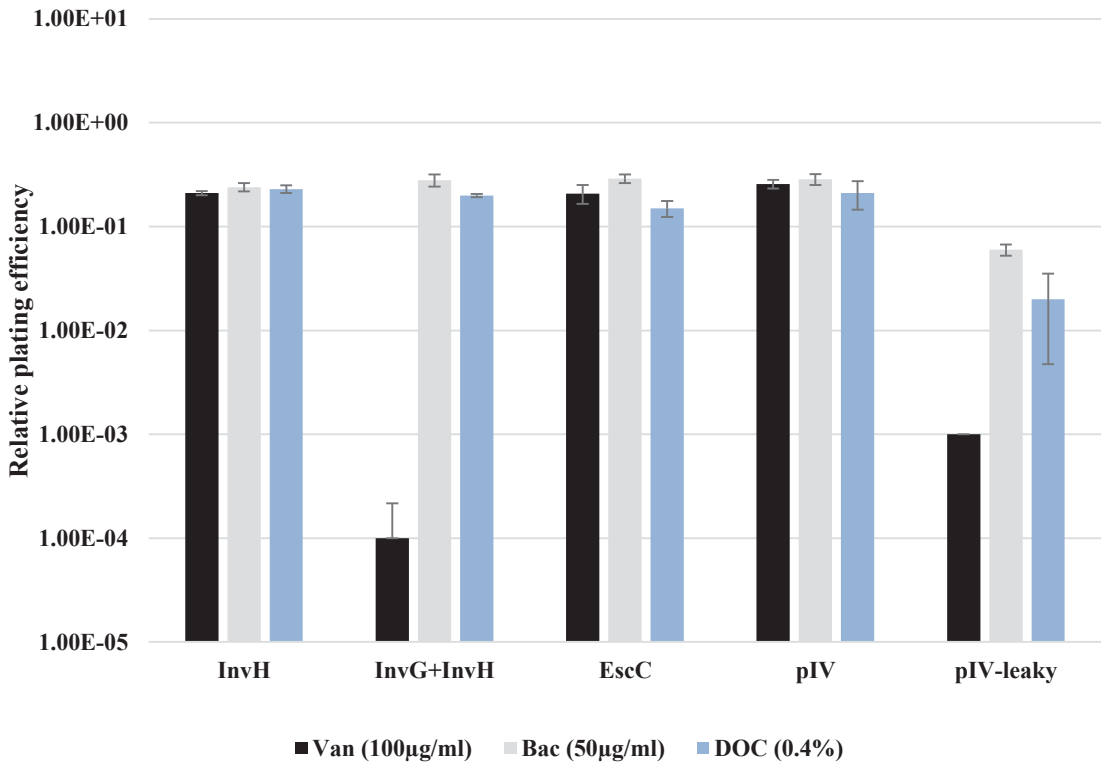

Figure 5.6 Relative plating efficiency of cells expressing InvG in the presence of large antibiotics and DOC.

Plating efficiency of the strain K2204 transformed with plasmids expressing wild type InvH or InvG+InvH in the presence of antibiotics and DOC was calculated as a ratio of plating in the presence *vs*. absence of particular antibiotic/detergent**.** Plasmids expressing wild-type EscC, pIV and a pIV-leaky mutant were used as controls. InvG, pGZ119EH-InvG; InvH, pCOLADuet-1 (with *tac* promoter) InvH; pIV, pPMR132 (expressing wild-type pIV); pIV leaky, pPMR132-S324G; EscC, pCR-Blunt-EscC (WT). All plates contained 0.1 mM IPTG. Error bars indicate the standard deviation from three biological replicates.

To examine whether InvG in the context of T3SS in *S.* Typhimurium (LT2 strain) results in sensitivity to large antibiotics or whether this phenotype occurs, when overexpressed in the absence of other components of the system in *E. coli* K12, *S.* Typhimurium (LT2 strain) was tested for sensitivity to Van, Bac and DOC (Figure 5.7). To insure the expression of the T3SS, a high osmolarity medium (300mM NaCl), known to induce the T3SS expression, was used (Zhao et al., 2001). This experiment showed that *S.* Typhimurium (LT2) was resistant to antibiotics, but slightly sensitive to DOC. These results indicated that observed sensitivity of InvG-expressing cells was due to its expression in *E. coli* K12 which contains different LPS (reported to be important for targeting of secretins to outer membrane and assembly of channel) and/or due to the absence of the remaining proteins of T3SS that could be required for proper targeting. Alternatively, the resistance to Van could be a consequence of curtailing the T3SS expression in majority of the cells in the culture due to toxicity in the absence of positive selection, as reported (Sturm et al., 2011).

E. coli cultures co-expressing InvG and InvH grew in the presence of maltoheptaose as a sole carbon source, confirming the leaky gate. However, colonies on this medium were tiny and transparent, reflecting most likely the cell lysis due to the InvG toxicity, as observed in the rich medium.

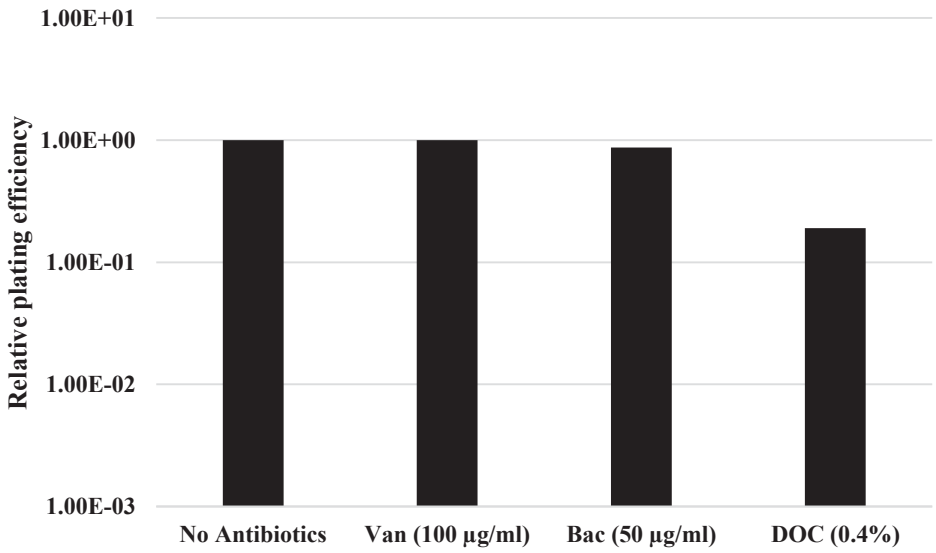

Figure 5.7 Antibiotic and deoxycholate sensitivity assay of *S.* typhimurium LT2.

Relative plating efficiency of *S. typhimurium* LT2 strain was calculated as a ratio of titre in the presence of Van, Bac and DOC relative to titre in the absence of these molecules.

5.2.2 InvG targeting in *Escherichia coli*

InvG expression appeared to be toxic for the *E. coli* K12. As this is a leaky secretin, the toxicity would be achieved primarily by assembly of the channel in the inner membrane, resulting in compromised proton motive force due to a massive proton and ion leakage. This is consistent with partial relief of toxicity in the presence of the pilotin InvH, which has been reported to improve targeting of InvG to outer membrane in *E. coli* (Daefler and Russel, 1998). To monitor localization of InvG in *E. coli*, custom-made antiserum against an N-terminal peptide was developed and the fractionated extract of *E. coli* co-expressing InvG and InvH, was precipitated by TCA and analysed by SDS-PAGE and western blotting. When fractionation was carried out 1 h post-induction of InvG (and InvH) by IPTG; the same time-point at which the EscC-expressing cells were fractionated (Figure 5.8), InvG was identified in all fractions (soluble, inner membrane, outer membrane and aggregates. In particular, monomer and multimer bands were detectable in the aggregate fraction (Figure 5.8a), similarly to EscC. The equivalent experiment in EscC gave an extremely strong monomer band and a ladder of multimers in the aggregate fraction; weak bands were detected in all three other fractions, with the soluble fraction band being stronger than the bands in the inner and outer membrane fractions (Figure 5.8). Therefore, InvG in the presence of co-expressed pilotin InvH has a similar distribution to that of EscC on its own after 1 h of expression (Figure 5.8) . At this time point, massive cell lysis was observed, reflected by decrease in culture density (as determined by a drop of culture OD). As the OD stopped increasing about 30 min after addition of IPTG, another experiment where cells were harvested and fractionated at 20 min post-induction was performed (Figure 5.8b). The signal of InvG monomers was now the strongest in the soluble fraction. In both fractionation experiments, massive increase of the phage shock protein PspA was detected. This reflects high stress to the inner membrane caused by insertion of InvG leaky secretin. Previously, *E. coli* B strain C41 (DE3) derived from BL21 (DE3) with deletion of two proteases genes, *lon* (cytoplasmic; suppressor of envelope stress responses and *ompT* (periplasmic) that degrades misfolded periplasmic proteins and with one uncharacterized mutation, was successfully used for the expression of InvG co-expressed with InvH (Crago and Koronakis, 1998; Miroux and Walker, 1996). The wild-type secretins generally fold into extremely stable multimers (partially resistant to boiling in SDS) that can only be

dissociated at a very low pH (by TCA precipitation). This is supported for both EscC and InvG by detection of multimers in the aggregate fraction (Figure 5.8a) after the TCA precipitation and boiling in SDS (Figure 5.8b), suggesting extremely high stability. Interestingly, at 20 min time point most of the InvG is found in the soluble fraction, suggesting potentially failure to integrate into the membranes which upon extended incubation accumulated as e.g. insoluble aggregates. At 20 min, strong PspA signal was detected in the outer membrane and aggregate fractions, which is the sign of disturbance of outer membrane assembly, resulting in inclusion of phospholipids. In contrast, at the 1 h time point PspA is found in the soluble and inner membrane fractions only, with only a very minor signal in the outer membrane, suggesting that the cells that survived until that time point have an outer membrane that is free of inner membrane and that they did not suffer from defects in the outer membrane assembly.

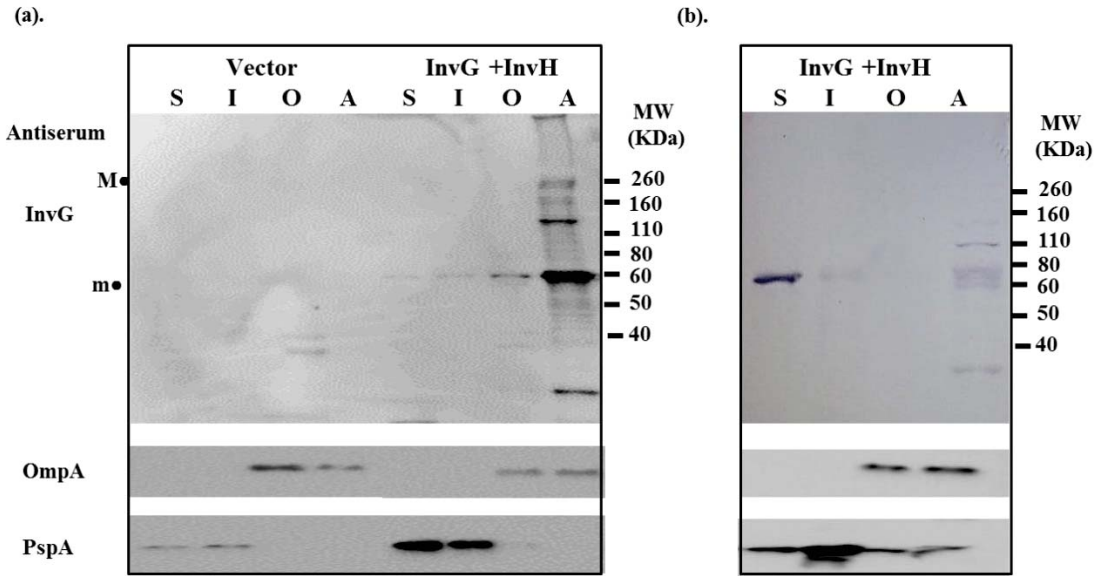

Figure 5.8 Subcellular localization of InvG.

Subcellular fraction of the cultures co-expressing InvG and InvH induced for 1 h (a) or 20 min (b) were subjected to a TCA precipitation to dissociate the InvG multimers and separated by SDS-PAGE (M, multimer; m, monomer). Lanes: S, soluble; I, inner membrane; O, outer membrane; A, aggregate.

5.3 Stress responses required for survival of E. coli K12 expressing EscC and InvG

Expression of EscC and InvG was toxic to the *E. coli* K12 laboratory strain K2204. Based on reports for secretins pIV, PulD and EscC, toxicity of secretins is observed when the leaky channels are targeted to the inner membrane, presumably due to the existence of constitutive pore and/or full opening of the secretin gates, compromising inner membrane integrity and therefore uncoupling proton pumping by electron transport chain from the synthesis of ATP by the synthase which is powered by the proton motive force. While all secretins that integrate into the inner membrane induce the *psp* response, only the leaky secretins are fully or partially toxic to *E. coli*, possibly signifying a limited ability of the stress responses (including *psp*) to mitigate very severe inner membrane stress (Brissette et al., 1990; Flores-Kim and Darwin, 2012; Possot et al., 1992; Russel and Kazmierczak, 1993). For example, the *psp* response is not required for survival of "mild" secretin stress induced by wild-type pIV (Weiner et al., 1991), it is required for survival of cells expressing a highly leaky mutant of pIV (Spagnuolo, unpublished) and T3SS secretin YscC of *Yersinia enterolytica* (Darwin, 2005). Spagnuolo (unpublished) found that the transcription activator of the *psp* response, PspF is required for survival of the *E. coli* K12 expressing a highly leaky secretin pIV. To examine the requirement for the *psp* response for survival of EscC and InvG expression in *E. coli* K12, the plating efficiency of strains containing the null mutations in *pspA* or *pspF* genes was compared to those in the wild-type background as a measure of the synthetic lethality of this combination (Figure. 5.9; 5.10).

It was found that in the absence of PspF, InvG/InvH expression decreased the plating efficiency of the host cells to 7.6×10^{-4} (Figure 5.9; 5.10). Therefore, InvG expression has a major effect is on the inner membrane, similar to that observed for a severely leaky pIV mutant (pIV^{E392K}; Spagnuolo, unpublished).

Synthetic lethality was also observed between the EscC expression and *pspF* null mutation, however the plating efficiency dropped by a much smaller factor (of 8×10^{-2}) relative to the PspF-positive host cells (Figure 5.10). Therefore, the inner membrane stress EscC imposes on the host *E. coli* K12 cells is much less severe than does InvG/InvH combination.

Insertion of a severely leaky mutant of pIV secretin (pIV^{E392K}) into the outer membrane was shown to highly induce osmotic shock responses and to depend on a specific positive gene regulator for survival (Spagnuolo J., unpublished). A response known as the Rcs (regulation of capsular polysaccharide synthesis) phosphorelay system was one of highly induce response by this pIV leaky mutant. In this two-component system, RcsF and RcsC are the sensors while RcsB and RcsA are the effector molecules, which regulate transcription of the target genes by forming homodimers of RcsB or heterodimers of RcsA and RcsB (Huang et al., 2006). Of those, RcsB but not RcsA is required for survival of cells expressing highly leaky mutant of pIV secretin (Spagnuolo, unpublished)To test whether RcsA and/or RcsB are required for survival of cells expressing InvG and EscC, synthetic lethality of their expression in the *rcsA* and *rcsB* null mutants were tested for viability (Figure 5.9; 5.10).

RcsB mutant had mild (if any) effect on survival of EscC and InvG-expressing cells (within one order of magnitude), suggesting that these severity have a minor, if any effect on osmotic stress when expressed in *E. coli*. This is similar to wild-type pIV, but in contrast to severely leaky mutant pIV^{E392K}, which shows very strong osmotic stress and drop in plating efficiency of several orders of magnitude in combination with the *rcsB* null mutation (Spagnuolo, unpublished). This particular pIV mutant causes high sensitivity to Van, Bac and DOC and is more severe than pIV^{S324G}.

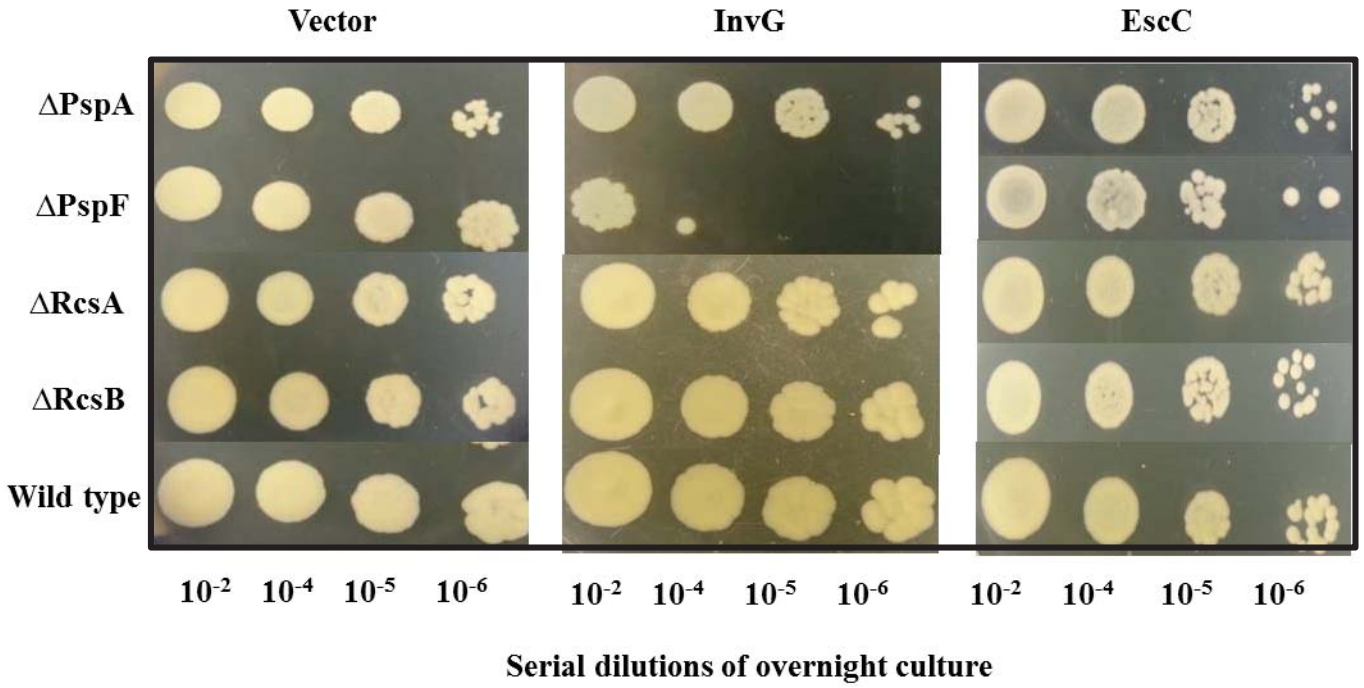

Figure 5.9 Estimation of cell viability with overnight cultures of null mutants of *pspA, pspF*, *rcsA and rcsB* expressing InvG/InvH, EscC and empty vector as control using drop method technique.

(a).

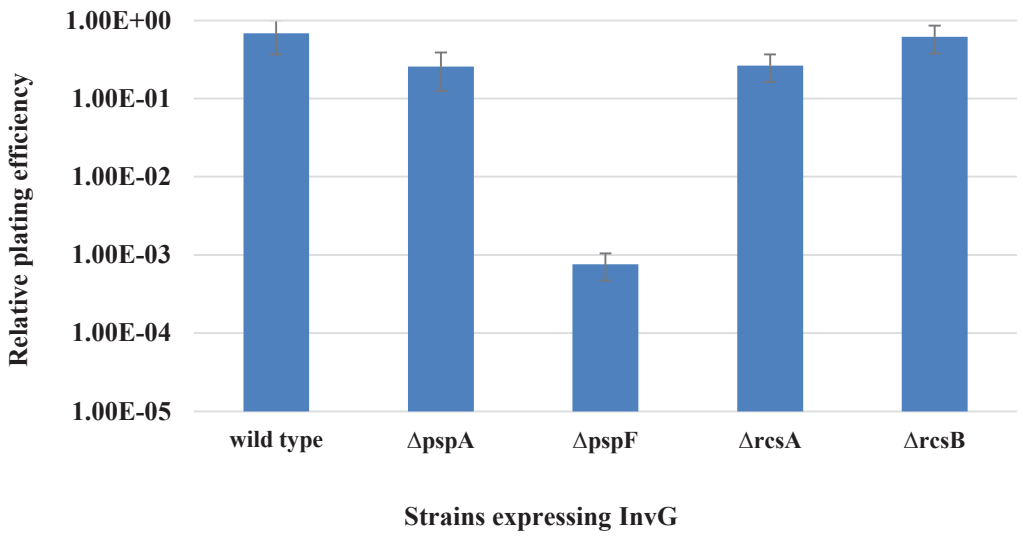

(b).

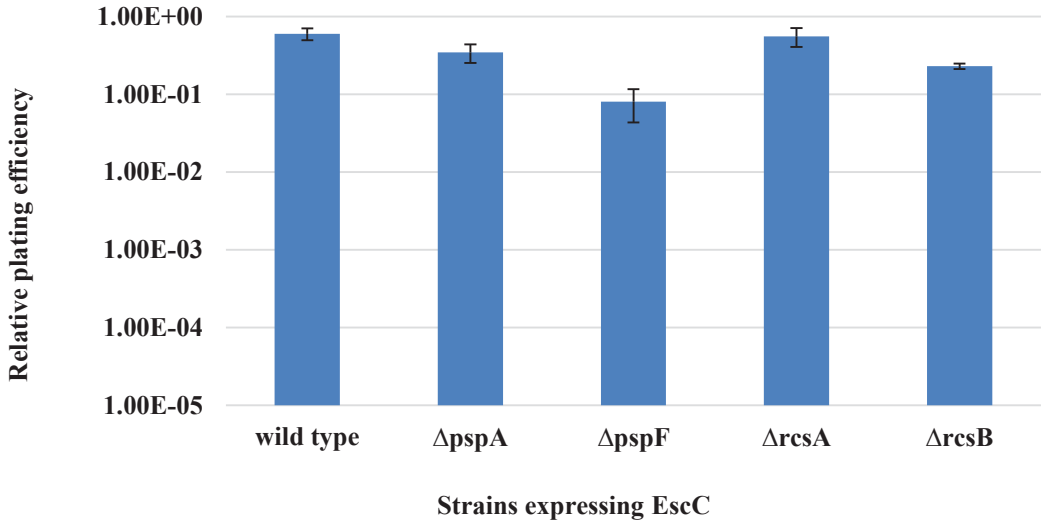

Figure 5.10 Plating efficiencies of InvG and EscC expressing stress response in null mutants.

Plating efficiency of wild-type and null mutants of following genes: *pspA*, *pspF*, *rcsA*, *rcsB*, expressing InvG (a) and EscC (b). The titres were determined by counting between 150 and 300 colonies per plate, on nine plates, representing three biological replicates (three plates for each). Error bars correspond to standard error of the counts on three plates.

5.4 Conclusions

This chapter has analysed the effects of T3SS secretins EscC and InvG on *E. coli* K12 envelope integrity, in order to establish the amenability of these secretins to mutagenesis approach we used for secretin pIV in order to identify the residues involved in gating.

Overall, our results show that both T3SS secretins are naturally "leaky", InvG more so than EscC. Both secretins were inefficient in targeting to the outer membrane, with more protein found in soluble than membrane fractions, and equal or more found in the inner than outer membrane fraction. Interestingly, most of both proteins was found in the aggregate fraction after 1 hr of induction. This was particularly surprising for InvG, which was co-expressed with the cognate pilotin InvH. While InvH relieved extreme toxicity of InvG, indicating a decrease of inner membrane targeting, consistently with a reported improvement of targeting to the outer membrane (Daefler and Russel, 1998), it did not prevent the inner membrane targeting, as shown in cell fractionation experiments and reflected by decreased plating efficiency in the presence vs. absence of induction by IPTG. The secretin-mediated toxicity is unlikely to be limited to expression in *E. coli* K12. It has been shown that induction of T3SS expression and assembly in S. Typhimurium retards the growth and results in curtailing of T3SS gene expression in the absence of selective pressure (Sturm et al., 2011), leading to majority of cells in a culture losing the T3SS production, particularly in the late log culture. The T3SS toxicity could be caused by the leaky secretins, which are the first component that is expressed and which initiates the T3SS assembly.

Consistent with insertion into the inner membrane, both secretins have strongly induced the *psp* response triggered by inner membrane stress. Furthermore, like a severely leaky mutant of secretin pIV, expression in the genetic background that cannot express the *psp* response genes, the toxicity was further increased for InvG than EscC. This correlates with a higher toxicity and more severe leaky phenotype of InvG, based on toxicity and ability to take up >600 Da molecules such as maltoheptaose and Van. The essentiality of the *psp* in relief of the secretin stress therefore places the relevant components of the Psp response, in particular the positive regulator PspF, as potential targets for design of antibacterials that will result in elimination of T3SS-containing (and therefore virulence factor-secreting) enterobacteria.

Chapter 6: Discussion

6.1 PulD C-terminal domain has pIV-homologous GATE1 and GATE2 regions

In this work, we functionally characterized the 13 PulD leaky mutants that increase the penetration of > 600 Da molecules through the PulD secretin channel. ,These mutations were obtained by random mutagenesis and selection experiment carried out by (Whitaker., 2012), but they were not characterised prior to the commencement of this thesis work. The analysis of these 13 leaky mutations in PulD outlined the potential regions involved in the formation of the "gate" or septum structure/regions were found to correspond to the two segments in the secretin homology domain, corresponding to those originally identified in the secretin pIV (Spagnuolo et al., 2010) (Figure 3.1). Alignment of pIV and PulD revealed mutations in the residues that were identical (G458, G466, E480, R481, S516, S517, R529 and G547) or similar (I475, A514 and T518, S519) between the two secretins (annotated here according to the PulD preprotein numbering). These residues, when replaced by another residue or deleted (in-frame deletions), resulted in a leaky phenotype in both secretins.

While pIV and PulD secretins have high identity (29%) of the amino acid primary sequence in their secretin homology domain (Pfam PF00263), and general structure as determined by the cryo-EM and SPA, their symmetries (corresponding to the number of monomers in the channel) are different; pIV is a multimer of 14, whereas PulD is multimer of 12 subunits, hence packing of the monomers may be somewhat different. Recently, a high-resolution cryo-EM structure of the PulD secretin homology domain has been published. The level of detail in this structure allowed differentiation of concentric zones within the septum structure, in which the thick centre (the plug) is connected to the walls of the channel by a grid-like zone. This "grid" appears to contain pores of about 1 nm in diameter, consistent with the ability of PulD to permit passage of small solutes with a similar cut-off as porins (Disconzi et al., 2014; Tosi et al., 2014). However, PulD, like other secretins, secrete folded proteins (PulA), which require diameters of 6 nm or more in order to allow passage of these large folded

polypeptide chains, hence the septum is expected to fully rearrange in order to establish an "active" fully open channel with no detectable septum. Such rearrangement was observed in the T3SS secretin InvG and other T3SS secretins (by cryo-EM and SPA) whose open channel conformation is stabilised by permanent lodgement of a multiprotein rod within the channel (Marlovits et al., 2006; Marlovits et al., 2004; Marlovits and Stebbins, 2009). The phenotype of leaky mutants could therefore be caused by widening of the pores in the grid that forms the septum relative to those in a wild-type PulD, allowing passage of maltopentaose (MW=829 Da) and other >600 Da molecules (depending on the pore size) which cannot pass through the wild-type PulD channel. Alternatively, the leaky phenotype can be caused by an increased tendency of the septum to spontaneously open in the absence of substrate, removing in the process the "flood gate" and freeing the path for the molecules that could not pass through the grid. The latter type of mutants is expected to allow passage of very large molecules and folded proteins through the channel. The presence of mutants with a minor increase in the pore size is evident from the lack of sensitisation to vancomycin (MW=1449 Da) in majority of pIV leaky mutants, particularly those that mapped to the central section of the GATE1 region. In PulD, mutations in the N-terminal cluster (G365C and A369T), did not increase sensitivity to vancomycin, in addition to some of the mutations in the GATE1 (G466C) and GATE2 (A534T). All point mutants were expressed and functional in secretion of PulA, hence they did not form defective multimers. With respect to the mutants that showed sensitivity to vancomycin, a large diameter of grid pore and/or increased frequency of septum opening are equally possible.

In pIV, leaky mutations at the two fringes of GATE1 region and most of the GATE2 mutants showed sensitivity to vancomycin. Similarly, in PulD, mutations at the ends of GATE1, G458S and Δ477-481 showed the highest sensitivity to vancomycin (Table 3.1). Further analysis of these two mutants showed that they have increased sensitivity to larger antimicrobial molecules, daptomycin (MW=1621 Da) and DOC micelle (~1,200-5,000 Da). Furthermore, the Δ477-481 mutant was tested positive for sensitivity to bacteriocin F (MW=5199 Da), a glycoprotein that only kills Gram-positive bacteria (M. Patchett and A. Kerr, unpublished data). This deletion mutation removes five residues at the C-terminal end of GATE1, of which four are identical in pIV. Mutant of the pIV homolog of PulD residue E480 (pIV E293K) showed

extremely high sensitivity to vancomycin and bacitracin (Spagnuolo et al., 2010), as well as mucoid growth and strong induction of envelope stress responses characteristic of hyperosmotic shock, consistent with a dramatic effect on integrity of the outer membrane. This region of GATE1, therefore, is possibly involved in stabilising the septum structure, its mutation resulting in increased frequency of gate opening.

Just upstream of this region, residues 470-474 in GATE1 were shown to be involved in structural maturation of PulD multimer rather than the pore size or channel opening (Guilvout et al., 2014). Three mutations, T470I and G472I/P, were shown to assemble non-functional membrane-associated multimer which does not form a channel in an *in vitro* transcription/translation/lipid insertion system. The multimers of these mutants are completely disassembled upon heating in the presence of SDS/urea, to which the wild-type PulD multimer is resistant. The TEM/single particle analyses showed that the transmembrane (saucer) region of the T470I multimer is in a dramatically different conformation in comparison to the wild-type PulD multimer or channel-forming mutants. Other mutants of the same region, T470V/S and G472A, as well as Gly replacement of the 470-474 segment ($G_{470\text{-}474}$) form at least partially functional multimers. As our selection requires a multimer that forms a channel, it is unlikely that mutations having role in both the determining the pore size and assembly of the channel would have been selected. This is consistent with the absence of leaky mutations at positions 470-474. Interestingly, leaky point mutations in this region were identified in pIV (Spagnuolo et al., 2010), albeit these particular residues were not identical between the two secretins and may not be affecting maturation of the multimer into a channel in pIV.

The five residues missing from the Δ477-481 is not functional in secretion of enzyme pullulanase (PulA), although it forms a multimer. Therefore these residues may have some role in the opening of the channel by interacting with neighbouring monomers in the course of conformational change that occurs at the time of PulA secretion. Mutations in the secretin pIV in this segment, in which 4 out of 5 residues are identical between the two secretins, result in both severely leaky (E292K) and non-functional (F288L) mutations, suggesting functional conservation. Therefore, absence of specific interactions in the channel formed by Δ477-481 PulD mutant perhaps made it non-functional for PulA secretion. These findings indicate the importance of these five

residues at the C-terminal end of GATE1 segment in folding or assembly of the septum and periplasmic vestibule, the latter of which would be required for secretion of the cognate substrates, PulA or filamentous phage. Given the severely leaky phenotype of the PulD Δ477-481 deletion mutant, for which the existence of a channel is a prerequisite, these residues are unlikely to be required for the assembly of the transmembrane portion of the channel.

The severely leaky mutant G458S (at the N-terminal end of the GATE1 segment) was functional in secretion of PulA (46% relative to the wild-type), therefore despite the increased septum permeability or instability of its structure, the function of the multimer in secretion of its cognate substrate was preserved. Interestingly, this residue is conserved in pIV and a leaky mutant in this position was isolated using the same strategy by (Spagnuolo et al., 2010). However, the leaky mutation in pIV had Asp replacing the wild-type Gly, in contrast to Ser or Ala in PulD mutants. In contrast to the two PulD mutants, the pIV leaky mutant in the homologous position was not sensitive to Van; hence the effect of mutation on the channel was likely limited to a small change in the grid pore size.

Interestingly, the G458S mutant was isolated previously in a different screen, for suppression of toxicity of the signal-sequence-less PulD expressed in the cytoplasm and shown to have multimerisation defects in the *in vitro* transcription-translation liposome-targeting system (Guilvout et al., 2011). However, the authors showed that the full-length $PulD_{G458S}$ mutant (including the signal sequence) was not functional in secretion of PulA, in a complementation strain that expressed the *pul* genes (apart from PulD) from a single-copy chromosomal insertion. We used a different complementing strain, in which the *pul* operon was expressed from a pBR322-derived Amp^R plasmid (pCHAP8243), containing the origin of replication typically producing 20 copies of plasmid per cell (Bolivar et al., 1977), therefore the copy number of genes and expression of proteins, including the PulD-specific PulS chaperone (pilotin) required for PulD multimerisation, outer membrane targeting and protection from periplasmic proteases, was higher. This most likely resulted in the observed relatively high amount of the G458S multimer in this work, resulting in a functional channel.

It is worth noting that many leaky mutants, including G458S, were toxic to *E. coli* in combination with the complementing plasmid pCHAP8243 containing the full *pul*

operon complement, but were non-toxic in combination with plasmid pAH181 expressing PulS only. The toxicity of the *pul* operon often resulted in segregation of the plasmid pCHAP8243 and consequently low amount of PulD in the cells due to the absence of PulS and PulA encoded by this plasmid. For this reason, freshly transformed cells were always used in the experiments and multiple cultures were set for each mutant, accompanied by monitoring of the PulD production and segregation of the Amp^R marker in each of the cultures assayed for PulA secretion (Figure 3.3). These experiments showed that, for G458S and other leaky point mutants that were all functional the amount and fraction of secreted PulA was positively correlated with the amount of PulD mutant protein and % of Amp^R cells in the culture. The exception to this was the deletion mutant Δ477-481, which was not functional even in the cells in which it was present in high amount.

6.2 GATE1 pIV-PulD swap chimeras provide insight into the secretin homology domain function and structure

To identify the specific functional domains of the related proteins, analyses of chimeras constructed by precise fusion of protein domains from the related proteins has been a very helpful in structure and function analysis of the proteins (Dunn et al., 1993). For example, this approach has been successfully used in the past to illustrate the structure and functional analysis of ABC transporters and in the development of chimeric antitoxins and vaccines for anthrax (Geillon et al., 2014; Wu et al., 2010). Moreover, functional determinants of closely related proteins like porins were also identified by constructing chimeric proteins (Mizuno et al., 1987; Tommassen et al., 1985; Van Der Ley et al., 1987).

To probe functional compartmentalisation among the secretin domains and the segments involved in gating, the engineered chimeras between pIV and PulD were analysed in this thesis. The first type of chimeras was the swaps of the GATE1 region between the two secretins. Of the two proteins, the $pIV_{(PulDGATE1)}$ chimera showed 10 fold higher phagemid titres in comparison to the negative control, but six orders of magnitude below the wild-type pIV. This is an indication that $pIV_{(PulDGATE1)}$ channel was assembled in the outer-membrane and functional, albeit at a very low efficiency or frequency. The formation of the channel was consistent with the observation that strain expressing $pIV_{(PulDGATE1)}$ was somewhat leaky to maltopentaose (MW 828 Da)

in the Δ*lamB* background. This suggested that PulD GATE1 segment which is shorter by three residues in comparison to the pIV GATE1, on its replacement in pIV might have formed a leaky channel. However, expression of this chimera was not detected in the total cell lysate, suggesting that $pIV_{(PulDGATE1)}$ chimeric secretin has delayed folding and most of the protein was degraded by periplasmic proteases, despite co-expression of its cognate chaperone (pilotin PulS) in the same cells.

The reverse chimera $PulD_{(pIVGATE1)}$ was found to be non-functional in an assay of PulA secretion into the medium. It is worth mentioning, though, that this assay range is only two orders of magnitude due to a high background of PulA leakage from dead and lysed cells, hence, unlike the phagemid assembly assay used for the reverse swap that has a range of seven orders of magnitude, low-activity mutants cannot be detected. With respect to the gate/septum properties, the $PulD_{(pIVGATE1)}$ chimera was not leaky to any of the > 600 Da molecules which can pass through the severely leaky PulD mutants in the GATE1 region, G458S and Δ477-481. To the contrary, the $PulD_{(pIVGATE1)}$ swap was slightly more resistant to rifampicin and vancomycin in quantitative dose-response growth assays, suggesting that they may have slightly tighter gate than PulD (Figure 4.11). Unexpectedly, contrary to the $pIV_{(PulDGATE1)}$ chimera, this $PulD_{(pIVGATE1)}$ chimeric protein was identified in the cells in similar amount to that of the wild-type PulD (hence if was a fast folder) and formed multimers of the same size as did the wild-type PulD. Overall pIV GATE1 sequence, despite being 3 residues longer than that of PulD, did not interfere with folding of the multimer and assembly of the channel.

Overall our analysis of the GATE1 swap chimeras indicates that this region in both pIV and PulD interacts with the neighbouring counterparts in folding, as reflected by the instability of the $pIV_{(PulDGATE1)}$ chimera, however its interactions with the rest of the protein in the terms of folding may be limited, given that the reverse chimera $PulD_{(pIVGATE1)}$ formed a multimer of similar size to that of the wild-type PulD. This region, however, appears to have an important role in secretion, as multimers of a deletion mutant lacking five residues of GATE1 (Δ477-481) and the $PulD_{(pIVGATE1)}$ form multimers that cannot secrete PulA . According to predicted transmembrane β-strands PulD and pIV GATE regions have a loop-like topology (Figure 6.1) which is in agreement with an outer membrane multimeric lipoprotein, CsgG whose crystal

structure was resolved recently (Goyal et al., 2014). CsgG is the curli pilin secretion channel that has radial symmetry and a septum across the channel, albeit it has a smaller diameter and contains a smaller number of subunits (9) in comparison to the secretins, as it secretes unfolded pilus subunits. However, it is morphologically similar in that the lumen of the channel is interrupted with a septum. Interestingly, the septum is formed through the interactions of loop-like structures, one contributed by each monomer (Goyal et al., 2014). Moreover, crystal structure revealed that the septum-forming loop in CsgG is supported by 1 α-helice and 2 β-strands located in the periplasm and outer membrane, respectively. In the absence of high-resolution structure, the TMBETA prediction for transmembrane β-strands in the pIV and PulD secretin homology domain predicted 10-11 β-strands. However, this prediction is not valid for outer membrane proteins with majority of the sequence beyond the transmembrane segment. For example, in the case of TolC channel that has a large periplasmic structure TMBETA predicted 21 transmembrane β-strands, whereas the X-ray structure demonstrated the existence of only 3 (Koronakis et al., 2000). In support of this, a recent Cryo–EM of $PscC^{c}$ revealed 36 density points visualizing surrounding the entire PscC ring, suggest that each monomer could become inserted into the membrane three times (assuming 12-fold symmetry) (Tosi et al., 2014).

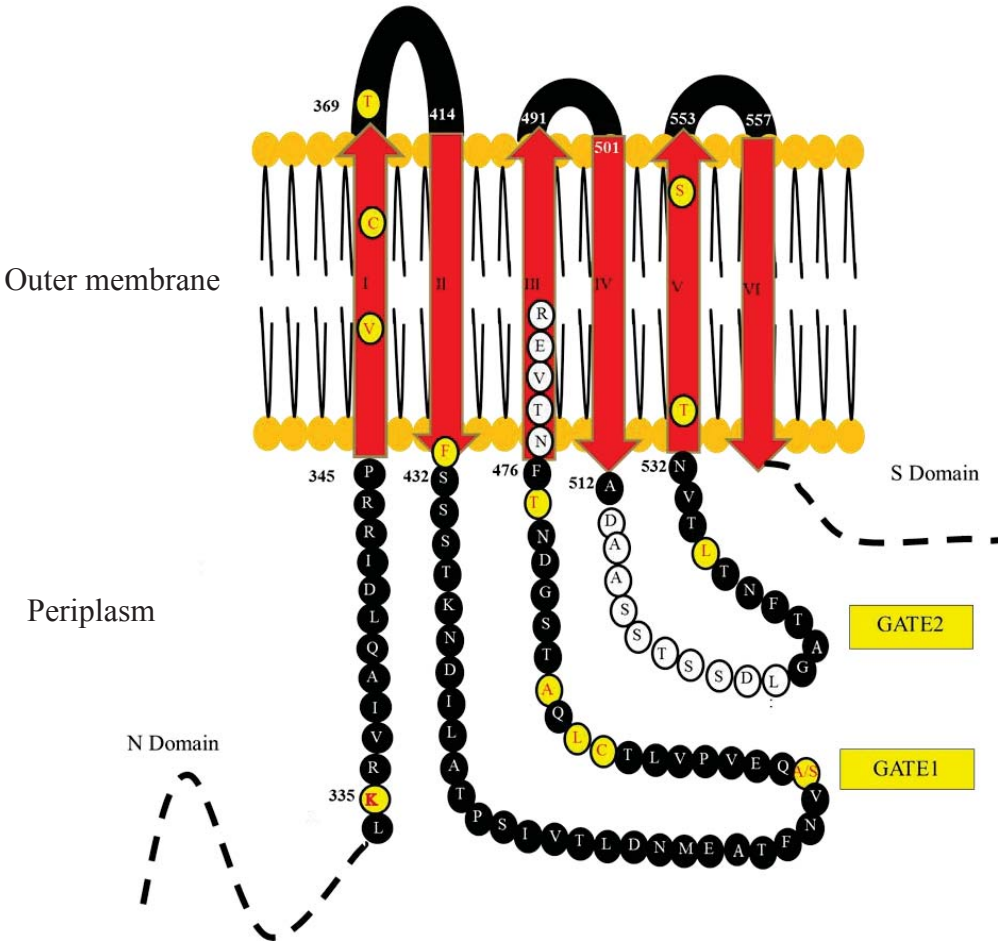

Figure 6.1 Proposed outer membrane topology model of PulD with transmembrane β-strands (red arrow) surrounding the two GATE regions.

Black dashed lines indicate the N and S domains (structures not modelled). The residues of the secretin homology domain predicted to be located at the periplasmic side of the outer membrane were shown as black circles (apart from the positions of leaky mutants that are yellow and deletions that are white), while loops at the external face of the outer membrane are showed as black arcs. Numbers correspond to PulD. Modified with permission from (Reichow et al., 2010; Spagnuolo et al., 2010; Whitaker., 2012)

6.3 N-C pIV-PulD chimeras

Multiple structure-function analyses including deletions, insertions and limited proteolysis suggested that the PulD core region, required for assembly of the channel, is composed of N3, C and S domains, whereas the N0-N2 domains were deemed involved in the interactions with the inner membrane components of the T2SS and not required for folding and assembly of the channel (Chami et al., 2005; Guilvout et al., 2008; Nouwen et al., 1999).

To probe the inter-domain interactions, N-C chimeras between pIV and PulD were constructed and analysed. Although the pIV-PulD N-C chimeras have been constructed in the past (Daefler et al., 1997b), they were not guided by current structural information from the high-resolution studies and modelling of the N0, N1, N2 and N3 domains, hence the joints of chimeras mostly placed with in the folding units. For this reason structure-informed N-C fusions were constructed here and analysed. This analysis resulted in unexpected findings with respect to the interactions between the N-terminal subdomains and the N3-C domains.

Firstly, a chimera that was composed of N0 domain from pIV and the core domain of PulD (N3CS) – previously collectively termed as the "C" domain (Chami et al., 2005; Guilvout et al., 1999; Nouwen et al., 1999) was constructed. However, this chimera could not be detected in the cells; hence its folding has been greatly retarded, resulting in periplasmic proteolysis despite the presence of PulS. This indicates that a correct N0 (N1-N2)-N3 interactions are required for folding of the secretin or one or more of its domains. Alternatively, the pIV N0 domain cannot fold in the absence of the cognate N3, targeting the chimera to the periplasmic proteases that recognise unfolded proteins (DegP). Conversely, mismatched interactions could actively prevent correct folding of the PulD N3 domain. This was not expected as the N0 domain is thought to be flexible with respect to N3 in many secretins, including pIV and PulD, given that they do not form a distinct structure in the Cryo-EM SAP analysis presumably due to having no fixed orientation with respect to the rest of the channel (Korotkov et al., 2009). Overall, this chimera suggests that interaction with cognate N3 is required for correct folding of pIV N0 domain.

The second type of chimera was constructed between the pIV N0N3 domains and the PulD CS moiety; this chimera therefore breaks the PulD "core" domain N3C.

Unexpectedly, this chimera was detectable in high amount in the cells and formed a TCA- and SDS-resistant multimer (Figure 4.8). This was not expected, given that the N3C is assumed to be the core domain of PulD channel. The stability of this fusion means that either PulD N3 is not required for multimerisation, or that the pIV N3 forms the same set of contacts with the PulD C domain as does the PulD N3, hence the folding, outer membrane targeting and multimerisation are not affected. This assumption is in agreement with the recent study where the C-terminal (secretin homology) domain of the T3SS secretin PscC from *Pseudomonas aeruginosa* was shown to be sufficient for the formation of channel (Tosi et al., 2014).

A third chimera N0N3(pIV)347-429*del*CS(PulD) was constructed where pIV N0N3 domains were linked to a truncated C domain (containing a deletion of 83 residues from the N-terminal end of the secretin homology domain of PulD (out of a total of 230 residues). This chimera was detected in the cell lysate and was targeted to the outer membrane. This was again unexpected, as the complete secretin homology domain of PulD was assumed to be required for folding and targeting of secretins. This finding also has repercussions on modelling of the deleted region, ruling out the presence of three TMBETA-predicted transmembrane β-strands within the deleted region (Figure 4.1), as this would potentially have a more detrimental effect on membrane targeting and multimer formation than removal of a periplasmic domain. Therefore, it is very likely that the sequence upstream of GATE1 does not represent transmembrane β strands, but rather contribute to assembly of an independently folding periplasmic portion of the channel, potentially corresponding to a subdomain or a loop in the periplasmic "cup" that was not required for folding, but is required for substrate recognition or secretion This assumption is in agreement with the model of PulD secretin homology domain obtained by a threading modelling program I-TASSER (Figure 6.2) where the N-terminal 96 residues of the C-domain sequence are predicted to fold into a separate domain with little or no contact with the rest of the C-domain. Interestingly, a segment roughly corresponding to this region was the only that, when replaced with the corresponding pIV sequence, did not abolish the pullulanase secretion by PulD.

Although the I-TASSER model does not match the TMBETA prediction in the terms of the number and position of β-strands in the rest of the secretin homology domain, and is modelled on a water-soluble adhesin from Streptococcal pilus subunit, it

predicts the correct number of transmembrane segments (4), three β-strands forming a β-sheet and a α-helix. This is consistent with the 48 density points visualized in recent Cryo–EM of $PulD^{N3C}$ surrounding the entire PulD ring, (assuming 12-fold symmetry) (Tosi et al., 2014).

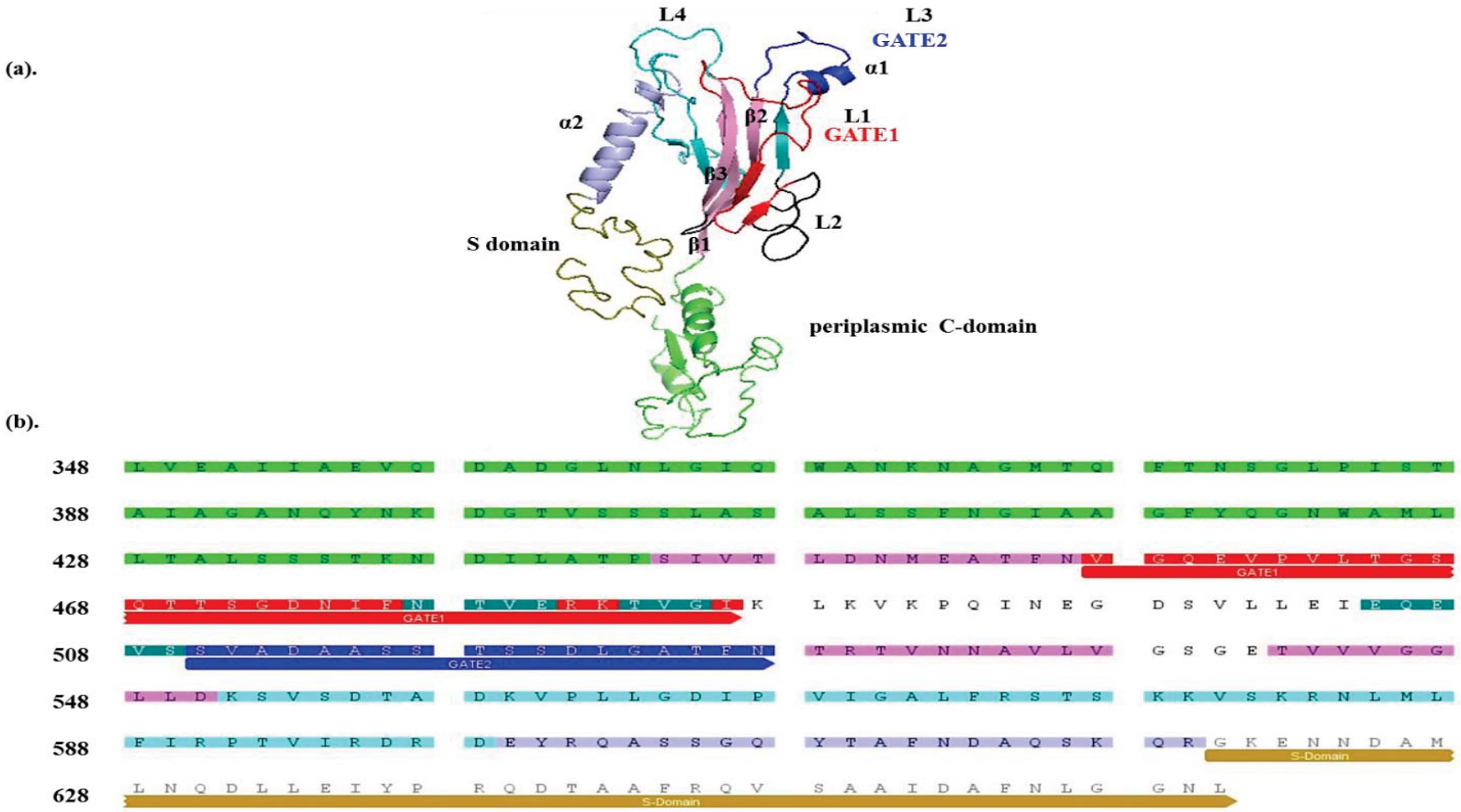

Figure 6.2 Model of PulD secretin homology (C-terminal) domain predicted by I-TASSER (Yang et al., 2015)**.**

Ribbon model (a) and the corresponding structural elements highlighted in the primary sequence (b). Domains and structures are highlighted as follows: β-strands (pink), GATE1 (L1 segment; red); inter-gate segment (L2 segment; black text; not highlighted). GATE2

(L3 segment; blue), post-gate segment (L4, cyan); trans membrane α-helix (α2) (light blue); S-domain (brown). (Numbering corresponds to the full-length PulD preprotein sequence. PulD is modelled using GBS104 (tip pilin of *Streptococcus agalactiae*) protein as a template (Krishnan et al., 2013); the C value for the model fit is -1.58 (C range is -5 to 2, 2 being the best fit).

Neither of the two chimeric secretins that were stable and targeted to the outer membrane was functional in the phagemid assembly or pullulanase secretion assays. This is in agreement with the results obtained using the N-C secretin chimeras of two closely related phages f1 and Ike that had a limited functionality, which was increased by acquisition of compensatory mutations in the N0 and/or N3 domains, resulting in the fully functional chimeras (Daefler et al., 1997b). Together with the results of this thesis work, the published findings show that the pIV N-terminal N0 or N0N3 domain is not autonomous and that it must interact with the C-terminal domain during assembly and secretion of phage This is quite possible as, like other secretins, the septum in pIV is expected to fully rearrange in order to establish an "active" fully open channel for secretion of phage, whose diameter is 6 nm. Such rearrangement was observed by cryo-EM and single particle analysis of the T3SS secretin InvG and other T3SS secretins within the needle complex, in which the base of the needle is lodged within the secretin lumen (Marlovits et al., 2006; Marlovits et al., 2004; Marlovits and Stebbins, 2009).

Multiple lines of evidence show that the interaction of secretins with the inner membrane components of the T2SS or FPSS is mediated through N0 domain of the secretin and in some cases also involve the N3 domain (Gerard-Vincent et al., 2002) (Douzi et al., 2011; Korotkov et al., 2011; Korotkov et al., 2006; Login et al., 2010).With respect to the T2SS, substrate secretion, recent studies using surface plasmon resonance revealed direct interactions between the inner membrane component, GspC, substrate and pseudopilus tip (Douzi et al., 2011). This set of interactions suggests that the inner membrane component of the T2SS, GspC, might recruit the substrate and transfer it to the pseudopilus tip which then carries it towards the secretin through which it is translocated. If this is the case, the observed failure of pIV-PulD chimeras to secrete pullulanase could clearly be explained by the lack of the required interactions between the N0N3 domains of pIV and the inner membrane component of the T2SS, PulC, required for connecting the inner membrane component of the T2SS to the exit port (the secretin).

Despite the established GspC-GspD and pI/pXI-pIV, it is worth mentioning that some filamentous phage, like CTXΦ of *V. cholerae*, do not encode a secretin and use the T2SS secretin EpsD that normally secretes the cholera toxin CtxAB (Davis et al., 2000). EpsD has the same domain organisation as other T2SS secretins, including four

N-terminal subdomains and 12-fold symmetry as PulD. In this case, it appears that the phage inner membrane component, pI/pXI, despite having no homology to the EpsC (GspC, forms interactions with EpsD that allow secretion of the CTX filamentous phage, albeit at a very low efficiency (~1 per 1000 Vibrio cells in the culture under the inducing conditions. This, of course, is much lower than the 10,000 phage per 1 cell for the wild-type f1 (or M13 filamentous phage, hence it is as inefficient as non-functional chimeric secretin N0N3(pIV)CS(PulD) in this thesis.

6.3 Secretins of T3SS are naturally leaky

Secretins of T3SS such as InvG and EscC, are part of a much larger structure, the needle complex, which comprises an external needle and a basal body that traverses both cell membrane and peptidoglycan layer. To determine whether the gating regions are conserved in T3SS secretins InvG and EscC with those identified in pIV and PulD, we cloned InvG, InvH and EscC and expressed them in the *E. coli* K12. Their expression in the *E. coli* laboratory strain with Δ*lamB* background allowed growth on the minimal media containing, as the sole carbon source, oligosaccharide maltopentaose which cannot pass through the secretin of T2SS (PulD) and FPSS secretin (pIV). The leaky phenotype is consistent with observations for another T3SS secretin, YscC of *Yersinia enterocolitica*, which in lipid bilayer forms stable high-conductance channel contrary to pIV and PulD, which show conductance only upon application of relatively high voltage, reflecting a requirement for opening of the septum to allow ion conductance. However, stable conductance of YscC reflects constitutively open conformation (Burghout et al., 2004b), hence the secretins of T3SS are naturally leaky when expressed without the rest of the basal body components. Once assembled, the complete T3SS needle complex is a stable structure, and once the needle base and the needle are assembled within the secretin barrel, it remains continuously open, and the channel must be plugged at the inner membrane component of the T3SS machinery. In other systems, such as T2SS and FPSS, the secretion seems to be more dynamic with respect to the secretins, and secretin septum is closed when not actively involved in secretion of substrates.

The secretin-mediated toxicity is unlikely to be limited to expression in *E. coli* K12. It has been shown that induction of T3SS expression and assembly in *Salmonella* Typhimurium retards the growth and results in curtailing of T3SS gene expression in

the absence of selective pressure (Sturm et al., 2011), leading to majority of cells in a culture losing the T3SS production, particularly in the late log culture. The T3SS toxicity could be caused by the leaky secretins, which are the first component that is expressed and which initiates the T3SS assembly.

Consistent with insertion into the inner membrane, both secretins have strongly induced the *psp* response to inner membrane stress. The essentiality of the *psp* in relief of the secretin stress therefore places the relevant components of the Psp response, in particular the positive regulator PspF, as potential targets for design of antibacterials that will result in elimination of T3SS-containing (and therefore virulence factor-secreting) enterobacteria.

6.4 Conclusions

This work has focused on PulD secretin from the standpoint of gating and communication between the N- and the C-terminal domain in the targeting to the outer membrane and the function in secretion. This work has shown that, although this region can be mutated and the function retained, the in-frame deletion mutant loses function despite assembling into a multimer, indicating the importance of correct folding and/or interactions with the substrate and/or other domains or subunits of PulD in secretion. The importance of this segment for folding was shown by instability of pIV containing the PulD GATE1 sequence, albeit the opposite chimera was stable.

Analysis of the N-C chimeras showed that folding of pIV N0 requires either the presence of or interactions with N3; furthermore, it showed that PulD N3 is not required for folding and multimerisation of the C domain, or that pIV N3 domain forms the necessary contacts. It also showed that the N-terminal 83 residues of the C domain were not required for folding, and therefore may form an independently folding periplasmic domain devoid of transmembrane β-strands.

The ability of two leaky PulD GATE1 mutants to sensitise *E. coli* to a set of widely used >600 Da antibiotics and to detergent sodium deoxycholate, as well as its conservation among the T2SS and it role in substrate secretion qualifies this structure as a potential drugable target for T2SS that would sensitise pathogenic bacteria to large antibiotics and prevent the virulence factor secretion.

This work showed that secretins of type III secretion system have intrinsically leaky gates. The toxicity of the leaky mutants in partially leaky EscC likely prevented isolation of severely leaky mutants by the random mutagenesis and selection procedure. This is consistent with the toxicity of T3SS secretins and published work indicating that the expression of T3SS retards growth of the host bacteria. In the case of InvG, the phage shock protein positive regulator, controlling all but one *psp* genes, was required for survival of the expressing cells, whereas the dependence of less toxic and less leaky secretin EscC was less dependent on PspF. The protective effect of psp was not mediated by the most highly induced Psp protein PspA, but rather one of other Psp proteins. This brings about PspF as a potential target for killing bacteria expressing the T3SS, thereby attenuating specifically the toxin-secretin cells.

Work presented in this thesis suggests that the use of molecules (which target the secretins and open the channels) in conjunction with large-size antibiotics may be a viable strategy for treatement of the infections caused by pathogenic Gram-negative bacteira that have the secretin channels in their outer membrane. Molecules targeting secretin of one secretion system may be effective against secretins of other secretion systems due to conserved nature of the C-terminal trans-membrane domain among the members of the secretin family (Veenendaal et al., 2009).

6.5 Future directions

This thesis has made hypotheses on structure and function of PulD and pIV based on mutagenesis and constructions of the chimeras. In order to get ultimate information on the gating of the secretins, high resolution structural details are required. To characterise the mechanism by which mutations render PulD leaky, *in vitro* electrophysiological assays are required (Marciano et al., 1999).

Short of the high resolution structure, a protein evolution experiment where non-functional chimeras of pIV and PulD will be subjected to mutagenesis and the functional mutants will be isolated by selection of self-assembling phagemids in the phagemid complementation assay developed in this thesis, in order to identify residues involved in interaction between the N and C moieties of the secretins.

Given that the T2SS secretins are potential targets for gate-opening and secretin-inhibiting molecules, a screen for molecules that will render *E. coli* leaky to > 600 Da antibiotics will be carried out to identify the PulD/PulS-dependent antibacterial molecules and validated in the presence and absence of PulD/PulS expression.

This work has shown that the secretins EscC and InvG expressed out of the context of the T3SS is leaky, however it is possible that in the context of the complete basal body the secretin gate would be stable and not leaky. To determine whether this is the case, the secretins should be co-expressed with other components of the basal body, either in the laboratory strains of *E. coli* or in the species and strains where they are originally expressed. If the secretins are not leaky in this context, mutagenesis of the plasmid expressing the whole set of basal body-encoding genes would be carried out to identify leaky mutations in the secretin and other basal body components involved in gating.

The effect of the basal body and the complete T3SS on induction of the Psp response should also be investigated, as well as synthetic lethality of the T3SS expression and *ΔpspF*. In the case that the synthetic lethality is confirmed, PspF would be considered a target for killing of T3SS-expresing, toxin-secreting cells. The screening of the molecules which would prevent induction of the Psp response will be undertaken to identify the PspF inhibitors. These molecules will further be validated for killing bacteria that express T3SS and secrete toxins.

References

Albers, S.-V., and Pohlschroeder, M. (2009). Diversity of archaeal type IV pilin-like structures. Extremophiles *13*, 403-410.

Anderson, D.M., and Schneewind, O. (1997). A mRNA signal for the type III secretion of Yop proteins by Yersinia enterocolitica. Science *278*, 1140-1143.

Angstrom, J., Teneberg, S., and Karlsson, K.A. (1994). Delineation and comparison of ganglioside-binding epitopes for the toxins of *Vibrio cholerae*, *Escherichia coli* and *Clostridium tetan*i, evidence for overlapping epitopes. Proceedings of the National Academy of Sciences of the United States of America *91*, 11859-11863.

Arts, J., van Boxtel, R., Filloux, A., Tommassen, J., and Koster, M. (2007). Export of the pseudopilin XcpT of the *Pseudomonas aeruginosa* type II secretion system via the signal recognition particle-Sec pathway. Journal of Bacteriology *189*, 2069-2076.

Askora, A., Kawasaki, T., Usami, S., Fujie, M., and Yamada, T. (2009). Host recognition and integration of filamentous phage phiRSM in the phytopathogen, *Ralstonia solanacearum*. Virology *384*, 69-76.

Ayers, M., Howell, P.L., and Burrows, L.L. (2010). Architecture of the type II secretion and type IV pilus machineries. Future Microbiology *5*, 1203-1218.

Baba, T., Ara, T., Hasegawa, M., Takai, Y., Okumura, Y., Baba, M., Datsenko, K.A., Tomita, M., Wanner, B.L., and Mori, H. (2006). Construction of *Escherichia coli* K-12 in-frame, single-gene knockout mutants: the Keio collection. Molecular Systems Biology *2*. Doi: 10.1038/msb4100050.

Bennett, N.J., Gagic, D., Sutherland-Smith, A.J., and Rakonjac, J. (2011). Characterization of a dual-function domain that mediates membrane insertion and excision of ff filamentous bacteriophage. Journal of Molecular Biology *411*, 972-985.

Berry, J.-L., Phelan, M.M., Collins, R.F., Adomavicius, T., Tonjum, T., Frye, S.A., Bird, L., Owens, R., Ford, R.C., Lian, L.-Y., *et al.* (2012). Structure and assembly of a trans-periplasmic channel for type IV pili in *Neisseria meningitidis*. PLoS pathogens *8*. Doi: 10.1371/journal.ppat.1002923.

Bitter, W., Koster, M., Latijnhouwers, M., de Cock, H., and Tommassen, J. (1998). Formation of oligomeric rings by XcpQ and PilQ, which are involved in protein transport across the outer membrane of *Pseudomonas aeruginosa*. Molecular Microbiology *27*, 209-219.

Blocker, A., Komoriya, K., and Aizawa, S. (2003). Type III secretion systems and bacterial flagella: Insights into their function from structural similarities. Proceedings of the National Academy of Sciences of the United States of America *100*, 3027-3030.

Bolivar, F., Rodriguez, R.L., Greene, P.J., Betlach, M.C., Heyneker, H.L., Boyer, H.W., Crosa, J.H., and Falkow, S. (1977). Construction and characterization of new cloning vehicles .2. Multipurpose cloning system. Gene *2*, 95-113.

Boor, K.J. (2006). Bacterial stress responses: What doesn't kill them can make them stronger. Plos Biology *4*, 18-20.

Bouley, J., Condemine, G., and Shevchik, V.E. (2001). The PDZ domain of OutC and the N-terminal region of OutD determine the secretion specificity of the type II out pathway of *Erwinia chrysanthemi*. Journal of Molecular Biology *308*, 205-219.

Brissette, J.L., and Russel, M. (1990). Secretion and membrane integration of a filamentous phage-encoded morphogenetic protein. Journal of Molecular Biology *211*, 565-580.

Brissette, J.L., Russel, M., Weiner, L., and Model, P. (1990). Phage shock protein, a stress protein of *Escherichia-coli*. Proceedings of the National Academy of Sciences of the United States of America *87*, 862-866.

Brissette, J.L., Weiner, L., Ripmaster, T.L., and Model, P. (1991). Characterization and sequence of the *Escherichia coli* stress-induced psp operon. Journal of Molecular Biology *220*, 35-48.

Brok, R., Van Gelder, P., Winterhalter, M., Ziese, U., Koster, A.J., de Cock, H., Koster, M., Tommassen, J., and Bitter, W. (1999). The C-terminal domain of the *Pseudomonas* secretin XcpQ forms oligomeric rings with pore activity. Journal of Molecular Biology *294*, 1169-1179.

Buchan, D.W., Minneci, F., Nugent, T.C., Bryson, K., and Jones, D.T. (2013). Scalable web services for the PSIPRED protein analysis workbench. Nucleic Acids Research *41*, 349-357.

Buddelmeijer, N., Krehenbrink, M., Pecorari, F., and Pugsley, A.P. (2009). Type II secretion system secretin PulD localizes in clusters in the *Escherichia coli* outer membrane. Journal of Bacteriology *191*, 161-168.

Buettner, D. (2012). Protein export according to schedule: Architecture, assembly, and regulation of type III secretion systems from plant- and animal-pathogenic bacteria. Microbiology and Molecular Biology Reviews *76*, 262-310.

Burghout, P., Beckers, F., de Wit, E., van Boxtel, R., Cornelis, G.R., Tommassen, J., and Koster, M. (2004a). Role of the pilot protein YscW in the biogenesis of the YscC secretin in *Yersinia enterocolitica*. Journal of Bacteriology *186*, 5366-5375.

Burghout, P., van Boxtel, R., Van Gelder, P., Ringler, P., Muller, S.A., Tommassen, J., and Koster, M. (2004b). Structure and electrophysiological properties of the YscC secretin from the type III secretion system of *Yersinia enterocolitica*. Journal of Bacteriology *186*, 4645-4654.

Burrows, L.L. (2005). Weapons of mass retraction. Molecular Microbiology *57*, 878-888.

Campbell, J. (2010). High-throughput assessment of bacterial growth inhibition by optical density measurements. Current protocols in chemical biology *2*, 195-208.

Castanie-Cornet, M.P., Cam, K., and Jacq, A. (2006). RcsF is an outer membrane lipoprotein involved in the RcsCDB phosphorelay signaling pathway in *Escherichia coli*. Journal of Bacteriology *188*, 4264-4270.

Chami, M., Guilvout, I., Gregorini, M., Remigy, H.W., Muller, S.A., Valerio, M., Engel, A., Pugsley, A.P., and Bayan, N. (2005). Structural insights into the secretin PulD and its trypsin-resistant core. Journal of Biological Chemistry *280*, 37732-37741.

Chandran, V., Fronzes, R., Duquerroy, S., Cronin, N., Navaza, J., and Waksman, G. (2009). Structure of the outer membrane complex of a type IV secretion system. Nature *462*, 1011-1066.

Chen, L.M., Bagrodia, S., Cerione, R.A., and Galan, J.E. (1999). Requirement of p21-activated kinase (PAK) for *Salmonella typhimurium*-induced nuclear responses. Journal of Experimental Medicine *189*, 1479-1488.

Cherepanov, P.P., and Wackernagel, W. (1995). Gene disruption in *Escherichia coli* - TcR and Km(R) cassettes with the option of flp-catalyzed excision of the antibiotic-resistance determinant. Gene *158*, 9-14.

Chin-Yi, C., Nace, G.W., and Irwin, P.L. (2003). A 6 x 6 drop plate method for simultaneous colony counting and MPN enumeration of *Campylobacter jejuni*, *Listeria monocytogenes*, and *Escherichia coli*. Journal of Microbiology Methods *55*, 475-479.

Chiu, C.H., Su, L.H., and Chu, C. (2004). *Salmonella enterica* serotype Choleraesuis: Epidemiology, pathogenesis, clinical disease, and treatment. Clinical Microbiology Reviews *17*, 311-322.

Clavel, T., Lazzaroni, J.C., Vianney, A., and Portalier, R. (1996). Expression of the *tolQRA* genes of *Escherichia coli* K-12 is controlled by the RcsC sensor protein involved in capsule synthesis. Molecular Microbiology *19*, 19-25.

Coburn, B., Sekirov, I., and Finlay, B.B. (2007). Type III secretion systems and disease. Clinical Microbiology Reviews *20*, 535-549.

Collin, S., Guilvout, I., Nickerson, N.N., and Pugsley, A.P. (2011). Sorting of an integral outer membrane protein via the lipoprotein-specific Lol pathway and a dedicated lipoprotein pilotin. Molecular Microbiology *80*, 655-665.

Collins, R.F., Beis, K., Dong, C., Botting, C.H., McDonnell, C., Ford, R.C., Clarke, B.R., Whitfield, C., and Naismith, J.H. (2007). The 3D structure of a periplasm-spanning platform required for assembly of group 1 capsular polysaccharides in *Escherichia coli*. Proceedings of the National Academy of Sciences of the United States of America *104*, 2390-2395.

Collins, R.F., Frye, S.A., Kitmitto, A., Ford, R.C., Tonjum, T., and Derrick, J.P. (2004). Structure of the *Neisseria meningitidis* outer membrane PilQ secretin complex at 12 A resolution. Journal of Biological Chemistry *279*, 39750-39756.

Cornelis, G.R. (2006). The type III secretion injectisome. Nature Reviews Microbiology *4*, 811-825.

Crago, A.M., and Koronakis, V. (1998). *Salmonella* InvG forms a ring-like multimer that requires the InvH lipoprotein for outer membrane localization. Molecular Microbiology *30*, 47-56.

Craig, L., and Li, J. (2008). Type IV pilli: paradoxes in form and function. Current Opinion in Structural Biology *18*, 267-277.

d'Enfert, C., Reyss, I., Wandersman, C., and Pugsley, A.P. (1989). Protein secretion by Gram-negative bacteria: characterization of two membrane proteins required for pullulanase secretion by *Escherichia coli* K-12. Journal of Biological Chemistry *264*, 17462-17468.

Daefler, S., Guilvout, I., Hardie, K.R., Pugsley, A.P., and Russel, M. (1997a). The C-terminal domain of the secretin PulD contains the binding site for its cognate chaperone, PulS, and confers PulS dependence on plV(f1) function. Molecular Microbiology *24*, 465-475.

Daefler, S., and Russel, M. (1998). The *Salmonella typhimurium* InvH protein is an outer membrane lipoprotein required for the proper localization of InvG. Molecular Microbiology *28*, 1367-1380.

Daefler, S., Russel, M., and Model, P. (1997b). Module swaps between related translocator proteins pIV(f1), pIV(IKe) and PulD: Identification of a specificity domain. Journal of Molecular Biology *266*, 978-992.

Darwin, A.J. (2005). The phage-shock-protein response. Molecular Microbiology *57*, 621-628.

Darwin, A.J. (2013). Stress relief during host infection: The phage shock protein response supports bacterial virulence in various ways. PLoS pathogens *9*. Doi: 10.1371/journal.ppat.1003388.

Dautin, N., and Bernstein, H.D. (2007). Protein secretion in Gram-negative bacteria via the autotransporter pathway. In Annual Review of Microbiology, pp. 89-112.

Davis, B.M., Lawson, E.H., Sandkvist, M., Ali, A., Sozhamannan, S., and Waldor, M.K. (2000). Convergence of the secretory pathways for cholera toxin and the filamentous phage, CTXphi. Science *288*, 333-335.

Deng, L.W., and Perham, R.N. (2002). Delineating the site of interaction on the pIII protein of filamentous bacteriophage fd with the F-pilus of *Escherichia coli*. Journal of Molecular Biology *319*, 603-614.

Deng, W., Puente, J.L., Gruenheid, S., Li, Y., Vallance, B.A., Vazquez, A., Barba, J., Ibarra, J.A., O'Donnell, P., Metalnikov, P., *et al.* (2004). Dissecting virulence: systematic and functional analyses of a pathogenicity island. Proceedings of the National Academy of Sciences of the United States of America *101*, 3597-3602.

Diepold, A., Amstutz, M., Abel, S., Sorg, I., Jenal, U., and Cornelis, G.R. (2010). Deciphering the assembly of the *Yersinia* type III secretion injectisome. European Molecular Biology Organization Journal *29*, 1928-1940.

Diepold, A., Wiesand, U., and Cornelis, G.R. (2011). The assembly of the export apparatus (YscR,S,T,U,V) of the Yersinia type III secretion apparatus occurs independently of other structural components and involves the formation of an YscV oligomer. Molecular Microbiology *82*, 502-514.

Disconzi, E., Guilvout, I., Chami, M., Masi, M., Huysmans, G.H.M., Pugsley, A.P., and Bayan, N. (2014). Bacterial secretins form constitutively open pores akin to general porins. Journal of Bacteriology *196*, 121-128.

Dorsey, F.C., Fischer, J.F., and Fleckenstein, J.M. (2006). Directed delivery of heat-labile enterotoxin by enterotoxigenic *Escherichia coli*. Cellular Microbiology *8*, 1516-1527.

Douet, V., Loiseau, L., Barras, F., and Py, B. (2004). Systematic analysis, by the yeast two-hybrid, of protein interaction between components of the type II secretory machinery of *Erwinia chrysanthemi*. Research in Microbiology *155*, 71-75.

Douzi, B., Ball, G., Cambillau, C., Tegoni, M., and Voulhoux, R. (2011). Deciphering the Xcp *Pseudomonas aeruginosa* type II secretion machinery through multiple interactions with substrates. Journal of Biological Chemistry *286*, 40792-40801.

Dunn, B., Stearns, T., and Botstein, D. (1993). Specificity domains distinguish the Ras-related Gtpases Ypt1 and Sec4. Nature *362*, 563-565.

Dunstan, R.A., Heinz, E., Wijeyewickrema, L.C., Pike, R.N., Purcell, A.W., Evans, T.J., Praszkier, J., Robins-Browne, R.M., Strugnell, R.A., Korotkov, K.V.*, et al.* (2013). Assembly of the type II secretion system such as found in *Vibrio cholerae* depends on the novel pilotin Asps. PLoS pathogens 9(1): Doi:10.1371/journal.ppat.1003117.

Durand, E., Alphonse, S., Brochier-Armanet, C., Ball, G., Douzi, B., Filloux, A., Bernard, C., and Voulhoux, R. (2011). The assembly mode of the seudopilus a hallmark to distinguish a novel secretion system subtype. Journal of Biological Chemistry *286*, 24407-24416.

Economou, A., Christie, P.J., Fernandez, R.C., Palmer, T., Plano, G.V., and Pugsley, A.P. (2006). Secretion by numbers: protein traffic in prokaryotes. Molecular Microbiology *62*, 308-319.

Elliott, S.J., Sperandio, V., Giron, J.A., Shin, S., Mellies, J.L., Wainwright, L., Hutcheson, S.W., McDaniel, T.K., and Kaper, J.B. (2000). The locus of enterocyte effacement (LEE)-encoded regulator controls expression of both LEE- and non-LEE-encoded virulence factors in enteropathogenic and enterohemorrhagic *Escherichia coli*. Infection and Immunity *68*, 6115-6126.

Fabrega, A., and Vila, J. (2013). *Salmonella enterica* serovar Typhimurium skills to succeed in the host: Virulence and regulation. Clinical microbiology reviews *26*, 308-341.

Feng, J.N., Model, P., and Russel, M. (1999). A trans-envelope protein complex needed for filamentous phage assembly and export. Molecular Microbiology *34*, 745-755.

Ferguson, A.D., Breed, J., Diederichs, K., Welte, W., and Coulton, J.W. (1998). An internal affinity-tag for purification and crystallization of the siderophore receptor FhuA, integral outer membrane protein from *Escherichia coli* K-12. Protein Science *7*, 1636-1638.

Flores-Kim, J., and Darwin, A.J. (2012). Links between type III secretion and extracytoplasmic stress responses in *Yersinia*. Frontiers in Cellular and Infection Microbiology *2*. Doi: 10.3389/fcimb.2012.00125.

Francetic, O., Buddelmeijer, N., Lewenza, S., Kumamoto, C.A., and Pugsley, A.P. (2007). Signal recognition particle-dependent inner membrane targeting of the PulG

pseudopilin component of a type II secretion system. Journal of Bacteriology *189*, 1783-1793.

Francetic, O., and Pugsley, A.P. (2005). Towards the identification of type II secretion signals in a nonacylated variant of pullulanase from *Klebsiella oxytoca*. Journal of Bacteriology *187*, 7045-7055.

Fujii, Kitaoka, M., and Hayashi, K. (2004). One-step random mutagenesis by error-prone rolling circle amplification. Nucleic Acids Research *32*. Doi:10.1093/nar/gnh147e145.

Fujii, Kitaoka, M., and Hayashi, K. (2014). Error-prone rolling circle amplification greatly simplifies random mutagenesis. Methods in Molecular Biology (Clifton, NJ) *1179*, 23-29.

Gagic, D., Wen, W., Collett, M.A., and Rakonjac, J. (2013). Unique secreted-surface protein complex of *Lactobacillus rhamnosus*, identified by phage display. Microbiology open *2*, 1-17.

Galan, J.E. (1999). Interaction of *Salmonella* with host cells through the centisome 63 type III secretion system. Current Opinion in Microbiology *2*, 46-50.

Galan, J.E. (2009). Common themes in the design and function of bacterial effectors. Cell Host and Microbe *5*, 571-579.

Galan, J.E., and Collmer, A. (1999). Type III secretion machines: Bacterial devices for protein delivery into host cells. Science *284*, 1322-1328.

Galan, J.E., and Wolf-Watz, H. (2006). Protein delivery into eukaryotic cells by type III secretion machines. Nature *444*, 567-573.

Galan, J.E., and Zhou, D. (2000). Striking a balance: modulation of the actin cytoskeleton by *Salmonella*. Proceedings of the National Academy of Sciences of the United states of America *97*, 8754-8761.

Gauthier, A., Thomas, N.A., and Finlay, B.B. (2003). Bacterial injection machines. Journal of Biological Chemistry *278*, 25273-25276.

Geillon, F., Gondcaille, C., Charbonnier, S., Van Roermund, C.W., Lopez, T.E., Dias, A.M.M., Pais de Barros, J.-P., Arnould, C., Wanders, R.J., Trompier, D., *et al.* (2014). Structure-Function Analysis of Peroxisomal ATP-binding Cassette Transporters Using Chimeric Dimers. The Journal of biological chemistry *289*, 24511-24520.

Genin, S., and Boucher, C.A. (1994). A superfamily of proteins involved in different secretion pathways in Gram-negative bacteria - modular structure and specificity of the n-terminal domain. Molecular & General Genetics *243*, 112-118.

Gerard-Vincent, M., Robert, V., Ball, G., Bleves, S., Michel, G.P.F., Lazdunski, A., and Filloux, A. (2002). Identification of XcpP domains that confer functionality and specificity to the *Pseudomonas aeruginosa* type II secretion apparatus. Molecular Microbiology *44*, 1651-1665.

Giltner, C.L., Nguyen, Y., and Burrows, L.L. (2012). Type IV Pilin Proteins: Versatile Molecular Modules. Microbiol Mol Biol Rev *76*, 740-772.

Gokhale, R.S., and Khosla, C. (2000). Role of linkers in communication between protein modules. Current Opinion in Chemical Biology *4*, 22-27.

Goyal, P., Krasteva, P.V., Van Genven, N., Gubellini, F., Van den Broeck, I., Troupiotis-Tsailaki, A., Jonckheere, W., Pehau-Arnaudet, G., Pinkner, J.S., Chapman, M.R., *et al.* (2014). Structural and mechanistic insights into the bacterial amyloid secretion channel CsgG. Nature *516*, 250-253.

Greener, A., and Callahan, M. (1994). XL1-Red: a highly efficient random mutagenesis strain. In Stratagene Newsletter: Strategies in Molecular Biology, 32-34.

Greener, A., Callahan, M., and Jerspeth, B. (1997). An efficient random mutagenesis technique using an *E. coli* mutator strain. Molecular Biotechnology *7*, 189-195.

Gromiha, M.M., Ahmad, S., and Suwa, M. (2005). TMBETA-NET: discrimination and prediction of membrane spanning beta-strands in outer membrane proteins. Nucleic Acids Research *33*, 164-167.

Gueguen, E., Savitzky, D.C., and Darwin, A.J. (2009). Analysis of the *Yersinia enterocolitica* PspBC proteins defines functional domains, essential amino acids and new roles within the phage-shock-protein response. Molecular Microbiology *74*, 619-633.

Guilvout, I., Chami, M., Berrier, C., Ghazi, A., Engel, A., Pugsley, A.P., and Bayan, N. (2008). *In vitro* multimerization and membrane insertion of bacterial outer membrane secretin PulD. Journal of Molecular Biology *382*, 13-23.

Guilvout, I., Chami, M., Disconzi, E., Bayan, N., Pugsley, A.P., and Huysmans, G.H.M. (2014). Independent domain assembly in a trapped folding intermediate of multimeric outer membrane secretins. Structure *22*, 582-589.

Guilvout, I., Chami, M., Engel, A., Pugsley, A.P., and Bayan, N. (2006). Bacterial outer membrane secretin PulD assembles and inserts into the inner membrane in the absence of its pilotin. European Molecular Biology Organization Journal *25*, 5241-5249.

Guilvout, I., Hardie, K.R., Sauvonnet, N., and Pugsley, A.P. (1999). Genetic dissection of the outer membrane secretin PulD: are there distinct domains for multimerization and secretion specificity? Journal of Bacteriology *181*, 7212-7220.

Guilvout, I., Nickerson, N.N., Chami, M., and Pugsley, A.P. (2011). Multimerization-defective variants of dodecameric secretin PulD. Research in Microbiology *162*, 180-190.

Hager, A.J., Bolton, D.L., Pelletier, M.R., Brittnacher, M.J., Gallagher, L.A., Kaul, R., Skerrett, S.J., Miller, S.I., and Guina, T. (2006). Type IV pili-mediated secretion modulates *Francisella* virulence. Molecular Microbiology *62*, 227-237.

Han, X., Kennan, R.A., Parker, D., Davies, J.K., and Rood, J.I. (2007). Type IV fimbrial biogenesis is required for protease secretion and natural transformation in *Dichelobacter nodosus*. Journal of Bacteriology *189*, 5022-5033.

Hansen, J.K., and Forest, K.T. (2006). Type IV pilin structures: Insights on shared architecture, fiber assembly, receptor binding and type II secretion. Journal of Molecular Microbiology and Biotechnology *11*, 192-207.

Hapfelmeier, S., Stecher, B., Barthel, M., Kremer, M., Muller, A.J., Heikenwalder, M., Stallmach, T., Hensel, M., Pfeffer, K., Akira, S., *et al.* (2005). The salmonella pathogenicity island (SPI)-2 and SPI-1 type III secretion systems allow *Salmonella* serovar Typhimurium to trigger colitis via MyD88-dependent and MyD88-independent mechanisms. Journal of Immunology *174*, 1675-1685.

Hardie, K.R., Lory, S., and Pugsley, A.P. (1996). Insertion of an outer membrane protein in *Escherichia coli* requires a shaperone-like protein. European Molecular Biology Organization journal *15*, 978-988.

Hardt, W.D., Chen, L.M., Schuebel, K.E., Bustelo, X.R., and Galan, J.E. (1998). *S.* Typhimurium encodes an activator of Rho GTPases that induces membrane ruffling and nuclear responses in host cells. Cell *93*, 815-826.

Hernandez, L.D., Hueffer, K., Wenk, M.R., and Galan, J.E. (2004). *Salmonella* modulates vesicular traffic by altering phosphoinositide metabolism. Science *304*, 1805-1807.

Hernandez, L.D., Pypaert, M., Flavell, R.A., and Galan, J.E. (2003). A *Salmonella* protein causes macrophage cell death by inducing autophagy. Journal of Cell Biology *163*, 1123-1131.

Ho, S.N., Hunt, H.D., Horton, R.M., Pullen, J.K., and Pease, L.R. (1989). Site-directed mutagenesis by overlap extension using the polymerase chain reaction. Gene *77*, 51-59.

Hodgkinson, J.L., Horsley, A., Stabat, D., Simon, M., Johnson, S., da Fonseca, P.C., Morris, E.P., Wall, J.S., Lea, S.M., and Blocker, A.J. (2009). Three-dimensional

reconstruction of the *Shigella* T3SS transmembrane regions reveals 12-fold symmetry and novel features throughout. Nature Structural and Molecular Biology *16*, 477-485.

Hope, G.C., and Dean, A.C.R. (1974). Pullulanase synthesis in *Klebsiella* (aerobacter) *aerogenes* strains growing in continuous culture. Biochemical Journal *144*, 403-411.

Horstman, N.K., and Darwin, A.J. (2012). Phage shock proteins B and C prevent lethal cytoplasmic membrane permeability in *Yersinia enterocolitica*. Molecular Microbiology *85*, 445-460.

Huang, Y.H., Ferrieres, L., and Clarke, D.J. (2006). The role of the Rcs phosphorelay in enterobacteriaceae. Research in Microbiology *157*, 206-212.

Hueck, C.J. (1998). Type III protein secretion systems in bacterial pathogens of animals and plants. Microbiology and Molecular Biology Reviews *62*, 379-433.

Johnson, T.L., Fong, J.C., Rule, C., Rogers, A., Yildiz, F.H., and Sandkvist, M. (2014). The type II secretion system delivers matrix proteins for biofilm formation by *Vibrio cholerae*. Journal of Bacteriology *196*, 4245-4252.

Joly, N., Engl, C., Jovanovic, G., Huvet, M., Toni, T., Sheng, X., Stumpf, M.P.H., and Buck, M. (2010). Managing membrane stress: the phage shock protein (Psp) response, from molecular mechanisms to physiology. FEMS Microbiology Reviews *34*, 797-827.

Jovanovic, G., Lloyd, L.J., Stumpf, M.P.H., Mayhew, A.J., and Buck, M. (2006). Induction and function of the phage shock protein extracytoplasmic stress response in *Escherichia coli*. Journal of Biological Chemistry *281*, 21147-21161.

Jovanovic, G., Weiner, L., and Model, P. (1996). Identification, nucleotide sequence, and characterization of PspF, the transcriptional activator of the *Escherichia coli* stress-induced psp operon. Journal of Bacteriology *178*, 1936-1945.

Jyot, J., Balloy, V., Jouvion, G., Verma, A., Touqui, L., Huerre, M., Chignard, M., and Ramphal, R. (2011). Type II secretion system of *Pseudomonas aeruginosa: In vivo* evidence of a significant role in death due to lung infection. Journal of Infectious Diseases *203*, 1369-1377.

Kaelin, W.G., Krek, W., Sellers, W.R., Decaprio, J.A., Ajchenbaum, F., Fuchs, C.S., Chittenden, T., Li, Y., Farnham, P.J., Blanar, M.A., *et al.* (1992). Expression cloning of a cDNA-encoding a retinoblastoma-binding protein with e2f-like properties. Cell *70*, 351-364.

Kimbrough, T.G., and Miller, S.I. (2000). Contribution of type III secretion components to needle complex formation. Proceedings of the National Academy of Sciences of the United States of America *97*, 11008-11013.

Kirn, T.J., Bose, N., and Taylor, R.K. (2003). Secretion of a soluble colonization factor by the TCP type 4 pilus biogenesis pathway in *Vibrio cholerae*. Molecular Microbiology *49*, 81-92.

Kobayashi, R., Suzuki, T., and Yoshida, M. (2007). *Escherichia coli* phage-shock protein A (PspA) binds to membrane phospholipids and repairs proton leakage of the damaged membranes. Molecular Microbiology *66*, 100-109.

Koronakis, V., Sharff, A., Koronakis, E., Luisi, B., and Hughes, C. (2000). Crystal structure of the bacterial membrane protein TolC central to multidrug efflux and protein export. Nature *405*, 914-919.

Korotkov, Johnson, T.L., Jobling, M.G., Pruneda, J., Pardon, E., Heroux, A., Turley, S., Steyaert, J., Holmes, R.K., Sandkvist, M.*, et al.* (2011). Structural and functional studies on the interaction of gspc and gspd in the type II secretion system. PLoS pathogens *7*. Doi: 10.1371/journal.ppat.1002228.

Korotkov, Pardon, E., Steyaert, J., and Hol, W.G. (2009). Crystal structure of the N-terminal domain of the secretin GspD from ETEC determined with the assistance of a nanobody. Structure *17*, 255-265.

Korotkov, Sandkvist, M., and Hol, W.G.J. (2012). The type II secretion system: biogenesis, molecular architecture and mechanism. Nature Reviews Microbiology *10*, 336-351.

Korotkov, K.V., Krumm, B., Bagdasarian, M., and Hol, W.G. (2006). Structural and functional studies of EpsC, a crucial component of the type 2 secretion system from *Vibrio cholerae*. Journal of Molecular Biology *363*, 311-321.

Kosarewicz, A., Koenigsmaier, L., and Marlovits, T.C. (2012). The blueprint of the type-3 injectisome. Philosophical Transactions of the Royal Society Biological Sciences *367*, 1140-1154.

Koster, M., Bitter, W., de Cock, H., Allaoui, A., Cornelis, G.R., and Tommassen, J. (1997). The outer membrane component, YscC, of the Yop secretion machinery of *Yersinia enterocolitica* forms a ring-shaped multimeric complex. Molecular Microbiology *26*, 789-797.

Koves, K., Vigh, S., Somogyvarivigh, A., Gorcs, T., Miller, J., Melrose, R., and Arimura, A. (1992). Immunohistochemical demonstration of Pacap immunoreactivity in the peripheral nervous-System. Regulatory Peptides *37*, 329-329.

Kowal, J., Chami, M., Ringler, P., Mueller, S.A., Kudryashev, M., Castano-Diez, D., Amstutz, M., Cornelis, G.R., Stahlberg, H., and Engel, A. (2013). Structure of the dodecameric

Yersinia enterocolitica secretin YscC and its trypsin-resistant core. Structure *21*, 2152-2161.

Krishnan, V., Dwivedi, P., Kim, B.J., Samal, A., Macon, K., Ma, X., Mishra, A., Doran, K.S., Ton-That, H., and Narayana, S.V.L. (2013). Structure of *Streptococcus agalactiae* tip pilin GBS104: a model for GBS pili assembly and host interactions. Acta Crystallographica Section D-Biological Crystallography *69*, 1073-1089.

Kubori, T., Sukhan, A., Aizawa, S.I., and Galan, J.E. (2000). Molecular characterization and assembly of the needle complex of the *Salmonella typhimurium* type III protein secretion system. Proceedings of the National Academy of Sciences of the United States of America *97*, 10225-10230.

Laemmli, U.K. (1970). Cleavage of structural proteins during assembly of head of bacteriophage-T4. Nature *227*, 680-685.

Lario, P.I., Pfuetzner, R.A., Frey, E.A., Creagh, L., Haynes, C., Maurelli, A.T., and Strynadka, N.C.J. (2005). Structure and biochemical analysis of a secretin pilot protein. European Molecular Biology Organization Journal *24*, 1111-1121.

Lathem, W.W., Grys, T.E., Witowski, S.E., Torres, A.G., Kaper, J.B., Tarr, P.I., and Welch, R.A. (2002). StcE, a metalloprotease secreted by *Escherichia coli* O157 : H7, specifically cleaves C1 esterase inhibitor. Molecular Microbiology *45*, 277-288.

Lee, H.M., Wang, K.C., Liu, Y.L., Yew, H.Y., Chen, L.Y., Leu, W.M., Chen, D.C.H., and Hu, N.T. (2000). Association of the cytoplasmic membrane protein XpsN with the outer membrane protein XpsD in the type II protein secretion apparatus of *Xanthomonas campestris* pv. campestris. Journal of Bacteriology *182*, 1549-1557.

Lefebre, M.D., and Galan, J.E. (2014). The inner rod protein controls substrate switching and needle length in a *Salmonella* type III secretion system. Proceedings of the National Academy of Sciences of the United States of America *111*, 817-822.

Leotta, G.A., Miliwebsky, E.S., Chinen, I., Espinosa, E.M., Azzopardi, K., Tennant, S.M., Robins-Browne, R.M., and Rivas, M. (2008). Characterisation of Shiga toxin-producing *Escherichia coli* O157 strains isolated from humans in Argentina, Australia and New Zealand. BioMed Central Microbiology *8*, 46.

Lessl, M., Balzer, D., Lurz, R., Waters, V.L., Guiney, D.G., and Lanka, E. (1992). Dissection of Incp conjugative plasmid transfer - definition of the transfer region Tra2 by mobilization of the Tra1 region in trans. Journal of Bacteriology *174*, 2493-2500.

Li, Y., Hu, Y., Francis, M.S., and Chen, S. (2015). RcsB positively regulates the *Yersinia* Ysc-Yop type III secretion system by activating expression of the master transcriptional regulator LcrF. Environmental microbiology *17*, 1219-1233.

Loeb, T. (1960). Isolation of a bacteriophage specific for the f+ and hfr mating types of *Escherichia coli* K-12. Science *131*, 932-933.

Login, F.H., Fries, M., Wang, X., Pickersgill, R.W., and Shevchik, V.E. (2010). A 20-residue peptide of the inner membrane protein OutC mediates interaction with two distinct sites of the outer membrane secretin OutD and is essential for the functional type II secretion system in *Erwinia chrysanthemi*. Molecular Microbiology *76*, 944-955.

Loquet, A., Sgourakis, N.G., Gupta, R., Giller, K., Riedel, D., Goosmann, C., Griesinger, C., Kolbe, M., Baker, D., Becker, S.*, et al.* (2012). Atomic model of the type III secretion system needle. Nature *486*, 276-279.

Lostroh, C.P., and Lee, C.A. (2001). The *Salmonella* pathogenicity island-1 type III secretion system. Microbes Infection *3*, 1281-1291.

Lowry, O.H., Rosebrough, N.J., Farr, A.L., and Randall, R.J. (1951). Protein measurement with the folin phenol reagent. Journal of Biological Chemistry *193*, 265-275.

Lu, H.M., Motley, S.T., and Lory, S. (1997). Interactions of the components of the general secretion pathway: role of *Pseudomonas aeruginosa* type IV pilin subunits in complex formation and extracellular protein secretion. Molecular Microbiology *25*, 247-259.

Lybarger, S.R., Johnson, T.L., Gray, M.D., Sikora, A.E., and Sandkvist, M. (2009). Docking and Assembly of the type II Secretion Complex of *Vibrio cholerae*. Journal of Bacteriology *191*, 3149-3161.

Majdalani, N., and Gottesman, S. (2005). The Rcs phosphorelay: A complex signal transduction system. In Annual Review of Microbiology, pp. 379-405.

Marciano, Russel, M., and Simon, S.M. (1999). An aqueous channel for filamentous phage export. Science *284*, 1516-1519.

Marciano, Russel, M., and Simon, S.M. (2001). Assembling filamentous phage occlude pIV channels. Proceedings of the National Academy of Sciences of the United States of America *98*, 9359-9364.

Marlovits, T.C., Kubori, T., Lara-Tejero, M., Thomas, D., Unger, V.M., and Galan, J.E. (2006). Assembly of the inner rod determines needle length in the type III secretion injectisome. Nature *441*, 637-640.

Marlovits, T.C., Kubori, T., Sukhan, A., Thomas, D.R., Galan, J.E., and Unger, V.M. (2004). Structural insights into the assembly of the type III secretion needle complex. Science *306*, 1040-1042.

Marlovits, T.C., and Stebbins, C.E. (2009). Type III secretion systems shape up as they ship out. Current Opinion in Microbiology, 47-52.

Martelli, P.L., Fariselli, P., Krogh, A., and Casadio, R. (2002). A sequence-profile-based HMM for predicting and discriminating beta barrel membrane proteins. Bioinformatics (Oxford, England) *18 Suppl 1*, S46-53.

Martin, P.R., Hobbs, M., Free, P.D., Jeske, Y., and Mattick, J.S. (1993). Characterization of pilQ, a new gene required for the biogenesis of type 4 fimbriae in *Pseudomonas aeruginosa*. Molecular Microbiology *9*, 857-868.

Marvin, D.A., and Hohn, B. (1969). Filamentous bacterial viruses. Bacteriology Reviews *33*, 172-209.

Marvin, D.A., Symmons, M.F., and Straus, S.K. (2014). Structure and assembly of filamentous bacteriophages. Progress in Biophysics and Molecular Biology *114*, 80-122.

Matson, J.S., Withey, J.H., and DiRita, V.J. (2007). Regulatory networks controlling *Vibrio cholerae* virulence gene expression. Infection and Immunity *75*, 5542-5549.

Mattick, J.S., Whitchurch, C.B., and Alm, R.A. (1996). The molecular genetics of type-4 fimbriae in *Pseudomonas aeruginosa* - A review. Gene *179*, 147-155.

McCann, H.C., and Guttman, D.S. (2008). Evolution of the type III secretion system and its effectors in plant-microbe interactions. New Phytologist *177*, 33-47.

McGhie, E.J., Brawn, L.C., Hume, P.J., Humphreys, D., and Koronakis, V. (2009). Salmonella takes control: effector-driven manipulation of the host. Current Opinion in Microbiology *12*, 117-124.

Mergulhao, F.J.M., and Monteiro, G.A. (2004). Secretion capacity limitations of the Sec pathway in *Escherichia coli*. Journal of Microbiology and Biotechnology *14*, 128-133.

Mergulhao, F.J.M., Taipa, M.A., Cabral, J.M.S., and Monteiro, G.A. (2004). Evaluation of bottlenecks in proinsulin secretion by *Escherichia coli*. Journal of Biotechnology *109*, 31-43.

Michaelis, S., Chapon, C., Denfert, C., Pugsley, A.P., and Schwartz, M. (1985). Characterization and expression of the structural gene for pullulanase, a maltose-inducible secreted protein of *Klebsiella pneumoniae*. Journal of Bacteriology *164*, 633-638.

Miki, T., Okada, N., Shimada, Y., and Danbara, H. (2004). Characterization of *Salmonella* pathogenicity island 1 type III secretion-dependent hemolytic activity in *Salmonella enterica* serovar Typhimurium. Microbial Pathogenesis *37*, 65-72.

Miller, J.H. (1972). Experiments in Molecular Genetics. (Cold Spring Harbor, New York: Cold Spring Harbor Laboratory).

Minamino, T., Morimoto, Y.V., Hara, N., and Namba, K. (2011). An energy transduction mechanism used in bacterial flagellar type III protein export. Nature Communications *2*. Doi:10.1038/ncomms1488.

Miroux, B., and Walker, J.E. (1996). Over-production of proteins in *Escherichia coli*: Mutant hosts that allow synthesis of some membrane proteins and globular proteins at high levels. Journal of Molecular Biology *260*, 289-298.

Mizuno, T., Kasai, H., and Mizushima, S. (1987). Construction of a series of ompc-ompf chimeric genes by invivo homologous recombination in *Escherichia coli* and characterization of their translational products. Molecular and General Genetics *207*, 217-223.

Model, P., Jovanovic, G., and Dworkin, J. (1997). The *Escherichia coli* phage-shock-protein (*psp*) operon. Molecular Microbiology *24*, 255-261.

Mohammadi-Barzelighi, H., Bakhshi, B., Lari, A.R., and Pourshafie, M.R. (2011). Characterization of pathogenicity island prophage in clinical and environmental strains of *Vibrio cholerae*. Journal of Medical Microbiology *60*, 1742-1749.

Morgan, J.K., Ortiz, J.A., and Riordan, J.T. (2014). The role for TolA in enterohemorrhagic *Escherichia coli* pathogenesis and virulence gene transcription. Microbial Pathogenesis *77*, 42-52.

Mullan, L.J., and Bleasby, A.J. (2002). Short EMBOSS User Guide. European Molecular Biology Open Software Suite. Briefings in Bioinformatics *3*, 92-94.

Natale, P., Brueser, T., and Driessen, A.J.M. (2008). Sec- and Tat-mediated protein secretion across the bacterial cytoplasmic membrane - Distinct translocases and mechanisms. Biochim Biophys Acta-Biomembr *1778*, 1735-1756.

Nataro, J.P., and Kaper, J.B. (1998). Diarrheagenic *Escherichia coli*. Clinical microbiology reviews *11*, 142-201.

Neidhardt, F.C., Bloch, P.L., and Smith, D.F. (1974). Culture medium for enterobacteria. Journal of Bacteriology *119*, 736-747.

Nikaido, H., and Rosenberg, E.Y. (1983). Porin channels in *Escherichia coli* - studies with liposomes reconstituted from purified proteins. Journal of Bacteriology *153*, 241-252.

Nouwen, N., Ranson, N., Saibil, H., Wolpensinger, B., Engel, A., Ghazi, A., and Pugsley, A.P. (1999). Secretin PulD: association with pilot PulS, structure, and ion-conducting channel formation. Proceedings of the National Academy of Sciences of the United States of America *96*, 8173-8177.

Opalka, N., Beckmann, R., Boisset, N., Simon, M.N., Russel, M., and Darst, S.A. (2003). Structure of the filamentous phage pIV multimer by cryo-electron microscopy. Journal of Molecular Biology *325*, 461-470.

Pages, J.-M., James, C.E., and Winterhalter, M. (2008). The porin and the permeating antibiotic: a selective diffusion barrier in Gram-negative bacteria. Nature Reviews Microbiology *6*, 893-903.

Peabody, C.R., Chung, Y.J., Yen, M.R., Vidal-Ingigliardi, D., Pugsley, A.P., and Saier, M.H. (2003). Type II protein secretion and its relationship to bacterial type IV pili and archaeal flagella. Microbiology-SGM *149*, 3051-3072.

Pescaretti, d.l.M.M., Farizano, J.V., Morero, R., and Delgado, M.A. (2013). A novel insight on signal transduction mechanism of RcsCDB system in *Salmonella enterica* Serovar Typhimurium. Plos One *8*. DOI: 10.1371/journal.pone.0072527.

Pineau, C., Guschinskaya, N., Robert, X., Gouet, P., Ballut, L., and Shevchik, V.E. (2014). Substrate recognition by the bacterial type II secretion system: more than a simple interaction. Molecular Microbiology *94*, 126-140.

Podschun, R., and Ullmann, U. (1998). *Klebsiella* spp. as nosocomial pathogens: Epidemiology, taxonomy, typing methods, and pathogenicity factors. Clinical Microbiology Reviews *11*, 589-603.

Possot, O., Denfert, C., Reyss, I., and Pugsley, A.P. (1992). Pullulanase secretion in *Escherichia coli* k-12 requires a cytoplasmic protein and a putative polytopic cytoplasmic membrane-protein. Molecular Microbiology *6*, 95-105.

Possot, O.M., Vignon, G., Bomchil, N., Ebel, F., and Pugsley, A.P. (2000). Multiple interactions between pullulanase secreton components involved in stabilization and cytoplasmic membrane association of PulE. Journal of Bacteriology *182*, 2142-2152.

Qi, M., Sun, F.-J., Caetano-Anolles, G., and Zhao, Y. (2010). Comparative genomic and phylogenetic analyses reveal the evolution of the core two-component signal transduction systems in enterobacteria. Journal of Molecular Evolution *70*, 167-180.

Rakonjac, J., Bennett, N.J., Spagnuolo, J., Gagic, D., and Russel, M. (2011). Filamentous bacteriophage: biology, phage display and nanotechnology applications. Current Issues Molecular Biology *13*, 51-76.

Rakonjac, J., and Conway, J.F. (2006). Bacteriophages: self-assembly and applications. In Molecular Bionanotechnology, B. Rehm, ed. (Norwich, UK: Horizon Scientific Press), 153-190.

Rakonjac, J., Feng, J.N., and Model, P. (1999). Filamentous phage are released from the bacterial membrane by a two-step mechanism involving a short C-terminal fragment of pIII. Journal of Molecular Biology *289*, 1253-1265.

Rapoza, M.P., and Webster, R.E. (1995). The products of *gene I* and the overlapping in-frame *gene XI* are required for filamentous phage assembly. Jounal of Molecular Biology *248*, 627-638.

Reichow, S.L., Korotkov, K.V., Hol, W.G.J., and Gonen, T. (2010). Structure of the cholera toxin secretion channel in its closed state. Nature Structural Molecular Biology *17*, 1226-1232.

Rice, S.A., Tan, C.H., Mikkelsen, P.J., Kung, V., Woo, J., Tay, M., Hauser, A., McDougald, D., Webb, J.S., and Kjelleberg, S. (2009). The biofilm life cycle and virulence of *Pseudomonas aeruginosa* are dependent on a filamentous prophage. ISME Journal *3*, 271-282.

Robinson, C.R., and Sauer, R.T. (1998). Optimizing the stability of single-chain proteins by linker length and composition mutagenesis. Proceedings of the National Academy of Sciences of the United States of America *95*, 5929-5934.

Roe, A.J., Yull, H., Naylor, S.W., Woodward, M.J., Smith, D.G.E., and Gally, D.L. (2003). Heterogeneous surface expression of EspA translocon filaments by *Escherichia coli* O157 : H7 is controlled at the posttranscriptional level. Infection and Immunity *71*, 5900-5909.

Rossier, O., Starkenburg, S.R., and Cianciotto, N.P. (2004). *Legionella pneumophila* type II protein secretion promotes virulence in the A/J mouse model of Legionnaires' disease pneumonia. Infection and Immunity *72*, 310-321.

Ruiz, N., Falcone, B., Kahne, D., and Silhavy, T.J. (2005). Chemical conditionality: a genetic strategy to probe organelle assembly. Cell *121*, 307-317.

Ruiz, N., Kahne, D., and Silhavy, T.J. (2006). Advances in understanding bacterial outer-membrane biogenesis. Nature Reviews Microbiology *4*, 57-66.

Russel, M. (1991). Filamentous phage assembly. Molecular Microbiology *5*, 1607-1613.

Russel, M. (1994). Mutants at conserved positions in *gene IV*, a gene required for assembly and secretion of filamentous phages. Molecular Microbiology *14*, 357-369.

Russel, M., and Kazmierczak, B. (1993). Analysis of the Structure and Subcellular Location of Filamentous Phage-pIV. Journal of Bacteriology *175*, 3998-4007.

Russel, M., Linderoth, N.A., and Sali, A. (1997). Filamentous phage assembly: Variation on a protein export theme. Gene *192*, 23-32.

Russel, M., and Model, P. (2006). Filamentous phage. In The Bacteriophages (Second Edition), R.C. Calendar, ed. (New York: Oxford University Press, Inc.), 146-160.

Sambrook, J., Fritsch, E.F., and Maniatis, T. (1989). Molecular cloning: A laboratory manual, 2nd edn (Cold Spring Harbor, NY: Cold Spring Harbor Laboratory Press).

Sambrook, J., and Russell, D.W. (2001). Molecular cloning: a laboratory manual (3rd. Edn.), 3rd edn (Cold Spring Harbor: Cold Spring Harbor).

Sandkvist, M. (2001). Type II secretion and pathogenesis. Infection and Immunity *69*, 3523-3535.

Sandkvist, M., Hough, L.P., Bagdasarian, M.M., and Bagdasarian, M. (1999). Direct interaction of the EpsL and EpsM proteins of the general secretion apparatus in *Vibrio cholerae*. Journal of Bacteriology *181*, 3129-3135.

Sani, M., Allaoui, A., Fusetti, F., Oostergetel, G.T., Keegstra, W., and Boekema, E.J. (2007). Structural organization of the needle complex of the type III secretion apparatus of *Shigella flexneri*. Micron *38*, 291-301.

Sanowar, S., Singh, P., Pfuetzner, R.A., Andre, I., Zheng, H., Spreter, T., Strynadka, N.C.J., Gonen, T., Baker, D., Goodlett, D.R.*, et al.* (2010). Interactions of the transmembrane polymeric rings of the S*almonella enterica* serovar Typhimurium type III secretion system. mBio. Doi: 10.1128/mBio.00158-10.

Satyshur, K.A., Worzalla, G.A., Meyer, L.S., Heiniger, E.K., Aukema, K.G., Misic, A.M., and Forest, K.T. (2007). Crystal structures of the pilus retraction motor PilT suggest large domain movements and subunit cooperation drive motility. Structure *15*, 363-376.

Sauvonnet, N., Vignon, G., Pugsley, A.P., and Gounon, P. (2000). Pilus formation and protein secretion by the same machinery in *Escherichia coli*. European Molecular Biology Organization Journal *19*, 2221-2228.

Schmidt, H., and Hensel, M. (2004). Pathogenicity islands in bacterial pathogenesis. Clinical Microbiology Reviews *17*, 14-56.

Schraidt, O., Lefebre, M.D., Brunner, M.J., Schmied, W.H., Schmidt, A., Radics, J., Mechtler, K., Galan, J.E., and Marlovits, T.C. (2010). Topology and organization of the *Salmonella typhimurium* type III secretion needle complex components. PLoS Pathogens *6*, (4): DOI: 10.1371/journal.ppat.1000824.

Schraidt, O., and Marlovits, T.C. (2011). Three-dimensional model of *Salmonella's* needle complex at subnanometer resolution. Science *331*, 1192-1195.

Schuch, R., and Maurelli, A.T. (2001). MxiM and MxiJ, base elements of the Mxi-Spa type III secretion system of *Shigella*, interact with and stabilize the MxiD secretin in the cell envelope. Journal of Bacteriology *183*, 6991-6998.

Seo, J., Savitzky, D.C., Ford, E., and Darwin, A.J. (2007). Global analysis of tolerance to secretin-induced stress in *Yersinia enterocolitica* suggests that the phage-shock-protein system may be a remarkably self-contained stress response. Molecular Microbiology *65*, 714-727.

Sheppard, D.N., and Welsh, M.J. (1999). Structure and function of the CFTR chloride channel. Physiological reviews *79*, S23-45.

Silver, L.L. (2011). Challenges of antibacterial discovery. Clinical Microbiology Reviews *24*, 71-109.

Sithivong, N., Izumiya, H., Munnalath, K., Phouthavane, T., Chomlasak, K., Sisavath, L., Vongdouangchanh, A., Vongprachanh, P., Watanabe, H., and Ohinishi, M. (2010). Cholera outbreak, Laos, 2007. Emerging Infectious Diseases *16*, 745-746.

Sledjeski, D.D., and Gottesman, S. (1996). Osmotic shock induction of capsule synthesis in *Escherichia coli* K-12. Journal of Bacteriology *178*, 1204-1206.

Sohel, I., Puente, J.L., Ramer, S.W., Bieber, D., Wu, C.Y., and Schoolnik, G.K. (1996). Enteropathogenic *Escherichia coli:* Identification of a gene cluster coding for bundle-forming pilus morphogenesis. Journal of Bacteriology *178*, 2613-2628.

Spagnuolo, J., Opalka, N., Wen, W.X., Gagic, D., Chabaud, E., Bellini, D., Bennett, M., Norris, G.E., Darst, S.A., Russel, M., *et al.* (2010). Identification of the gate regions in the primary structure of the secretin pIV. Molecular Microbiology *76*, 17.

Spreter, T., Yip, C.K., Sanowar, S., Andre, I., Kimbrough, T.G., Vuckovic, M., Pfuetzner, R.A., Deng, W.Y., Yu, A.C., Finlay, B.B., *et al.* (2009). A conserved structural motif mediates formation of the periplasmic rings in the type III secretion system. Nature Structural Molecular Biology *16*, 468-476.

Strozen, T.G., Stanley, H., Gu, Y., Boyd, J., Bagdasarian, M., Sandkvist, M., and Howard, S.P. (2011). Involvement of the GspAB complex in assembly of the type II secretion system secretin of *Aeromonas* and *Vibrio* species. Journal of Bacteriology *193*, 2322-2331.

Sturm, A., Heinemann, M., Arnoldini, M., Benecke, A., Ackermann, M., Benz, M., Dormann, J., and Hardt, W.-D. (2011). The cost of virulence: Retarded growth of *Salmonella*

Typhimurium cells expressing type III secretion system 1. PLoS pathogens *7*. DOI: 10.1371/journal.ppat.1002143.

Szostek, B.A., and Rathera, P.N. (2013). Regulation of the swarming inhibitor Disa in *Proteus mirabilis*. Journal of Bacteriology *195*, 3237-3243.

Takeda, S., Fujisawa, Y., Matsubara, M., Aiba, H., and Mizuno, T. (2001). A novel feature of the multistep phosphorelay in *Escherichia coli:* a revised model of the RcsC -> YojN -> RcsB signalling pathway implicated in capsular synthesis and swarming behaviour. Molecular Microbiology *40*, 440-450.

Thanassi, D.G., Bliska, J.B., and Christie, P.J. (2012). Surface organelles assembled by secretion systems of Gram-negative bacteria: diversity in structure and function. FEMS Microbiology Reviews *36*, 1046-1082.

Tikhonova, E.B., Wang, Q.J., and Zgurskaya, H.I. (2002). Chimeric analysis of the multicomponent multidrug efflux transporters from Gram-negative bacteria. Journal of Bacteriology *184*, 6499-6507.

Tommassen, J., Vanderley, P., Vanzeijl, M., and Agterberg, M. (1985). Localization of functional domains in *Escherichia coli* K-12 outer-membrane porins. European Molecular Biology Organization Journal *4*, 1583-1587.

Tosi, T., Estrozi, L.F., Job, V., Guilvout, I., Pugsley, A.P., Schoehn, G., and Dessen, A. (2014). Structural similarity of secretins from type II and type III secretion systems. Structure *22*, 1348-1355.

Toth, I.K., and Birch, P.R.J. (2005). Rotting softly and stealthily. Current Opinion in Plant Biology *8*, 424-429.

Tseng, Y.H., Lo, M.C., Lin, K.C., Pan, C.C., and Chang, R.Y. (1990). Characterization of filamentous bacteriophage-phi-lf from *Xanthomonas campestris* pv campestris. Journal of General Virology *71*, 1881-1884.

Van Der Ley, P., Burn, P., Agterberg, M., Van Meersbergen, J., and Tommassen, J. (1987). Analysis of structure-function relationships in *Escherichia coli* K-12 outer membrane porins with the aid of *ompC phoE* and hybrid genes. Molecular and General Genetics *209*, 585-591.

Van der Meeren, R., Wen, Y., Van Gelder, P., Tommassen, J., Devreese, B., and Savvides, S.N. (2013). New insights into the assembly of bacterial secretins structural studies of the periplasmic domain of XcpQ from *Pseudomonas aeruginosa*. Journal of Biological Chemistry *288*, 1214-1225.

Veenendaal, A.K.J., Sundin, C., and Blocker, A.J. (2009). Small-molecule type III secretion system inhibitors block assembly of the *Shigella* type III secreton. Journal of Bacteriology *191*, 563-570.

Vicente, A.C.P., Teixeira, L.F.M., Iniguez-Rojas, L., Luna, M.G., Silva, L., Andrade, J.R.C., and Guth, B.E.C. (2005). Outbreaks of cholera-like diarrhoea caused by enterotoxigenic *Escherichia coli* in the Brazilian Amazon Rainforest. Transactions of the Royal society of Tropical Medicine and Hygiene *99*, 669-674.

Wachter, C., Beinke, C., Mattes, M., and Schmidt, M.A. (1999). Insertion of EspD into epithelial target cell membranes by infecting enteropathogenic *Escherichia coli*. Molecular Microbiology *31*, 1695-1707.

Waldor, M., and Mekalanos, J.J. (1996). Lysogenic conversion by a filamentous phage encoding cholera toxin. Science *272*, 1910-1914.

Wehbi, H., Portillo, E., Harvey, H., Shimkoff, A.E., Scheurwater, E.M., Howell, P.L., and Burrows, L.L. (2011). The peptidoglycan-binding protein FimV promotes assembly of the *Pseudomonas aeruginosa* type IV pilus secretin. Journal of Bacteriology *193*, 540-550.

Weiner, L., Brissette, J.L., and Model, P. (1991). Stress-induced expression of the *Escherichia coli* phage shock protein operon is dependent on sigma-54 and modulated by positive and negative feedback mechanisms. Genes and Development *5*, 1912-1923.

Whitaker., R. (2012). Analysis of gate residues in the type 2 secretin PulD. Unpublished MSc thesis Massey University.

Wimley, W.C. (2002). Toward genomic identification of beta-barrel membrane proteins: Composition and architecture of known structures. Protein Science *11*, 301-312.

World Health, O. (2014). Antimicrobial resistance: 2014 global report on surveillance.

Wu, G., Hong, Y., Guo, A., Feng, C., Cao, S., Zhang, C.-C., Shi, R., Tan, Y., and Liu, Z. (2010). A chimeric protein that functions as both an anthrax dual-target antitoxin and a trivalent vaccine. Antimicrob Agents Ch *54*, 4750-4757.

Xie, K., and Dalbey, R.E. (2008). Inserting proteins into the bacterial cytoplasmic membrane using the Sec and YidC translocases. Nature Reviews Microbiology *6*, 234-244.

Yamagata, A., Milgotina, E., Scanlon, K., Craig, L., Tainer, J.A., and Donnenberg, M.S. (2012). Structure of an essential type IV pilus biogenesis protein provides insights into pilus and type II secretion systems. Journal of Molecular Biology *419*, 110-124.

Yang , R Yan, A Roy, D Xu, J Poisson, and Y Zhang. The I-TASSER Suite: Protein structure and function prediction. (2015). Nature Methods 12, 7-8.

Yen, M.R., Peabody, C.R., Partovi, S.M., Zhai, Y.F., Tseng, Y.H., and Saier, M.H. (2002). Protein-translocating outer membrane porins of Gram-negative bacteria. Biochimica et Biophysica Acta-Biomembranes *1562*, 6-31.

Yip, C.K., Finlay, B.B., and Strynadka, N.C. (2005). Structural characterization of a type III secretion system filament protein in complex with its chaperone. Nature Structural and Molecular Biology *12*, 75-81.

Zhao, L., Ezaki, T., Li, Z.Y., Kawamura, Y., Hirose, K., and Watanabe, H. (2001). Vi-suppressed wild strain *Salmonella typhi* cultured in high osmolarity is hyperinvasive toward epithelial cells and destructive of peyer's patches. Microbiology and Immunology *45*, 149-158.

Zhong, D., Lefebre, M., Kaur, K., McDowell, M.A., Gdowski, C., Jo, S., Wang, Y., Benedict, S.H., Lea, S.M., Galan, J.E., *et al.* (2012). The *Salmonella* type III secretion system inner rod protein PrgJ is partially folded. Journal of Biological Chemistry *287*, 25303-25311.